DYNAMIC MODELLING OF PROTON EXCHANGE MEMBRANE FUEL CELL SYSTEM FOR ELECTRIC BICYCLE

AZADEH KHEIRANDISH

FACULTY OF ENGINEERING

UNIVERSITY OF MALAYA

KUALA LUMPUR

2016

DYNAMIC MODELLING OF PROTON EXCHANGE MEMBRANE FUEL CELL SYSTEM FOR ELECTRIC BICYCLE

AZADEH KHEIRANDISH

THESIS SUBMITTED IN FULFILMENT OF

THE REQUIREMENTS FOR THE DEGREE OF

DOCTOR OF PHILOSOPHY

FACULTY OF ENGINEERING

UNIVERSITY OF MALAYA

KUALA LUMPUR

2016

UNIVERSITY OF MALAYA

ORIGINAL LITERARY WORK DECLARATION

Name of Candidate: Azadeh Kheirandish

Registration/Matric No: KHA110083

Name of Degree: DOCTOR OF PHILOSOPHY

Title of Project Paper/Research Report/Dissertation/Thesis ("this Work"):

"**DYNAMIC MODELLING OF PROTON EXCHANGE MEMBRANE FUEL CELL SYSTEM FOR ELECTRIC BICYCLE"**

Field of Study: AUTOMATION, CONTROL & ROBOTICS

I do solemnly and sincerely declare that:

(1) I am the sole author/writer of this Work;

(2) This Work is original;

(3) Any use of any work in which copyright exists was done by way of fair dealing and for permitted purposes and any excerpt or extract from, or reference to or reproduction of any copyright work has been disclosed expressly and sufficiently and the title of the Work and its authorship have been acknowledged in this Work;

(4) I do not have any actual knowledge nor do I ought reasonably to know that the making of this work constitutes an infringement of any copyright work;

(5) I hereby assign all and every rights in the copyright to this Work to the University of Malaya ("UM"), who henceforth shall be owner of the copyright in this Work and that any reproduction or use in any form or by any means whatsoever is prohibited without the written consent of UM having been first had and obtained;

(6) I am fully aware that if in the course of making this Work I have infringed any copyright whether intentionally or otherwise, I may be subject to legal action or any other action as may be determined by UM.

Candidate's Signature Date:

Subscribed and solemnly declared before,

Witness's Signature Date:

Name:

Designation

ABSTRACT

Fuel cell systems with high-energy efficiency provides clean energy with lower noise and emissions that have attracted significant attention of energy. Proton exchange membrane (PEM) fuel cell has high power density; long stack life and low-temperature operation condition, which makes it a prime candidate for the vehicles. Performance optimization of PEM fuel cell has been a topic of research in the last decade. The efficiency of fuel cells is not specific; it is a subordinate to the power density where the system operates. The fuel cell performance is least efficient when functioning under maximum output power conditions.

Modelling the PEM fuel cell is the fundamental step in designing efficient systems for achieving higher performance. In spite of affecting factors in PEM fuel cell functionality, providing a reliable model for PEM fuel cell is the key of performance optimization challenge. There have been two approaches for modelling and prediction of commercial PEM fuel cell namely, theoretical and empirical models. Since theoretical modeling is not achievable in experimental conditions, the empirical modeling has attracted significant attention in researches. Various types of algorithms have been utilized for modelling these systems to achieve a high accuracy for predicting the efficiency and controlling the system.

Recent models provide high accuracies using complex systems and complicated calculations using advanced optimization algorithms. However, designing an accurate dynamic model for prediction and controlling the system in a real time condition is a challenge in this field. By utilizing the state of the art soft computing algorithms in modeling the technical systems to reduce the complexity of the models artificial neural networks have had a great impact in this field. This study has multifold objectives and

aim to design models for a 250W proton exchange membrane fuel cell system that is used as the power plant in electric bicycle. Classical linear regression and artificial neural networks as the most popular and accurate algorithms have been optimized and used for modeling this system. In addition, for the first time fuzzy cognitive map has been utilized in modeling PEM fuel cell system and targeted to provide a dynamic cognitive map from the affective factors of the system. Controlling and modification of the system performance in various conditions is more practical by correlations among the performance factors of the PEM fuel cell resulted from fuzzy cognitive map. On the other hand, the information of fuzzy cognitive map modeling is applicable for modification of neural networks structure for providing more accurate results based on the extracted knowledge from the cognitive map and visualization of the system's performance.

ABSTRAK

Sistem sel bahan api dengan kecekapan tenaga tinggi menyediakan tenaga bersih dengan kadar bunyi dan pelepasan yang lebih rendah telah menarik perhatian besar tenaga. Sel bahan api membran pertukaran proton (PEM) fuel cell telah menjadi pilihan utama untuk kenderaan kerana mempunyai ketumpatan kuasa yang tinggi ; kadar hidup timbunan yang lama dan keadaan operasi di suhu rendah. Pengoptimuman prestasi PEM fuel cell telah menjadi topik penyelidikan untuk beberapa dekad yang lalu. Kecekapan sel bahan api tidak khusus ; ia adalah lebih rendah daripada ketumpatan kuasa di mana sistem beroperasi. Prestasi sel bahan api kurang berkesan apabila ianya berfungsi di dalam keadaan kuasa keluaran yang maksimum.

Pemodelan PEMFC adalah langkah asas dalam mereka bentuk sistem yang cekap untuk mencapai prestasi yang lebih tinggi. Selain faktor-faktor yang mempengaruhi prestasi PEMFC , menyediakan model yang boleh dipercayai adalah kunci kepada cabaran untuk mengoptimumkan prestasi PEMFC. Terdapat dua pendekatan untuk pemodelan dan ramalan komersial sel bahan api PEM iaitu model teori dan model empirikal. Oleh kerana pemodelan teori tidak boleh dicapai daripada kajian , pemodelan empirikal telah menarik perhatian yang besar dalam penyelidikan. Pelbagai jenis algoritma telah digunakan dalam pemodelan sistem ini untuk mencapai ketepatan yang tinggi dalam meramal kecekapan dan mengawal sistem.

Model terbaru menyediakan ketepatan tinggi dengan menggunakan sistem yang kompleks dan pengiraan yang rumit menggunakan algoritma pengoptimuman paling maju. Walau bagaimanapun, mereka bentuk model dinamik yang tepat untuk meramal dan mengawal sistem ini dalam keadaan masa sebenar adalah mencabar untuk bidang ini. Dengan menggunakan keadaan seni algoritma pengkomputeran lembut dalam pemodelan sistem teknikal untuk mengurangkan kerumitan model rangkaian neural tiruan

mempunyai impak yang besar dalam bidang ini. Kajian ini mempunyai objektif berganda dan bertujuan untuk mereka bentuk model untuk sebuah sistem sel bahan api membran pertukaran proton berkuasa 250W yang digunakan sebagai loji kuasa dalam basikal elektrik. Sebagai algoritma yang paling popular dan tepat, regresi linear klasik dan rangkaian neural tiruan telah dioptimumkan dan digunakan untuk model sistem ini. Di samping itu, buat kali pertama peta kognitif kabur telah digunakan dalam pemodelan sistem sel bahan api PEM dan bertujuan untuk menyediakan peta kognitif dinamik dari faktor keberkesanan sistem. Pengawalan dan pengubahsuaian prestasi sistem dalam pelbagai keadaan adalah lebih praktikal dengan korelasi antara faktor prestasi sel bahan api PEM hasil daripada peta kognitif kabur. Selain itu, maklumat daripada pemodelan peta kognitif kabur boleh digunakan untuk pengubahsuaian struktur rangkaian neural untuk memberikan hasil yang lebih tepat berdasarkan pengetahuan yang diekstrak dari peta kognitif dan visualisasi prestasi sistem.

ACKNOWLEDGMENT

I would like to express my special appreciation and thanks to my advisor Dr. Mahidzal Dahari for the continuous support of my Ph.D study and related research, for his patience, motivation, and his guidance and help during the time of my research. I could not have imagined having a better advisor and mentor for my PhD study.

I would like to extend my thanks to my dear friend, Dr. Farid Motlagh for his selfless support and professional research attitude that influenced me throughout my whole graduate study. Besides, I would also like to thank my best friend, Assoc. Prof Niusha Shafiabady for her kind support, guidance and her contributions to this research are greatly appreciated. I would like to take this opportunity to express my appreciation for my lovely friends: Sepideh Yazdani and Ali Askari and my beloved Jaana, for standing beside me throughout this entire journey and providing their help and support in many different ways.

A special thanks to my family for supporting me spiritually throughout writing this thesis and my life in general. Words cannot express how grateful I am to my mother, Azar Danesh, father, Reza Kheirandish, brother Mahyar and sister Mahsa for all of the sacrifices that you've made on my behalf. Your prayer for me was the reason that has sustained me this far. I would also like to thank all of my friends who supported me in writing, and invited me to strive towards my goal.

Azadeh Kheirandish

TABLE OF CONTENTS

LIST OF FIGURE

LIST OF TABLES

LIST OF SYMBOLS AND ABBREVIATIONS

Symbols

H_2	Hydrogen
e	Electron
O_2	Oxygen
H_2O	Water
OH^-	Hydroxide
CO_2	Carbon
CH_3OH	Methanol
$co_3^=$	Carbonate
V_{oper}	Operation voltage
η_{fc}	Fuel cell efficiency
n	Number of cells
$\eta_{fcsystem}$	Efficiency of system
$\Delta \boldsymbol{p}$	Pressure drop
V	volume (L) of an electrolyzer buffer tank
T	Temperature (K)
n	Number of random sample

x	Sample data with mean $\bar{X}$
S	Standard deviation
z-score	Standardization of data
x	Explanatory variable
$h\theta(x)$	Predicted value (hypothesis)
θ_0	Intercepts
θ	Estimated slope coefficient of the line
ε	Error term
y	Real value
h	Predicted value
MSE	Mean of the squares
$J(\theta)$	Cost function
m	Number of iterations
α	Learning rate value
θ	System weights
w_{kj}	Synaptic weights
x_m	Input
k	Neuron
u_k	Linear combiner outputs

b_k	Bias
v_k	Activation potential
$\varphi(.)$	Activation function
$F(x)$	Sum of square error
x	weights matrix and bias
$H(x)$	Hessian matrix
(x)	Vector of network error
$J(x)$	Jacobian matrix
$C_j(t)$	Activation degree of concept j^{th} at moment t
e_{ij}	Relationship strength from concept C_i to concept C_j
c	Real positive number
x	Value $C_j(t)$
C_i	Current activation of concept i^{th}
C_i	Current activation of concept j^{th}
$e_{ij}(k)$	Value of the weights between concepts $i^{th}\ and\ j^{th}$
η	Learning coefficient
$C(0)$	Value of concepts
$E(0)$	Connection matrix
W_{FINAL}	Final connection matrix

T_j	Mean target value of the concept C_j
e_{max}	Maximum difference
d_{ij}	Value of i^{th} concept at the j^{th} time point
K	Number of available data points
N	Number of concepts in modeled system
A	Simulated data vector for every output parameter
T	Real experimental value
N	Sample number
$DC_i^{estimated}$	Estimated and of decision concepts (DC)
DC_i^{real}	Real value decision concepts (DC)
K	Number of available iterations

ABBREVIATIONS

ICE	Internal combustion engine
AFC	Alkaline fuel cell
DMFC	Direct methanol fuel cell
SOFC	Solid oxide fuel cell
MCFC	Molten carbonate fuel cell
PAFC	Phosphoric acid fuel cell
PEMFC	Proton exchange membrane fuel cell
ANFIS	Adaptive neuro fuzzy inference system
ANN	Artificial neural network
LR	Linear regression
FCM	Fuzzy cognitive map
DAQ	Data acquisition
LHV	Lower heating value
DD-NHL	Data driven nonlinear Hebbian learning
RB-FCM	Rule-based FCM
LMBP	Levenberg-Marquardt back propagation
FCV	Fuel cell vehicle

GDL	Gas diffusion layer
GA	Genetic algorithm
BP	Back propagation
RBF	Radial basis function
NLP	Non-linear programming
MPC	Model predicted control
MBDO	Metamodel-Based Design Optimization
EPSO	Enhanced particle swarm optimization
IT	Information technology
DCNs	Dynamic Cognitive Networks
FGCMs	Fuzzy Gray Cognitive Maps
IFCMs	Intuitionistic Fuzzy Cognitive Maps
DRFCMs	Dynamic Random Fuzzy Cognitive Maps
E-FCMs	Evolutionary Fuzzy Cognitive Maps
FTCMs	Fuzzy Time Cognitive Map
RCMs	Rough Cognitive Maps
TAFCMs	Timed Automata-based fuzzy cognitive maps
BDD-FCMs	Belief-Degree Distributed Fuzzy Cognitive Maps
RBFCMs	Rule Based Fuzzy Cognitive Maps

FCN	Fuzzy Cognitive Network
DHL	Differential Hebbian Learning
BDA	Balanced Differential Algorithm
NHL	Nonlinear Hebbian Learning
AHL	Active Hebbian Learning
ES	Evolutionary Strategies
GA	Genetic Algorithms
RCGA	Real Coded Generic Algorithms
SI	Swarm Intelligence
Mas	Memetic Algorithms
SA	Simulated Annealing
CSA	Chaotic Simulated Annealing
TS	Tabu Search
ACO	Ant Colony Optimization
EGDA	Extended Great Deluge Algorithm
BB-BC	Bing Bang-Big Crunch
SOMA	Self-Organizing Migration Algorithms
IA	Immune Algorithms
NHL-DE	Hebbian learning algorithm and Differential Evolution algorithm

NHL-EGDA	Nonlinear Hebbian Learning algorithm and Extended Great Deluge Algorithm
NHL-RCGA	real-coded genetic algorithm and nonlinear Hebbian learning algorithm
ECU	Electronic Control Unit
HHV	Higher heating value
R	Ideal gas constant
RH	Related humidity
I	Current
qO_2	Oxygen flow rate
T	Temperature
qH_2	Hydrogen flow rate
V_{fc}	Fuel cell voltage
Eff	Efficiency
PCA	Principle component analysis
GD	Gradient Descent
m	Number of measurements
n	Number of trails
W_{ij}	Weights
DOC	Desired Output Concepts

mbf	Membership functions
μ_{nvs}	Membership function negatively very strong
μ_{ns}	Membership function negatively very strong
μ_{nm}	Membership function negatively medium
μ_{nw}	Membership function negatively weak
μ_{z}	Membership function zero
μ_{pw}	Membership function positively weak
μ_{pm}	Membership function positively medium
μ_{ps}	Membership function positively strong
μ_{pvs}	Membership function positively very strong
DC	Decision concepts

LIST OF APPENDICES

Chapter 1 : INTRODUCTION

1.1 Background of study

Fossil fuel depletion has created environmental problems such as pollution, climate change and global warning. However, the largest fields of oil have been discovered and production is clearly past its peak. Factors such as awareness of the health problems related to high air pollution levels and dwindling oil fuel reserves have increased interest in the replacement of internal combustion engine (ICE) vehicles. However, considerable problems regarding health and environment are the result of the use of too many vehicles worldwide, and for the sake of the health of the environment and humanity, decreasing the use of fossil energy sources with the aim of zero emission vehicles is helpful.

In vehicle industry, the major distinguished achievement is development of the internal combustion engine vehicle (Brandon & Hommann, 1996; Chen, Hsaio, & Wu, 1992). To date, several automobile companies and research organizations regarding the future generation of vehicles have focused on the production of hybrid vehicle technology for enhancement of fuel economy, increased efficiency and controlled emission (Faiz, Weaver, & Walsh, 1996; Kammen, 2002). Among the development of new energy technologies fuel cells with sufficient efficiency and low emission are considered one of the most promising vehicular power sources (Kordesch & Simader, 1996).

Figure 1.1 shows the theoretical voltage-current (V-I) curve of fuel cell for considering how the fuel cell voltage varies with output current, and it also display cause of voltage drop. Another important curve for developing the control strategy and drivetrain topology for electric vehicle power by fuel cell is efficiency versus power.

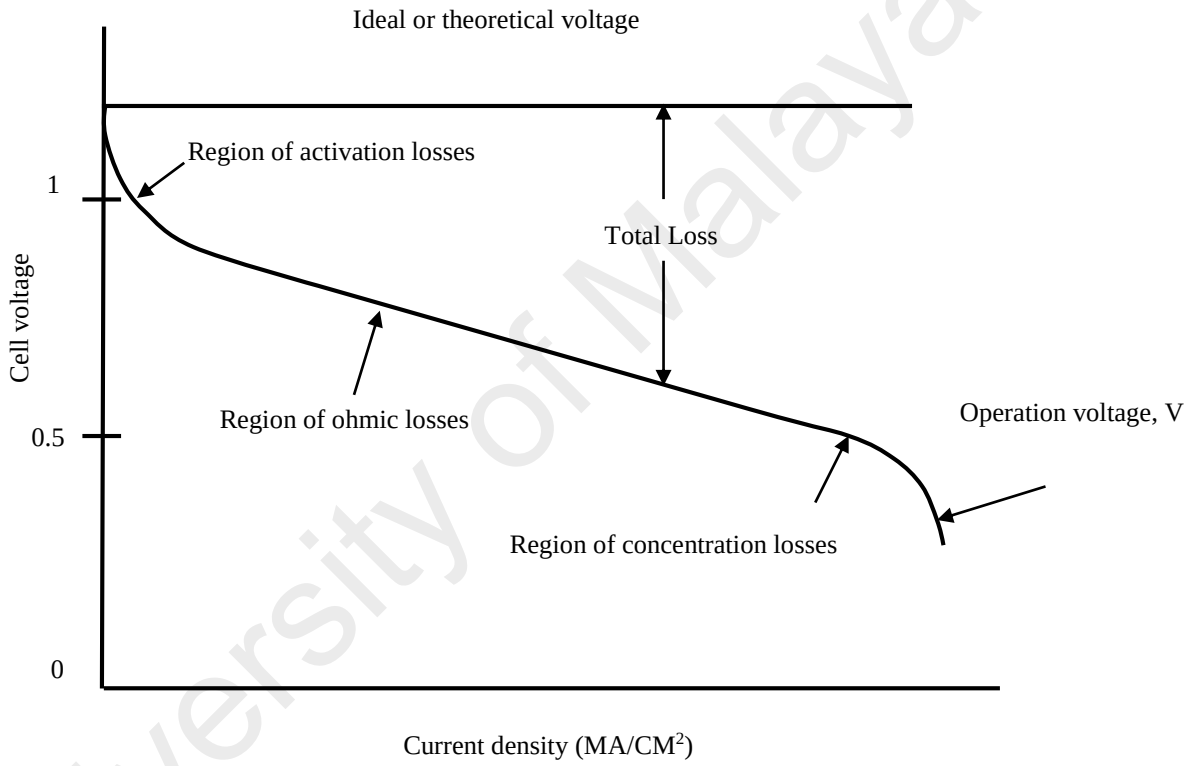

Figure 1.1: Ideal voltage versus current curve for fuel cell

Fuel cell powered electric vehicles have been considered a solution to the inherent issue of long charge and short range time of electric vehicles compared to traditional batteries. Fuel cells, discovered by British physicist William R Grove in 1839 (Blomen & Mugerwa, 2013) are electrochemical energy conversion devices which generate electricity by mixing hydrogen and oxygen in electrolyte. Fuel cells generate power with low emission, high efficiency and quiet operation compared to conventional power

generator. Fuel cells are categorized into six variable types based on their electrolyte type including:

1) Alkaline fuel cell (AFC) with a wide range of operation temperatures and are suitable to use in spacecraft (McLean, Niet, Prince-Richard, & Djilali, 2002).

2) Direct methanol fuel cell (DMFC), a rare commonly used fuel cell which operates at high temperature (Hamnett, 1997).

3) Solid oxide fuel cell (SOFC) with a high temperature threshold between 600 and 1000℃ (Hammou & Guindet, 1997).

4) Molten carbonate fuel cell (MCFC) to perform only at temperatures higher than 650℃ (Dicks, 2004).

5) Phosphoric acid fuel cell (PAFC) with operating temperature of 150-200℃ and is utilized in both stationary power and mobile applications, such as large vehicles (Bagotsky, 2012).

6) Proton exchange membrane fuel cell (PEMFC) with a lower operating temperature, which renders the fuel cell viable for both portable and stationary applications (Vishnyakov, 2006).

Power capacity of fuel cells are categorized according to their application including portable power, stationary, residential, and transportation. Proton exchange membrane fuel cell (PEMFC) is the most demanded type of fuel cell in popular technology due to its simplicity, solid membrane, quiet operation and low temperature operating range. In this project, PEM fuel cell has been used to run an electric bicycle. Chemical reactions of PEM fuel cells are as follows:

Anode side: $$2H_2 \rightarrow 4H^+ + 4e^-$$ (1-1)

Cathode side: $$O_2 + 4H^+ + 4e^- \rightarrow 2H_2O$$ (1-2)

Net reaction: $$2H_2 + O_2 \rightarrow 2H_2O$$ (1-3)

Modelling plays a significant role in research projects by allowing investigation of critical situations without presenting any real-life danger, which results in a better evaluation of system. For accurate modeling and to define better efficiency of system, PEM fuel cell modeling is required to draw the pattern for critical parameters. Several models have been developed to improve the design and operation of fuel cells, especially PEM fuel cell (Baschuk & Li, 2005; Ceraolo, Miulli, & Pozio, 2003; Contreras, Posso, & Guervos, 2010; Gong & Cai, 2014; Haji, 2011; Meidanshahi & Karimi, 2012; Oezbek, Wang, Marx, & Soeffker, 2013; Rowe & Li, 2001; Tiss, Chouikh, & Guizani, 2013), based on theoretical and empirical modeling. *Theoretical* modeling involves solving differential equations or integration or both to determine the PEM fuel cell performance from various physical parameters. *Empirical* modeling predicts a model by using experimental data without determining the process parameters in detail (Napoli, Ferraro, Sergi, Brunaccini, & Antonucci, 2013).

Since PEM fuel cell is a complex nonlinear system with multi-variables, optimizing model parameters for design improvement and performance enhancement using analytical models is challenging. Mathematical nature of theoretical models make them more complicated than empirical models (Ismail, Ingham, Hughes, Ma, & Pourkashanian, 2014; Jang, Cheng, Liao, Huang, & Tsai, 2012). Therefore, advanced algorithms are suggested to be developed in order to reduce the essential computational effort (Gong & Cai, 2014; Samsun et al., 2014). Soft computing techniques and machine

learning algorithms are reliable mediums to employ in empirical modeling for a more efficient prediction of affecting parameters on voltage–current (V–I) curve of fuel cell (Boscaino, Miceli, & Capponi, 2013).

In recent years, active empirical modelling techniques based on machine learning theory defined as adaptive neuro fuzzy inference system (ANFIS) (Rezazadeh, Mehrabi, Pashaee, & Mirzaee, 2012; Silva et al., 2014; Vural, Ingham, & Pourkashanian, 2009), support vector machine (SVM) (Q. Li, Chen, Liu, Guo, & Huang, 2014; Zhong, Zhu, & Cao, 2006; Zhong, Zhu, Cao, & Shi, 2007), and artificial neural network (ANN) which is a powerful tool for modelling the performance of PEM fuel cell (Jemeı, Hissel, Péra, & Kauffmann, 2003; Lee, Park, Yang, Yoon, & Kim, 2004; Ogaji, Singh, Pilidis, & Diacakis, 2006; S. Ou & L. E. Achenie, 2005) have been developed. The advantage of these models over theoretical model is that they are much simpler, enabling quick prediction and requiring less computational time.

Researches in this field aim to propose methods to predict the PEM fuel cell performance and to compare it with experimental data to indicate the accuracy of the model. Most of these studies applied algorithm to decrease the error in models. Furthermore, some researchers have proposed a control technology for optimal control of the system response (J. Hasikos, H. Sarimveis, P. Zervas, & N. Markatos, 2009; Jemeï, Hissel, Péra, & Kauffmann, 2008; J.-M. Miao, Cheng, & Wu, 2011; Sachin V Puranik, Ali Keyhani, & Farshad Khorrami, 2010; Wu, Shiah, & Yu, 2009). The focus of these models is on the design of PEM fuel cell rather than its application.

1.2 Problem statement

Recent development in fuel cell efficiency and performance is based on single cell or fuel cell while computing the whole system efficiency plays significant role to improve the performance and efficiency of the system. Despite a number of limitations of PEM fuel cell like high production cost of hydrogen, essential features such as zero emission, high efficiency and low operating temperature, fast start-up, make PEM fuel cells ideal for transportation. There is considerable difference between the actual and ideal efficiency of systems that their internal components are not changeable; therefore, controlling these system to operate in an optimized condition is challenging. In addition, both empirical and theoretical models of PEM fuel cell have been aimed to improve the design and operation of fuel cells, but this cannot be achieved without providing an accurate and reliable model of the system. Although there have been numerous fuel cell stack models in order to benefit from its design (Buchholz & Krebs, 2007; Hu, Cao, Zhu, & Li, 2010; Kong & Khambadkone, 2009; Kong, Yeau, & Khambadkone, 2006; Rouss et al., 2008; Zhang, Pan, & Quan, 2008), there has been few models for the whole PEM fuel cell system (Ahmed M Azmy & István Erlich, 2005; Jemeı et al., 2003; Jemeï et al., 2008).

Simulation model of whole fuel cell system in electric vehicle is essential to adjust the optimization ability of complete vehicle with auxiliary component. Therefore, the problem statement can be stated as developing a dynamic model for fuel cell system in electric bicycle with the ability to predict each variable of PEM fuel cell and the efficiency of whole system, providing a cognitive map from the PEM fuel cell with a linguistic relationship between variables to be used for control and real-time processing applications.

1.3 Objectives

Cognitive map can be used to evaluate the performance of PEMFC system and enable it to be used for controlling all variables in order to increase the efficiency .The main goal of this study is dynamic modelling of the PEM fuel cell performance in electric bicycle. The objectives of this study are as follows:

1- To define an accurate relation between efficiency and power density of system during different operation conditions based on experimental data.

2- To design a linear regression model for predicting output voltage and system efficiency based on (temperature, related humidity, current, hydrogen/oxygen flow rate).

3- To improve and optimize the PEM fuel cell empirical model using artificial neural networks.

4- To develop a fuzzy cognitive map (FCM) of PEM fuel cell variables and to provide the causality of these variables on each other for real-time control applications.

1.4 Methodology

The data has been collected from data acquisition (DAQ). Values of (temperature, related humidity, current, hydrogen/oxygen flow rate and voltage) were recorded from the PEM fuel cell system. With reference to the problem statement and objectives of this study, methodology is illustrated in separate phases. First phase of the study aims to define an accurate relation between efficiency and power density of system during different operation conditions based on experimental data. Fuel cell efficiency was calculated by using fuel cell's stack operating voltage (V_{oper}) versus hydrogen's lower heating value (LHV) equation. Since in the PEM fuel cell single cells are connected in series, the efficiency of single cell and fuel cell stack are equal. The whole system's efficiency has been computed using generated electric bicycle energy versus energy of consumed H_2. A detailed description of equations can be found in chapter 3.

In the second phase of the study, various models of PEM fuel cell were presented for better understanding of fuel cell system behavior and operation process. Both linear and non-linear models were used for modelling the PEM fuel cell electric bicycle: 1) linear regression model and 2) artificial neural network model and comparison of these two models for better performance estimation of PEM fuel cell system. These models were designed based on available variables including load current, temperature, related humidity, and hydrogen/oxygen flow rate as inputs with load voltage and system efficiency as output variables. Each of these models have been optimized in order to minimize the cost function of models and represent optimal value of decision variables to provide an accurate prediction of outputs.

Since using classical control theories to design a controller for system could compromise the efficiency of the system, in the final phase of this study a dynamic model was used to predict the system status based on the causality relations among PEM fuel

cell variables. Fuzzy cognitive map (FCM) was used for the first time as a convenient and powerful tool for dynamic system modelling based on experimental data. FCM is a combination of fuzzy logic and neural network through strategy of relation between all factors. Data driven nonlinear Hebbian learning method (DD-NHL) was used as a state of the art algorithm to design the cognitive map of PEMFC. FCM has been trained by the collected data to generate accurate causality relations between variables. The causality relations in this model were converted into fuzzy concepts in order to provide a rule-based FCM (RB-FCM). The main advantage of RBFCM is the flexibility of the model for providing an accurate dynamic model of the system for real-time control applications.

1.5 Scope of the study

In this study, a 25-Kg electric assisted bicycle special VRLA-battery 6-DZM-10 12V 10Ah is used to determine the overall efficiency of the system by using experimental data. The data collection is performed on a stationary bicycle while the tire could spin freely on traditional Kickstand. For this experiment, we attempted to keep the bicycle at the cruise condition (constant speed) with a fuel cell power average of 35.29 W, and fuel cell stack efficiency average of 48.45%. Parameters in the condition of this test are obtained in ambient temperature range 0℃ up to 35 ℃ and ambient relative humidity range of 30-80%.

The linear model was designed based on gradient descent algorithm and ANN was trained using Levenberg-Marquardt back propagation (LMBP) algorithm. Validation data was used to plot learning curve and error analysis for optimizing the models variables and structure. The RBFCM was used only for dynamic modeling of the system variables. However, due to the limited accessibility to inner auxiliaries and parameters of bicycle

and PEMFC, real-time control of the system input parameters was not feasible. However, the final design of RBFCM was accurate for dynamic training and prediction of system status to be used for controllers.

1.6 Outline of study

This thesis has been organized into five chapters.

Chapter 1 (present chapter) outlines brief introduction of the research area starting with the fuel cell general overview, problem statement, objective, methodology, and scope of the study. This chapter presents a general viewpoint to enable the reader to understand what has been done in this project.

Chapter 2 provides a background about type of fuel cells and their application in detail. This is followed by a discussion of the types of PEM fuel cell models and a brief review of linear regression model and artificial neural network models as effective methods to give a general idea of these empirical model approaches. The fuzzy cognitive map and its application have been also introduced in this section.

Chapter 3 describes the methodology employed in the current study including details of how data has been collected from bicycle and how the overall efficiency of system was calculated. The proposed procedure to model PEM fuel cell system is provided step by step and investigated to find optimal parameters to obtain more accurate and faster modelling. The fuzzy cognitive map was trained by using state of art Non-linear Hebbian learning algorithm which has been elaborated in detail in chapter 3.

Chapter 4 presented the result and discussion of implementation of calculated overall efficiency, linear regression and neural network prediction and fuzzy cognitive map model.

Chapter 5 provides the conclusion of this thesis and recommendations for future work.

Chapter 2 : LITERATURE REVIEW

2.1 Introduction

Over the past three decades, the major environmental issue in many countries around the world has been the global warming, lead to a dramatic increase in electrical energy demand. Many researchers have presented an alternative energy converter at an affordable price. These converters are generally eco-friendly (Purkrushpan & Peng, 2004)

During the past decade, research and development of electric vehicles have attracted significant attention due to various concerns such as reducing emission and air pollution from the combustion of fossil fuels. This kind of promising technology has minimum emission, significant improvement in fuel economy and higher efficiency than today's internal combustion engines (Kammen, 2002).

Currently, many researchers are working to produce clean electrical energy for future generation vehicles. One of the major challenges has been the inherent limitation of short range and long charge time historically related to electric power vehicles. The ideal solution compared to traditional battery power electric vehicles is fuel cell powered hybrid vehicles. The main focus of hybrid vehicles is electric cars and buses in developing countries because of air pollution, and smaller vehicles are widely used for transportation and utility purposes (Dockery et al., 1993). Z Qi (2009) (Garche et al., 2013) demonstrated various vehicular applications, such as bicycles, wheelchairs, forklifts, and scooters, that utilize PEM fuel cells instead of batteries.

Addressing all these issues surrounding the internal combustion engine vehicles and replacing these with low-emission, renewable fuel and high energy efficiency, the

good choice currently is hydrogen fuel cell vehicle (FCVs) which provides the chance for the consumer to be a both user and producer of energy (Rifkin, 2003). The background of fuel cell vehicles and the remaining issues for getting these vehicles on the road are discussed in section 2.3.

2.2 Background of the Study

2.2.1 Fuel Cell

A fuel cell is a device that releases a considerable amount of power in the form of electrical currents as hydrogen and oxygen atoms undergo an electrochemical reaction, the by-product of which is water molecules (F. Barbir & Gomez, 1997). A fuel cell is similar to battery in convert of chemical energy to electric energy; however, one distinct difference between them is that fuel cells continue to operate as long as fuel and air are supplied and there is no need to recharge. Sir William Grove invented the fuel cell in 1839 based on C.F Schoenbein's idea as he observed the fuel cell effect; Grove saw the capability of combining oxygen and hydrogen to make water (Bossel, Schönbein, & Grove, 2000)

Currently, fuel cells are categorized into six different types based on their electrolyte material, fuel diversity and operating temperature that make them suitable for different applications. The following sections briefly presented the main types of fuel cells and section 2.1.1.6 provides more details the of proton exchange membrane fuel cell (PEMFC).

2.2.1.1 Alkaline Fuel Cell (AFC)

Alkaline fuel cells (AFC) demonstrated by Francis Bacon in 1930 are one of most popular fuel cells developed to power NASA's Apollo space program. They contain an alkaline solution derived from an alkaline electrolyte. They can operate over a wide range of temperatures that depend on the fuel cell application, which constitutes the main advantage of these fuel cells over the other types. However, the significant technical disadvantage of this type of fuel cell is the carbon dioxide poisoning of the electrolyte. They react with hydrogen at the anode, releasing four electrons and producing water:

At anode: $$2H_2 + 4OH^- \rightarrow 4H_2O + 4e^-$$ (2-1)

Electrons react with oxygen and water at the cathode and produce new OH:

At cathode: $$O_2 + 4e^- + 2H_2O \rightarrow 4OH^-$$ (2-2)

For continuous reaction, the mobile ion OH^- should pass through the electrolyte, and for electrons to go from anode to cathode, there must be an electrical circuit (Lin, Kirk, & Thorpe, 2006). Figure 2.1 displays the principle of alkaline fuel cell.

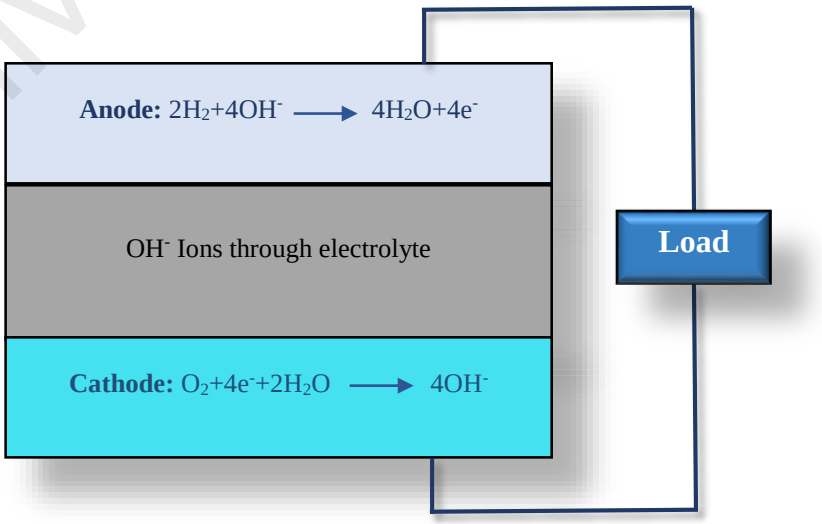

Figure 2.1: Alkaline fuel cell principle

2.2.1.2 Direct Methanol Fuel Cell (DMFC)

Direct methanol fuel cell was discovered by Dr. Surya Prakash and Dr. George A. Olah in 1990, and is the only fuel cell that consumes methanol for fuel instead of hydrogen. The utilization of these fuel cells is limited to applications in which the efficiency is superseded by the power density in terms of importance. Hence, the utilization of DMFCs is not as common as that of other fuel cells. Methanol is mixed with water at the anode and the mobile ion is H+ passes through the electrolyte and six electrons are released and transferred from anode to cathode:

At the anode: $$CH_3OH + H_2O \rightarrow 6H^+ + 6e^- + CO_2 \quad (2\text{-}3)$$

Electrons react with oxygen and hydrogen at the cathode and produce water:

At the cathode: $$\frac{3}{2}O_2 + 6H^+ + 6e^- \rightarrow 3H_2O \quad (2\text{-}4)$$

Overall reaction: $$CH_3OH + \frac{3}{2}O_2 \rightarrow 2H_2O + CO_2 \quad (2\text{-}5)$$

The issue about DMFC is that CO_2 is produced as a byproduct and the reaction at the anode is slow and provides less power(Frano Barbir, 2012). Figure 2.2 shows the principle of direct methanol fuel cell.

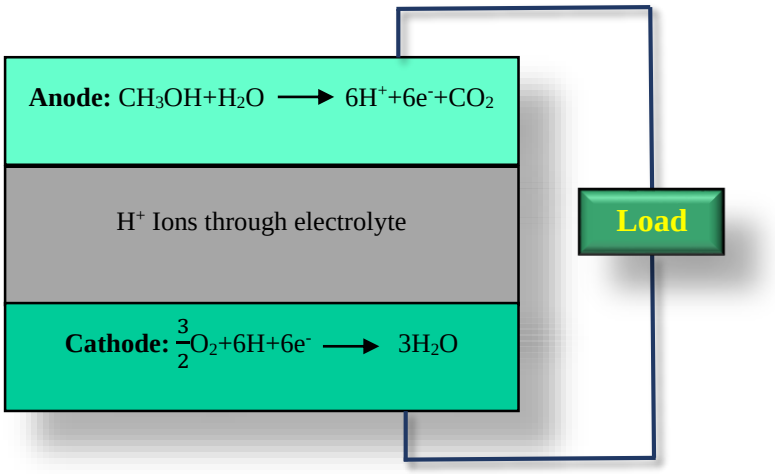

Figure 2.2: Direct methanol fuel cell principle

2.2.1.3 Solid Oxide Fuel Cell (SOFC)

Solid Oxide fuel cells (SOFC) are another type of fuel cell that was discovered by Walther Hermann Nernst, one of the earliest researchers of SOFC, in 1899. A high temperature threshold between 600 and 1000℃ constitutes the main concern for the utilization of SOFC in vehicles. SOFC contains a solid oxide or ceramic as the electrolyte to conduct the oxygen ions. Oxygen ion and hydrogen oxidation at the anode and produce water and electron:

At the anode: $$H_2 + O^{=} \rightarrow \mathrm{H_2O} + 2\mathrm{e}^{-} \quad (2\text{-}6)$$

At the cathode, oxygen reacts with electrons and produces oxygen ion:

At the cathode: $$\frac{1}{2}\mathrm{O_2} + 2\mathrm{e}^{-} \rightarrow O^{=} \quad (2\text{-}7)$$

Overall reaction: $$\frac{1}{2}\mathrm{O_2} + H_2 \rightarrow \mathrm{H_2O} \quad (2\text{-}8)$$

Hydrogen and carbon monoxide are two major fuels of solid oxide fuel cell (Fuerte, Valenzuela, & Daza, 2007). Figure 2.3 displays the principle of solid oxide fuel cell.

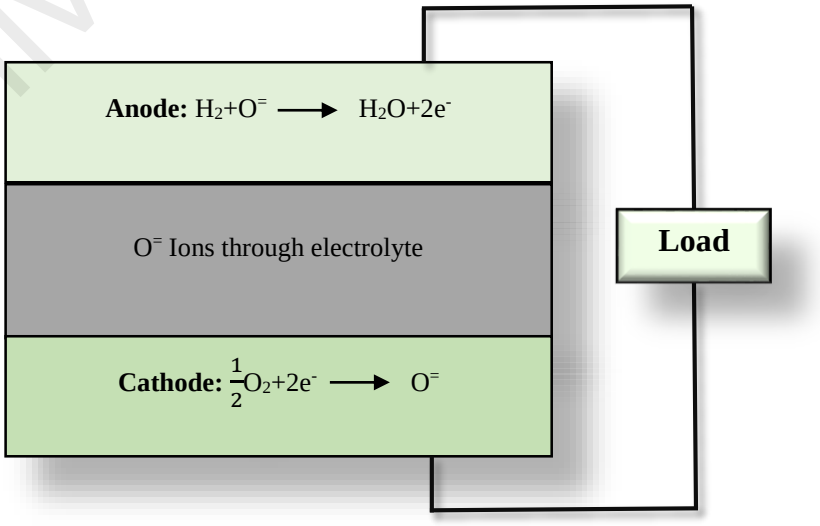

Figure 2.3: Solid oxide fuel cell principle

2.2.1.4 Molten Carbonate Fuel Cells (MCFC)

Molten carbonate fuel cell (MCFCs) was built by Erwin Baur in 1921 based on a mixture of molten salts that act as an electrolyte. These fuel cells can perform only at temperatures that are higher than 650℃. Carbonate and hydrogen react at the anode side and produce water and $CO_2$and electron:

At the anode: $H_2 + co_3^{=} \rightarrow \mathrm{H_2O} + \mathrm{CO_2} + 2\mathrm{e}^-$ (2-9)

Oxygen and by carbon dioxide react with electrons at the anode and produce carbonate anions.

At the cathode: $\frac{1}{2}\mathrm{O_2} + \mathrm{CO_2} + 2\mathrm{e}^- \rightarrow co_3^{=}$ (2-10)

The exothermic overall reaction is:

Overall reaction: $H_2 + \frac{1}{2}\mathrm{O_2} + \mathrm{CO_2} \rightarrow \mathrm{H_2O} + \mathrm{CO_2}$ (2-11)

To complete the circuit carbonate anions pass from the cathode to anode through the molten electrolyte. During oxygen reduction, carbon dioxide is passed to the cathode for use (Bischoff & Huppmann, 2002). Figure 2.4 shows the principle of molten carbonate fuel cell.

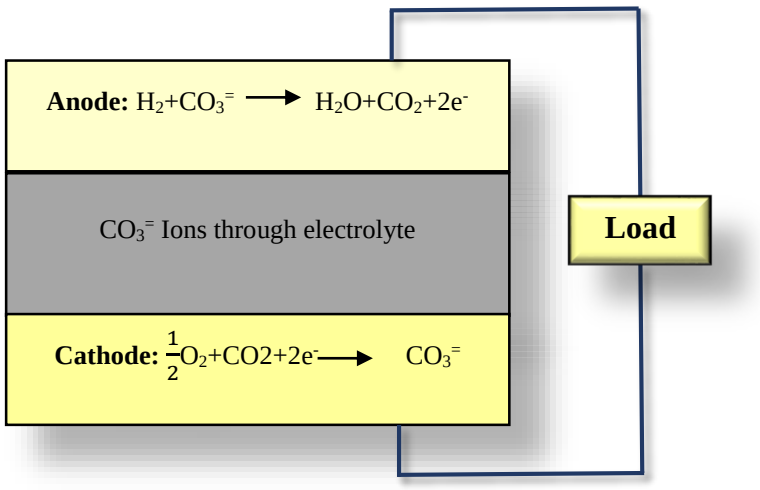

Figure 2.4: Molten carbonate fuel cell principle

2.2.1.5 Phosphoric Acid Fuel Cell (PAFC)

Phosphoric acid fuel cell (PAFCs) was developed by G. V. Elmore and H. A. Tanner in 1961 and uses liquid phosphoric acid as an electrolyte. The operating temperature of these devices is approximately (150-200)℃ . PAFCs are used in both stationary power and mobile applications such as large vehicles. The pre-heating requirements and its open-ended structure which requires the careful control of hydrogen flow are some of its drawbacks. Pure hydrogen at the anode breaks into hydrogen ion and produces four electrons.

At the anode: $2H_2 \rightarrow 4\mathrm{H}^+ + 4\mathrm{e}^-$ (2-12)

Hydrogen ions and oxygen and electrons at the cathode produce water, and electrons pass through the external circuit from anode to cathode.

At the cathode: $\mathrm{O}_2 + 4\mathrm{H}^+ + 4\mathrm{e}^- \rightarrow 2\mathrm{H}_2\mathrm{O}$ (2-13)

Overall reaction: $2H_2 + \mathrm{O}_2 \rightarrow 2\mathrm{H}_2\mathrm{O}$ (2-14)

The output is very low at the anode due to pure hydrogen and using Carbon monoxide in fuel increases it (Kasahara, Morioka, Yoshida, & Shingai, 2000). Figure 2.5 displays the principle of phosphoric acid fuel cell.

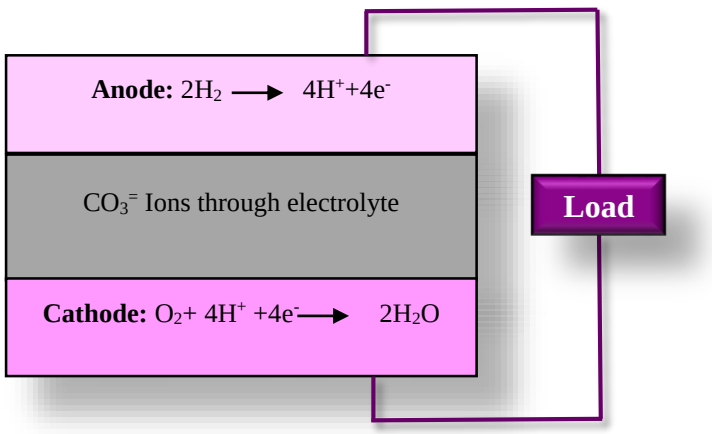

Figure 2.5: Phosphoric acid fuel cell

2.2.1.6 Proton Exchange Membrane Fuel Cells (PEMFC)

Proton exchange membrane fuel cell was invented by Willard Thomas Grubb and Leonard Niedrach of General Electric in the early 1960s. Some issues that accrued in fuel cells are removed; i.e. the requirement for expensive material, application in extreme conditions and it is one of the most promising systems that can be used for stationary application due to their size. In recent years, the high efficiency of PEMFCs has provided impressive capabilities for the transportation sector. Low temperature, high efficiency, silence and simplicity are distinguishing features that set PEMFCs apart from other fuel cells and allow PEM fuel cell to be operated in any orientation and easy start-up (Kheirandish, Kazemi, & Dahari, 2014).

Polymer membrane, catalyst layer, gas diffusion layer, and bipolar plate are the main components of PEM fuel cells. Polymer membrane located on the center of the fuel cell, separates the anode and cathode and hydrogen ions that pass through it. Hydrogen oxidation and oxygen reduction react on catalyst layer at anode and cathode respectively. Gas diffusion layer (GDL) is after catalyst layer at anode and cathode. These three layers are called membrane electrode assembly. The MEA is plated between bipolar plate that is commonly made of graphite (Larminie, 2003; Liu & Case, 2006). Figure 2.6 shows the structure of polymer electrolyte membrane.

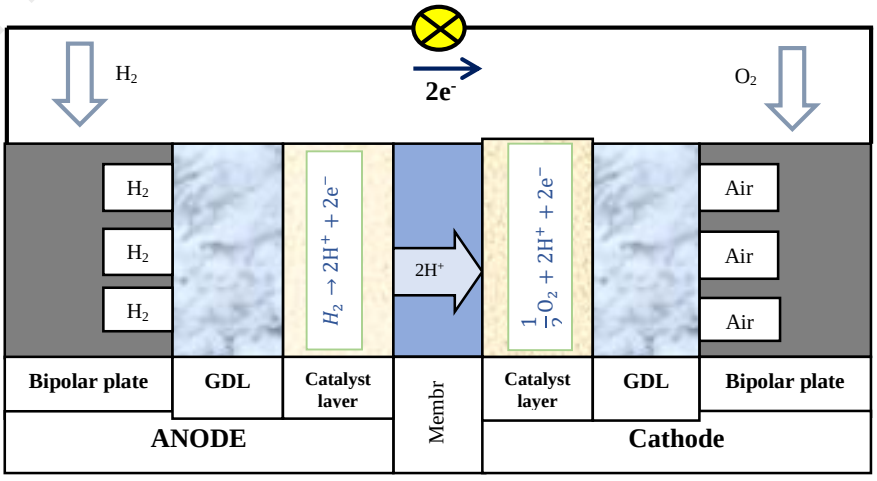

Figure 2.6: The structure of proton electrolyte membrane

Similar to other types of fuel cells, PEMs also consists of three significant parts: a cathode and an anode that act as electrolytes formed by platinum-catalysis and the membrane(Cook, 2002). In a PEM fuel cell reflex, the hydrogen oxidation and oxygen reduction reactions occur simultaneously at the anode and cathode (Asl, Rowshanzamir, & Eikani, 2010). Figure 2.7 shows the single cell of a fuel cell.

At the anode, the stream of hydrogen molecules are disarticulated into protons and electrons as follows:

At the anode: $H_2 \rightarrow 2\mathrm{H}^+ + 2\mathrm{e}^-$ (2-15)

Electrons are released from hydrogen and move along the external load circuit to the cathode; therefore, the flow of electrons creates the electrical output current. The electron arriving at the cathode from the external circuit concurrently reacts with oxygen molecules that are joined with a platinum catalyst of electrode and two protons (which have moved through the membrane) to create water molecules; this reduction is represented as follows:

At the cathode: $\frac{1}{2}\mathrm{O}_2 + 2\mathrm{H}^+ + 2\mathrm{e}^- \rightarrow \mathrm{H}_2\mathrm{O}$ (2-16)

Overall reaction: $H_2 + \frac{1}{2}\mathrm{O}_2 \rightarrow \mathrm{H}_2\mathrm{O}$ (2-17)

The chemical reaction is now complete. Despite the reaction, a portion of the energy is expended in the form of heat released from the respective redox reaction as a byproduct.

The typical single cell voltage produces 0.5-0.7 V under load condition to have maximum power. The single cells must be connected in series to create adequate electricity.

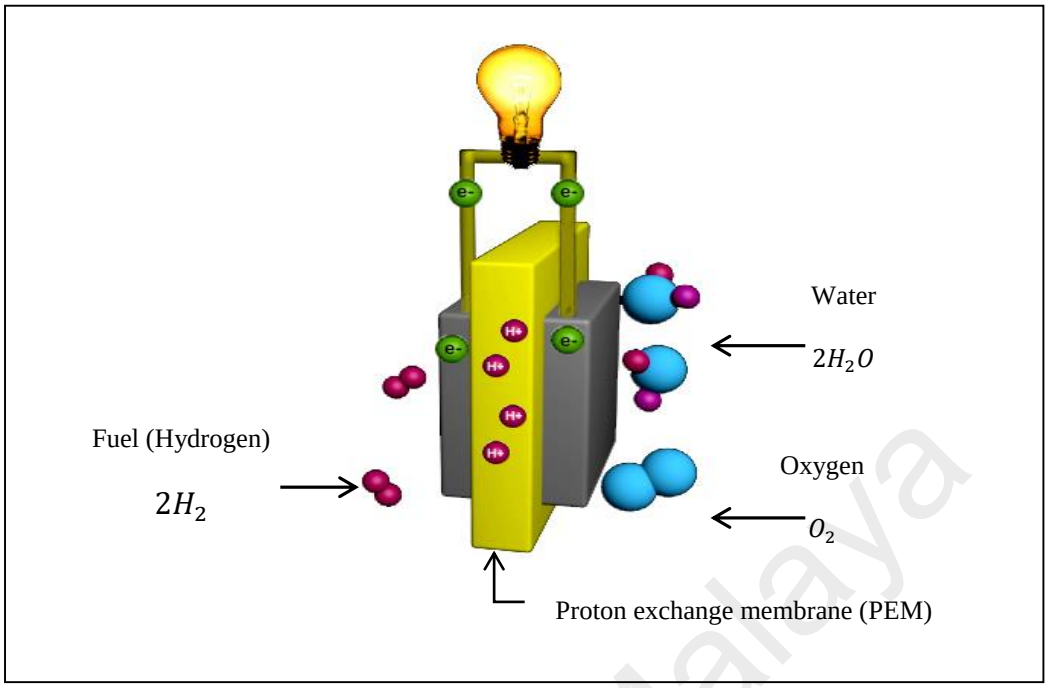

Figure 2.7: Schematic of reaction in PEMFC's single cell

PEM fuel cells are used in many applications without geographical restrictions, and their superior efficiency is being capitalized on in automobiles [for more detailed information see: (Baschuk & Li, 2000; Marr & Li, 1999)]. Using a proton conductive polymer membrane as an electrolyte leads to lower operating temperatures, which render the fuel cell viable for both portable and stationary applications. Factors such as being lightweight, a minuscule amount of corrosive fluid, a long stack lifetime, the generation of zero emissions, and higher efficiencies, render this fuel cell to be perfect for automobile applications (Yilanci, Dincer, & Ozturk, 2008)

A low temperature and high efficiency are two distinguishing features that set PEMFCs apart from other fuel cells (Wee, 2007). The operating temperature range of PEMFCs is 50-100℃, leads to a very quick commissioning ability. The total cost is also rather low because cheaper materials are viable at low temperature settings as the operation carries less risks. The efficiency of a PEM fuel cell is also much higher compared to that of an internal combustion engine in vehicles while direct hydrogen acts

as its input. Furthermore, the small load on a PEM fuel cell translates into higher efficiencies. For a normal driving time, a vehicle will require only a small amount of nominal engine power, and a PEM fuel cell is especially poignant in this regard because its efficiency is maximized when the loads are small. This efficiency peak stands in contrast to that of an internal combustion engine (Salemme, Menna, & Simeone, 2009). Evaluation between different types of fuel cells are shown in Table 2-1(Larminie, Dicks, & McDonald, 2003).

Table 2-1: Comparison of fuel cell types. (OT defines Operating Temperature in Centigrade scale)

Fuel cell type	Electrolyte	OT	Application	Advantages	Disadvantages
Alkaline Fuel Cell (AFC)	Potassium hydroxide	90-100	Military space	-Simple operation - low weight & volume - low temperature - not have corrosion problems	-extremely intolerant to CO_2 - relatively short lifetime
Direct Methanol Fuel Cell (DMFC)	Solid polymer membrane	0-100	Consumer goods Laptop Mobile phones	- Easy storage and transport -High energy storage	- low power output with respect to the hydrogen cells - Methanol is toxic and flammable
Solid Oxide Fuel Cell (SOFC)	Ceramic oxide	650-1000	Electric utility Auxiliary power Large distributed generation	-Fuel flexibility - Very fast chemical reactions -high efficiency	-slow start up - high temperature enhances corrosion & breakdown of cell component - Not a mature technology

Table 2.1 continued:

Fuel cell type	Electrolyte	OT	Application	Advantages	Disadvantages
Molten Carbonate Fuel Cells (MCFC)	Alkali carbonates	600-700	Electric utility Large distributed generation	-High speed reaction -High efficiency -suitable for combine heat and power	-Slow start up -Complex electrolyte management - Require preheating before starting work
Phosphoric Acid Fuel Cell (PAFC)	Phosphorous	150-200	Distributed generation	-Use air directly from atmosphere -high overall efficiency with CHP	-low current and power -large size -requires expensive platinum catalyst
Proton Exchange Membrane Fuel Cells (PEMFC)	Solid polymer membrane	50-100	Small distributed generation Backup power Portable power Transportation	-Low temperature -Quick start -Solid electrolyte reduces corrosion& electrolyte management problems -compact and robust -simple mechanical design -High efficiency	-High sensitivity fuel impurities -very expensive catalyst (platinum) and a membrane (solid polymer) -Low temperature -Waste heat temperature not Suitable for combined heat & power

2.2.2 Fuel Cell Applications

The electrical power produced by different types of fuel cells, ranges from milliwatts to megawatts. The application of fuel cells has been categorized based on their power capacity can be summarized as follows.

2.2.2.1 Portable Power

Fuel cells are developed to power portable devices such as cellular phone without recharging up to a month and power laptops longer than batteries. Fuel cells also can power digital handheld devices such as video recorder, pagers, portable power tools and low power remote devices such as smoke detectors, hotels locks and hearing aids. Proton exchange membrane (PEM) and Direct Methanol Fuel Cell (DMFC) are two fuel cells used as portable power banks. Figure 2.8 shows a laptop powered by fuel cell. (Dyer, 2002; Salameh, 2014).

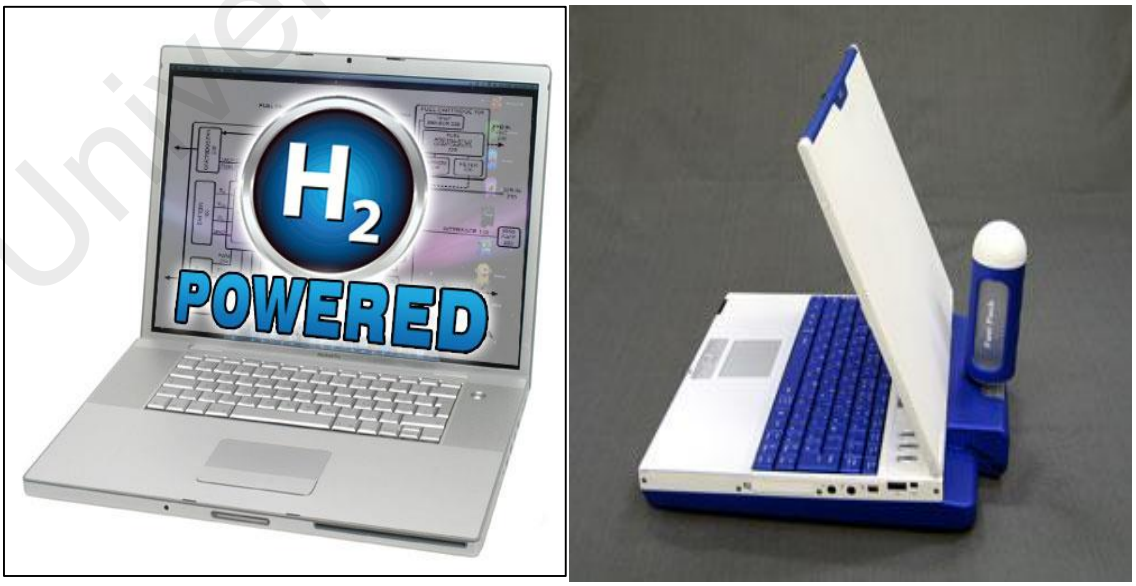

Figure 2.8: Laptop computer powered by fuel cell
(source: http://www.hydrogengas.biz/hydrogenfuelcelllaptop.html)

2.2.2.2 Stationary

Fuel cell systems can provide the main power for building applications such as schools, hotels, office buildings, and for back up the power for critical place such as airports and hospitals. Four stationary types of fuel cells that can be employed to generate power include solid oxide (SOFC), molten carbonate (MCFC), phosphoric acid (PAFC) and proton exchange membrane (PEM) fuel cells. Figure 2.9 shows a building that uses fuel cell to produce power(Salameh, 2014).

Figure 2.9: Fuel cells used for building
(source: http://www.fuelcells.org/uploads/bloom_constellation-place.jpg)

2.2.2.3 Residential

For small commercial and residential applications, small fuel cell could be applied. Clear Edge manufactures PEM fuel cells to generate power and heat simultaneously to warm swimming pools and provide hot water. Moreover, hot water or heating for home can use the heat from the reaction. Proton exchange membrane (PEM) fuel cell generally used in residential and small commercial building. Figure 2.10 shows the fuel cell uses in residential buildings (Salameh, 2014).

Figure 2.10: Fuel cell used in a residential building (source:http://www.cleantechinvestor.com/portal/interviews/1765-the-hydrogen-home.html)

2.2.2.4 Transportation

Design of vehicle powered by fuel cells is one of the solutions to the increasing cost of gasoline fuel and natural gas. Currently, fuel cells are developed for use in various vehicles such as buses, cars, forklifts, golf carts, airplanes, motorcycle, scooters and bicycles. In today's society, electric bicycle has become more popular as it is cost effective and more reliable. The fuel cells that are applied in this application are proton exchange (PEM) fuel cells. Figure 2.11 shows the fuel cells applied in a car (Salameh, 2014).

Figure 2.11: Fuel cell used in transportation
(source: http://www.fuelcells.org/uploads/Picture-003.jpg)

2.3 Fuel cell efficiency

During the past decade, detailed theoretical efficiency calculation methods have drawn increasing attention in many available publications for better performance of PEM fuel cell. Low efficiency and high production cost are some of the most serious challenges for previous fuel cell technologies. Therefore, many research groups have focused on this area as a key challenge for the commercialization stage. Fuel cells are expected to generate power for longer periods and at higher efficiencies compared to batteries.

Barbir and Gomez (1996) (Frano Barbir & Gomez, 1996) investigated the primary rule of efficiency of PEM fuel cell and surmised that the economics and operating efficiency of a fuel cell are interrelated. Kazim (Kazim, 2002, 2004, 2005) presented a novel approach on the determination on minimal operating efficiency in PEM fuel cell and its performance in different conditions. Ferng et al. (Ferng, Tzang, Pei, Sun, & Su, 2004) investigated the performance of single-cell PEM fuel cell analytically and experimentally. Yongping Hou et al. (Hou, Zhuang, & Wan, 2007) proposed models that detail the efficiency of fuel cells and investigated their theoretical and experimental efficiency while evaluating several influencing parameters that are related to the efficiency of a fuel cell. Meiyappan Siva Pandian (2010) (Pandian, Anwari, Husodo, & Hiendro, 2010) stipulated that enhancing the power output of PEM would reduce the efficiency, which would be detrimental to the economic aspect of the system. They carried out performance and efficiency testing of PEM fuel cell in different operating temperature and pressure.

In order to improve the efficiency and system performance of power density, optimization of product and to design a PEM fuel cell system in various conditions is very important and challenging.

2.4 Fuel Cell Modeling

A key issue for effective and efficient utilization of the PEM fuel cells and solar cells is optimal modelling. Models have been developed to represent the behaviour of the system at different operating conditions. However, the primary concern of vehicle modelling is overall characteristic of the stack.

Optimal modelling for better knowledge of impressive and efficient utilization of the PEM fuel cell performance is a significant issue. Models have been developed to estimate and optimize the real performance of fuel cell system through the a great deal actual phenomena and various operating conditions (Niu, Zhang, & Li, 2014).

The main advantages of modeling are cost effectiveness, investigation of critical situations without any real life danger and the system's virtualization in variable conditions. PEM fuel cell modeling is required to pattern critical parameters such as pressure, temperature and hydrogen consumption due to natural environment reaction inside the fuel cell. A large number of fuel cell models have been developed during the past few years to provide more comprehension of the fuel cell phenomena. There have been two approaches for PEM fuel cell modeling namely theoretical and empirical model.

2.4.1 Theoretical Models

Theoretical models are based on thermodynamic, electrochemical and fluid dynamic relationships. Phenomenological equations such as Stefan–Maxwell equation for the gas phase transport and Butler–Volmer equation for cell voltage are used in this description. In theoretical models, for determining the performance of fuel cell,

mathematical partial equations have been used. For different types of fuel cell stack and size, the convenient method for modelling is theoretical model, however, due to the non-linear nature of fuel cells, they are less accurate and reliable. Indeed theoretical modeling is not an easy task due to the dependence on specific knowledge of many parameters based on electrochemical phenomena and the reduced performance of the overall system due to computational intensity (Napoli et al., 2013). Several mathematical models have been presented to improve the design and operation of fuel cell but internal parameters need to be defined which are difficult to determine in fuel cell system and unfortunately many of these models are not accurate enough (Baschuk & Li, 2005; Ceraolo et al., 2003; Contreras et al., 2010; Gong & Cai, 2014; Haji, 2011; Meidanshahi & Karimi, 2012; Oezbek et al., 2013; Rowe & Li, 2001; Tiss et al., 2013).

2.4.2 Empirical Models

Using an experimental data for modelling is the most straightforward method to model fuel cells. Empirical model is based on soft computing and machine learning has provided a better understanding of predicting the parameters that affect the voltage-current (V-I) curve of fuel cell without evaluating physical and electrochemical phenomena in depth (Boscaino et al., 2013).

One of the advantages of this type of model is producing accurate results requiring very little computations. The accuracy of results is based on experimental procedures and instrumentation which are used to achieve the data (Chávez-Ramírez et al., 2010).

2.4.2.1 Linear Regression

Linear regression models are used for several purposes such as data description, parameter estimation, prediction and estimation and control. To summarize or describe a set of data the majority of scientists and engineers use regression analysis equations. Sometimes regression method can solve the problem in estimating the parameters. Regression method is used for prediction of response variable and also used for control purposes. **Figure 2.12** shows the regression model building process.

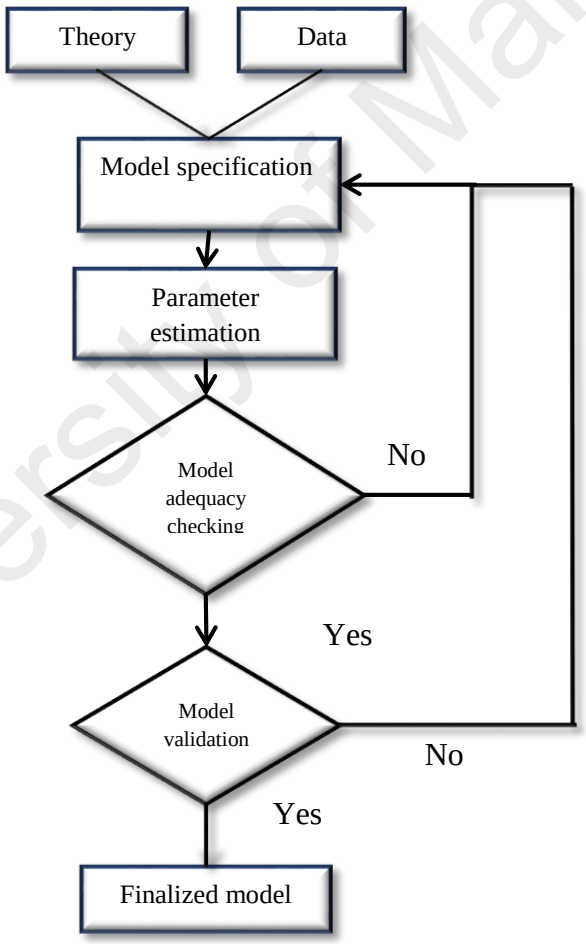

Figure 2.12: regression model building

A few works of linear regression have been reported. Ii.Q et al. (Q. Li et al., 2014) proposed model of locomotive PEM fuel cell based on support vector regression to investigate the effect of different operating conditions on dynamic locomotive behaviour. Zhi-Dan Zhong et al. (Zhong et al., 2006) designed a proton exchange membrane fuel cell (PEMFC) by using support vector machine to predict the behaviour of PEM fuel cell under different operating conditions. Dong'an Liu et al. (Peng & Lai, 2010) proposed a least squares-support vector machine to simulate the PEM fuel cell to investigate the effect of assembly error of the bipolar plate (BPP).

2.4.2.2 Artificial Neural Network Modelling

The implementation of new technology with capability of getting close to actual human being is the major objective of science (Funes, Allouche, Beltrán, & Jiménez, 2015). For various engineering problems such as modelling, control, signal processing and pattern recognition, artificial neural network has been applied (Powell, 1977). The beneficial properties that ANN can offer is the ability to predict the output using input data in form of both supervised and un-supervised learning methods. For modelling and prediction, the fuel cell due to its highly nonlinear system and neural network, can be an appropriate alternative choice.

2.4.2.2.1 Levenberg-Marquardt back propagation (LMBP)

The back propagation algorithm has been used for training ANN generalized by Rumelhart et al. in 1986 (Rumelhart, Hinton, & Williams, 1985, 1988). Backpropagation algorithm involves two phases: forward propagation and backward propagation. In forward propagation to produce the networks outputs, the effect of applied input vector

propagates through the network between layers (Furht & Marques, 2003). In backward propagation, the error signal produced by the subtracted the actual output and desired output of the network is then propagated backward through the network. To minimize the error the synaptic weights are adjusted.

Neural network modelling includes two phases: training phase and test and validation phase. Set of input-output parameters are applied to the network in training phase. According to the back propagation algorithm, an adjustment of synaptic weight is done until acceptable range of error signal is shown. When the network is trained, in test and validation phase, the network is exposed to unseen data to ensure its proper performance in real-life application.

The Levenberg-Marquardt algorithm is interpolated between gradient descent update and the Gauss-Newton update to approach second-order training with simplified form of Hessian matrix (Levenberg, 1944; Marquardt, 1963). Figure 2.13 shows the structure of neural network modelling.

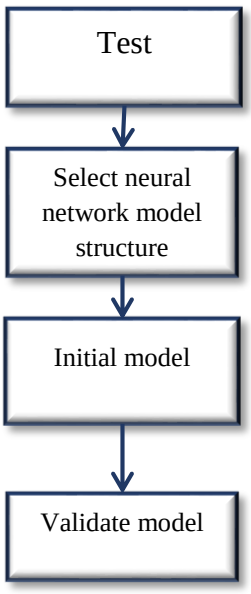

Figure 2.13: Steps of neural network modelling approach

Jemei et al. proposed back propagation network to model an entire fuel cell system. They considered the affected input on behavior of fuel cell with network by two inputs, one hidden layer and one output layer. The proposed ANN model is an efficient method to predict the stack voltage. The proposed model will be integrated in a complete vehicle powertrain(Jemei, Hissel, Péra, & Kauffmann, 2002).

Ou et al. tested various artificial neural network including; back propagation and radial basis function network for PEM fuel cell output voltage prediction show satisfactory performance. They studied the effects of platinum (pt) loading on the performance of fuel cell and developed and compared multiplicative and additive, two neural network hybrids model that consist of an ANN component and physical component by full-blown ANN model. The result demonstrated that the additive hybrid model has better accuracy than multiplicative model (S. Ou & L. E. K. Achenie, 2005).

Azmy et al. presented an artificial neural network (ANN) model for residential application to manage daily operation of PEM fuel cell using genetic algorithm (GA) to optimize the performance of fuel cell. The result shows good agreement between ANN model and optimal values and the proposed approach achieved both easy and fast adjustment of fuel cell setting(A. M. Azmy & I. Erlich, 2005).

Kong et al. presented an artificial neural network to improve model accuracy of the PEM fuel cell under different operation conditions. The network consisted of stack current as an input. In addition, fuel cell temperature effect on the stack was estimated from the fuel cell current. It was reported that a good balance was obtained between ANN model and experimental result(Kong et al., 2006).

Hatti et al. predicted the cell voltage of single cell by applying back propagation Levenberg-Marquardt training algorithm to improve system performance and analysis of

fuel cell system. The result shows good performance in the model and demonstrated that the present model is suitable for design and analysis of the cell voltage of fuel cell(Hatti, Tioursi, & Nouibat, 2006).

Saengrung et al. proposed two artificial neural network (ANN) including multiple layer perceptron (MLP) and radial basis function (RBF) to model the fuel cell performance of commercial proton exchange membrane (PEM). They considered the model using two inputs, air flow and stack temperature and two outputs, stack voltage and stack current and two hidden layers for back propagation and one hidden layer for multiple layer perceptron. The results show that ANN predicted the performance of PEM fuel cell with satisfactory accuracy in a short period of time (Saenrung, Abtahi, & Zilouchian, 2007).

Jemei et al. proposed an Artificial neural network for modeling the PEM fuel cell applied in an electric vehicle to evaluate the output variables and their variations. They used back propagation for training data, modeled by five inputs and two hidden layers and one output. The result shows that ANN is an efficient model for PEM fuel cell and it is possible to determine the parameters that influence the behavior of the fuel cell(Jemei, Hissel, Pera, & Kauffmann, 2008).

Hasikos et al. applied a Radial basis function of neural network to simulate and control the PEM fuel cell system, and optimize it by non-linear programming problem (NLP) which minimizes the consumption of hydrogen. Finally, they designed the Model predicted control (MPC) for the optimal control of the fuel cell system. Results showed that successful dynamic behavior model can be achieved and consumption of hydrogen minimized (J. Hasikos, H. Sarimveis, P. L. Zervas, & N. C. Markatos, 2009).

Chavez Ramirez et al. proposed an Artificial neural network to model the performance of PEM fuel cell. The approach model shows excellent accuracy in modelling the PEM system by considering 7 inputs, two hidden layers and 2 outputs. They concluded this model can be applied in complex systems and applications(Chavez-Ramirez et al., 2010).

Youssef et al. developed an ANN model by using Levenberg-Marquardt back propagation (LMBP) algorithm to simulate the performance of PEM fuel cell by ANN model without complex computation. The result show that polarization curve of ANN model had good compliance with experimental data (Youssef, Khalil, & AL-NAdi, 2010).

Puranik et al. presented an artificial neural network to model the 500-W proton exchange membrane (PEM) fuel cell to analyses the dynamic behavior after training and validating the model. The result show the effect of measurement noise on the performance of the model (Sachin V. Puranik, Ali Keyhani, & Farshad Khorrami, 2010).

Miao et al. proposed the Metamodel-Based Design Optimization (MBDO) to promote the performance of the power density of the proton exchange membrane fuel cell. PEM fuel cell was modeled by artificial neural network (ANN) based on back propagation with 5 inputs and one hidden layer and one output. They applied genetic algorithm (GA) to optimize the performance of PEM fuel cell. The experimental result showed that MBDO approach is effective for PEM fuel cell performance of power density(J.-M. Miao et al., 2011).

Bhagavatula et al.(Bhagavatula, Bhagavatula, & Dhathathreyan, 2012) investigated feedforward backpropagation neural networks to estimate the performance of a PEM fuel cell single cell in different temperature and flow rate. Result show that predictions were closely match with experimental data.

Chang et al. combined the back propagation neural network and Taguchi method to estimate the output voltage of PEM fuel cell accurately. They compared the proposed model and results indicated that the error of proposed method is much smaller than that of BPNN without applying the Taguchi method (K.-Y. Chang & Teng, 2012).

Meiler et al investigated multilayer perceptron neural networks and semi empirical models to identify the parameters of the model from limited experimental data. Five inputs and one output have been chosen to model input-output behaviour of nonlinear system. Both model were validated by using experimental data to investigate the model ability in identification of system parameters.(Meiler, Hofer, Nuhic, & Schmid, 2012).

Cheng et al. demonstrated the meta-modeling constructed by Radial basis function neural network to improve the power density in PEM fuel cell. They applied the Genetic algorithm (GA) to optimize the performance of PEM fuel cell and compared the results with experimental data. The result defined that proposed approach is effective and economical to improve the performance of PEM fuel cell (Cheng, Miao, & Wu, 2013).

Chang proposed hybrid model based on radial basis function (RBF) and enhanced particle swarm optimization (EPSO) to have an accurately and estimate of PEM fuel cell parameters. They modeled fuel cell using two inputs and one hidden layer and three outputs. The result showed that the proposed hybrid models can effectively estimate the parameters of PEM fuel cell(W.-Y. Chang, 2013).

Summary of artificial neural network's literature is shown in Table 2-2.

Table 2-2: Summary of previous works on ANN

Author (date)	Method for modelling	Objective	Results
Jemei et al. (2003)	Back propagation neural network (BP NN)	To consider the affected input on behavior of fuel cell system with network	Proposed ANN model is an efficient method to predict the stack voltage.
Ou and Achnie et al. (2005)	Back propagation (BP) and radial basis function(RBF) network	To develop a quantitatively good model and to study the effects of pt loading on the performance of fuel cell	The result demonstrated that the additive hybrid model has better accuracy than multiplicative model.
Azmy et al. (2005)	Artificial neural network (ANN) and genetic algorithm (GA)	To model PEM fuel cell for residential application to manage daily operation of it	The result shows the good agreement between ANN model and optimal values
Kong et al. (2006)	Artificial neural network (ANN)	To improve accurate model of the PEM fuel cell under different operation condition.	It was reported good agreement was obtained between ANN model and experimental result.
Hatti et al. (2007)	Back propagation Levenberg-Marquardt	To improve system performance and analysis of fuel cell system	The result show good performance in the model and investigated present model is suitable for design and analysis the cell voltage of fuel cell.

Table 2.2 continued:

Author (date)	Method for modelling	Objective	Results
Saengrung et al. (2007)	Back propagation (BP) and radial basis function (RBF)	To model the commercial (PEM) fuel cell performance.	The results show that ANN predicted the performance of PEM fuel cell with a satisfactory accuracy in short period of time.
Hasikos et al. (2009)	Radial basis function of neural network (RBF)	to simulate the PEM fuel cell model, and optimize it by non-linear programming problem (NLP)	Result show that successful dynamic behavior model can be achieve and minimize the consumption of hydrogen
Chavez Ramirez et al. (2010)	Artificial neural network (ANN)	To model the performance of PEM fuel cell.	The result show excellent accuracy in modelling the PEM system by considering 7 inputs, two hidden layer and 2 outputs
Youssef et al. (2010)	Levenberg-Marquardt back propagation (LMBP) algorithm.	To simulated performance of PEM fuel cell	The result shown that, polarization curve of ANN model had good agreement with experimental data.
Puranik et al. (2010)	Artificial neural network	To analysis the dynamic behaviors of PEM fuel cell	The result shows the effect of the measurement noise on the performance of the model.
Miao et al. (2011)	Back propagation (BP) artificial neural network (ANN) and Metamodel-Based Design Optimization	To promoting the performance of the power density of the proton exchange membrane fuel cell	The experimental result show that MBDO approach is effective for PEM fuel cell performance of power density

Table 2.2 continued:

Author (date)	Method for modelling	Objective	Results
Bhagavatula et al. (2011)	Feed forward back propagation	To estimate the performance of a PEM fuel cell single cell	Result show that predictions were closely match with experimental data.
Chang et al. (2012)	Combined the back propagation neural network and Taguchi method	To estimate the output voltage of PEM fuel cell accurately	They compared the proposed model and results indicated that the error of proposed method is much smaller than that of BPNN without applying the Taguchi method
Meiler et al. (2012)	Multilayer perceptron neural networks	To identify the parameters of the model from limited experimental data	Both model were validated by using experimental data to investigate the model ability in identification of system parameters.
Cheng et al. (2013)	Radial basis function neural network	To improve the power density in PEM fuel cell	The result defined that proposed approach is effective and economical to improve the performance of PEM fuel cell.
Chang (2013)	Radial basis function (RBF)	To have an accurately and reliable estimation of PEM fuel cell parameters.	The result show that the proposed hybrid models can effectively estimate the parameters of PEM fuel cell.

2.4.2.3 Fuzzy Cognitive Map

There is limited literature about multivariate regression other than neural methods. Soft computing is an alternative to hard and classic math for processing uncertain and incomplete data. This includes modelling relationships among highly interrelated variables with applications in curve fitting, regression, and generalization. Fuzzy Cognitive Maps (FCMs), which constitute an extension of cognitive maps, are a soft computing method for modelling complex systems using existence knowledge and human experience. They were introduced by Kosko as signed directed graphs for representing causal reasoning and computational inference processing, using a symbolic representation for the description and modelling of a system (Kosko, 1996). They describe complex systems using nodes/concepts (variables, weights, states, inputs, outputs) and directed links connecting them. The FCM model is used to analyse, simulate, and test the impact of the parameters and predict system behaviour. Fuzzy cognitive maps (FCM) are applied for relations between the elements and computing their "strength of impact" (Stach, Kurgan, Pedrycz, & Reformat, 2005). Basically, FCM integrated the present knowledge and information related to the system by using human experts to define the system's operation and behaviour and to find the factors required for the system. FCM is a distinctive approach in two domains; dynamic system modelling (Omid Motlagh, Tang, Khaksar, & Ismail, 2012) and controlling systems (O. Motlagh, Tang, Ismail, & Ramli, 2012).

Flexibility of system design, model and control is one of the features of FCM to show complex system behaviour. FCM has many desirable properties compared to expert systems or neural networks such as hidden inter-relationships. In addition, representing the structured information is easily displayed by FCM. For computing the inference,

simple numerical matrix operations are used (Kosko, 1996). Classical mathematical model has many problems like uncertainty and imprecise rules for modelling. Therefore, to analyse imprecise problems, fuzzy cognitive maps represent important parameters by nodes and denote causal relationship between these elements in given domain by edge.

Over the last decade, FCM has played an important role in various scientific area such as information technology, social and political science, engineering and robotics, medicine, environment and agriculture etc. (E. Papageorgiou, 2011). For instance, Information technology (IT) has several limitations in classifying, identifying and evaluating the indicator and these limitations can be solved by employing by FCM for successful modelling (Furfaro, Kargel, Lunine, Fink, & Bishop, 2010; Jose & Contreras, 2010; Lai, Zhou, & Zhang, 2009; X. Li, Ji, Zheng, Li, & Yu, 2009). In social and political science, for modelling and supporting the different policies especially in decision-making process in imminent crisis, FCM has emerged (Acampora & Loia, 2009; A. Andreou, Mateou, & Zombanakis, 2003; A. S. Andreou, Mateou, & Zombanakis, 2005; Joao Paulo Carvalho, 2010). In medicine domain, FCM has been applied for medical diagnosis and decision support including radiotherapy integrated structure and model for brain and bladder tumours, particular language impairment, managing urinary tract infections. (Georgopoulos, Malandraki, & Stylios, 2003; E. Papageorgiou, Papandrianos, Karagianni, Kyriazopoulos, & Sfyras, 2009; E. Papageorgiou et al., 2006; E. Papageorgiou, Stylios, & Groumpos, 2008; E. I. Papageorgiou, Papadimitriou, & Karkanis, 2009; Stylios & Georgopoulos, 2008). In environment and agriculture, FCM has been used for modelling a generic shallow lake, in agroforestry management to evaluate local knowledge, and in New Zealand to predict the dryland ecosystem to anticipate pest management outcomes. (Isaac, Dawoe, & Sieciechowicz, 2009; Kafetzis,

McRoberts, & Mouratiadou, 2010; Kok, 2009; Rajaram & Das, 2010; Ramsey & Norbury, 2009; Tan & Özesmi, 2006).

In engineering, FCM have been used for modelling and control of the system to analyse the failure modes and model the control system supervisory (Beeson, Modayil, & Kuipers, 2009; Gonzalez, Aguilar, & Castillo, 2009; Thodoris L Kottas, Boutalis, & Christodoulou, 2010; Thodoris L Kottas, Karlis, & Boutalis, 2010; E. I. Papageorgiou, Stylios, & Groumpos, 2006; Stylios & Groumpos, 2004). In the last decade the majority of FCM studies have been applied in the business and engineering fields for system control and prediction (E. Papageorgiou, 2011). In addition, decision making, management, interpreting, monitoring, classification, modelling and prediction are forms of typical problems solved by FCM. Table 2-3 shows some examples of the problems solved by FCM.

Table 2-3: Examples of problems solved by FCM

Scientific area	Problem solved by FCM
Information technology	Classification, modelling
Social and political	Decision-making
Medicine	Classification, decision support, modelling, prediction
Environment and agriculture	Policy making, knowledge representation, reasoning
Engineering (control, robotic)	Monitoring, prediction, navigation, learning

Different types of FCM extensions have been applied in various applications in scientific areas including:

1) *Dynamic Cognitive Networks (DCNs)* proposed by Y. Miao et al. in 2001 to explain and quantify the relationships between FCM concepts (Y. Miao, Liu, Siew, & Miao, 2001).
2) *Fuzzy Gray Cognitive Maps (FGCMs)* proposed by Jose L. Salmon in 2010 which is based on gray system theory for solving high uncertainly problems with incomplete and discrete data sets (Salmeron, 2010).
3) *Intuitionistic Fuzzy Cognitive Maps (IFCMs)* developed by D.K Iakovidis and E.I. Papageorgiou for decision-making models which define relations between two concepts by managing the degree of hesitancy at the output concept.
4) *Dynamic Random Fuzzy Cognitive Maps (DRFCMs)* proposed by Jose Aguilar in 2003 for modelling complex dynamic systems according to random neural models (Aguilar, 2003).
5) *Evolutionary Fuzzy Cognitive Maps (E-FCMs)* proposed by Cai et al. in 2010 which update the concept status in real time for simulation (Cai, Miao, Tan, Shen, & Li, 2010).
6) *Fuzzy Time Cognitive Map (FTCMs)* proposed by Kyung Sam Park et al. in 1995 for simulation between node's relationship including time (Park & Kim, 1995).
7) *Rough Cognitive Maps (RCMs)* proposed by Chunying et al. in 2011 based on Rough Sets theory for solving the rough weight problems(Chunying, Lu, Dong, & Ruitao, 2011).
8) *Timed Automata-based fuzzy cognitive maps (TAFCMs)* developed by Acampora et al. in 2011 in order to achieve realistic and consistent temporal computation(Acampora, Loia, & Vitiello, 2011).

9) *Belief-Degree Distributed Fuzzy Cognitive Maps (BDD-FCMs)* proposed by Ruan et al. in 2011 to express the complex relationship problems between concepts by belief structure (Ruan, Hardeman, & Mkrtchyan, 2011).

10) *Rule Based Fuzzy Cognitive Maps (RBFCMs)* proposed by J.P. Carvalho to avoid some limitations of FCM such as properties of other fuzzy systems not shared by FCM and not exploring the capability of using fuzzy rules. Complete and complex cognitive representation is allowed by RB-FCM as an improvement of Casual Fuzzy maps. It is composed of fuzzy nodes (concepts) and fuzzy links (relation). RB-FCM are essentially a fuzzy rule based system designed to answer the complexity and variety of qualitative system fuzzy mechanisms added to deal with different kinds of relations. In addition, what-if questions in cognitive map are answered by RB-FCM. Evolving concept of RB-FCM is defined by calculating the current values using previous inputs (João Paulo Carvalho & Tomè, 1999).

11) *Fuzzy Cognitive Network (FCN)* proposed by Kottas et al. in 2007 which is one of the effective extensions of fuzzy cognitive map (FCM) for supporting the continuous interaction with the system described (T. Kottas, Boutalis, Diamantis, Kosmidou, & Aivasidis, 2006).

Node and weight interactions are structures of the initial FCN graph. Nodes in FCNs are known as reference, control, output or simple operational nodes that describe the behavior of the system. Variables with constant or desired values are characterized by reference nodes. Control variables of system are characterized by control nodes and output variables of the system are represented by output nodes. All other nodes not mentioned previously are represented by simple operational nodes. Casual relationships between nodes are represented by weighted edges. FCN's primary weights are based on expert knowledge of the

function of system. In each iteration, weight values are updated by using modified delta rule, which provides smooth and fast coverage while at the same time, prevents the calculated values from being saturated.

Moreover, further enhancing and accelerating the updating mechanism is performed by utilizing information from earlier equilibrium point of system operation. This is achieved by dynamically building a database, which, for each encountered operational situation, assigns a fuzzy if-then rule connecting the involved weight and node values. In order to determine appropriate membership functions, range of the nodes and weights parameters are partitioned dynamically. This way, the speed of procedure is significantly enhanced by applying system's feedback which gradually begins with values closer to the desired ones for updating the weights (Boutalis, Kottas, & Christodoulou, 2009; Theodore L Kottas, Boutalis, & Christodoulou, 2007; Thodoris L Kottas, Karlis, et al., 2010).

The development method of FCM relies on human knowledge and experience. Numerous kinds of band concepts and relations between concepts are defined by experts, but many weaknesses are obtained by using learning method due to unreliable human experience and knowledge. Experts believe that for managing FCM, casual relationships and weight recalculations and potential uncontrollable convergence lead to undesired steady state because concept values are one of the main deficiencies. Several learning algorithms are proposed in order to overcome these problems.

2.4.2.3.1 Learning Algorithms

A learning algorithm is a mathematical method for determining the weights in order to train the FCM to model the behaviour of the system. Table 2-4 shows the common FCM training algorithms. Based on the learning paradigm, the learning algorithms are categorized into three groups:

1) *Hebbian-based* as well-known unsupervised algorithm is useful for FCM in order to enhance the efficiency and robustness and also to improve the dynamic behaviour and flexibility of FCM model. The most efficient Hebbian-based method for training the FCM are:

    a) *Differential Hebbian Learning (DHL)* proposed by J.A. Dickerson et al. as an unsupervised learning method for training FCM (Dickerson & Kosko, 1993).
    b) *Balanced Differential Algorithm (BDA)* proposed by A.V. Huerga that presented new rules for updating the values of weights on the edges (Huerga, 2002).
    c) *Nonlinear Hebbian Learning (NHL)* proposed by Papageorgiou et al. based on the nonlinear Hebbian learning rule for learning the structure of FCM (E. Papageorgiou et al., 2003).
    d) Active Hebbian Learning (AHL) proposed by Papageorgiou et al. based on the theory of sequence of activation concept (E. Papageorgiou, Stylios, & Groumpos, 2004).

e) Data-Driven Nonlinear Hebbian Learning (DD-NHL) proposed by Statch et al. based on same NHL learning principle and records historical data to learning process (E. Papageorgiou & Groumpos, 2004; Stach, Kurgan, & Pedrycz, 2008).

2) *Population-based,* which trained FCM based on new type of method to find models that simulate the input data. For training FCM, several population-based algorithms have been introduced such as (Koulouriotis, Diakoulakis, & Emiris, 2001):

a) Evolutionary Strategies (ES)
b) Genetic Algorithms (GA)
c) Real Coded Generic Algorithms (RCGA)
d) Swarm Intelligence (SI)
e) Memetic Algorithms (Mas)
f) Simulated Annealing (SA)
g) Chaotic Simulated Annealing (CSA)
h) Tabu Search (TS)
i) Ant Colony Optimization (ACO)
j) Extended Great Deluge Algorithm (EGDA)
k) Bing Bang-Big Crunch (BB-BC)
l) Self-Organizing Migration Algorithms (SOMA)
m) Immune Algorithms (IA)

3) Hybrid learning method which is based on historical data and initial experience updates the weights matrix. Hybrid approaches are known as(E. Papageorgiou & Groumpos, 2005; Ren, 2007; Yanchun & Wei, 2008):

a) Combined Nonlinear Hebbian Learning algorithm and Differential Evolution algorithm (NHL-DE)

b) Combined Nonlinear Hebbian Learning algorithm and Extended Great Deluge Algorithm (NHL-EGDA)

c) Combined real-coded genetic algorithm and nonlinear Hebbian learning algorithm (NHL-RCGA).

Table 2-4: Learning approaches and algorithms for FCM

Learning categories	**Learning approaches**	
	Author and year	**Name of approaches**
Hebbian-Based	Dickerson et al./1993	Differential Hebbian Learning (DHL)
	Huerga/ 2002	Balanced Differential Algorithm (BDA)
	Papageorgiou et al./2003	Nonlinear Hebbian Learning (NHL)
	Papageorgiou et al./ 2004	Active Hebbian Learning (AHL)
	Statch et al./ 2008	Data-Driven Nonlinear Hebbian Learning (DD-NHL)

Table 2.4 continued:

Learning categories	Learning approaches	
	Author and year	**Name of approaches**
Population based model	T. Back et al./ 1991	Evolutionary Strategy (ES)
	Koulouriotis et al./ 2001	Genetic Strategy (GS)
	Psaropoulos et al./ 2003	Particle Swarm Optimization (PSO)
	Stach et al./ 2005	Real-Coded Genetic Algorithms (RCGAs)
	Petalas et al./ 2005	Memetic Particle Swarm Optimization Algorithm (MPSO)
	Ghazanfari et al./ 2007	Simulated Annealing (SA)
	Alizadeh et al./2008	Chaotic Simulated Annealing (CSA)
	Ding et al./2011	Ant Colony Optimization (ACO)
	Baykasoglu et al./2011	Extended Great Deluge Algorithm (EGDA)
	Yesil et et al./ 2010	Big Bang-Big Crunch (BB–BC)
	Vascak/ 2010	Self-Organizing Migration Algorithms (SOMA)
	Lin et al./2009	Immune Algorithm (IA)
Hybrid Learning Method	Papageorgiou et al. /2005	Combine Nonlinear Hebbian Learning algorithm and the Differential Evolution algorithm (NHL-DE)
	Ren /2007	Combine Nonlinear Hebbian Learning and the Extended Great Deluge Algorithm (NHL-EGDA)
	Zhu et al. /2008	Combined real-coded genetic algorithm and nonlinear Hebbian learning algorithm (NHL-RCGA)

2.5 Summary

In this chapter, the fuel cell background is presented and in a brief review PEM fuel cell history and basic principle are described. Various main types of fuel cells such as electrochemical reaction are briefly explained. Currently, PEM fuel cell has a wide range of applications and the focus of this research is on this type of fuel cell. Depending on power capacity of fuel cell, the main applications are categorized into residential, portable, stationary and transportation. For the commercialized PEM fuel cell, study on improving efficiency and performance are the most serious challenges. In addition, accurate modeling of PEM fuel cell for improving efficiency has been a topic of interest for researchers in the last two decades. In this chapter a review of accurate recent models was provided and linear regression (LR), artificial neural network (ANN) and fuzzy cognitive map (FCM) are proposed for modelling the PEM fuel cell.

Chapter 3 : METHODOLOGY

3.1 Introduction

Based on the reviewed literature, modelling of complete electric vehicle with auxiliary parts is essential to adjust the optimization ability. In addition, a reliable model can benefit the system's efficiency with proper control methods to optimize its performance. Based on the problem statement, this study has multiple objectives: First, it aims to define the precise value of the whole system efficiency as well as its correlation with power and other affecting factors; second, it aims to design optimized linear and non-linear dynamic models of the system in order to enable real-time prediction of voltage and efficiency. Experimental data was collected by DAQ system from the electric bicycle; then, efficiency of whole system was calculated based on the collected data. In the next step, PEM fuel cell electric bicycle has been modelled by using both linear and non-linear approaches. Linear regression model and neural network models were used to predict the output voltage and efficiency. Finally, for the first time in this field, a dynamic fuzzy cognitive map was designed to define the causality of system concepts for active modeling of each system parameter. These steps are shown as a flowchart in Figure 3.1.

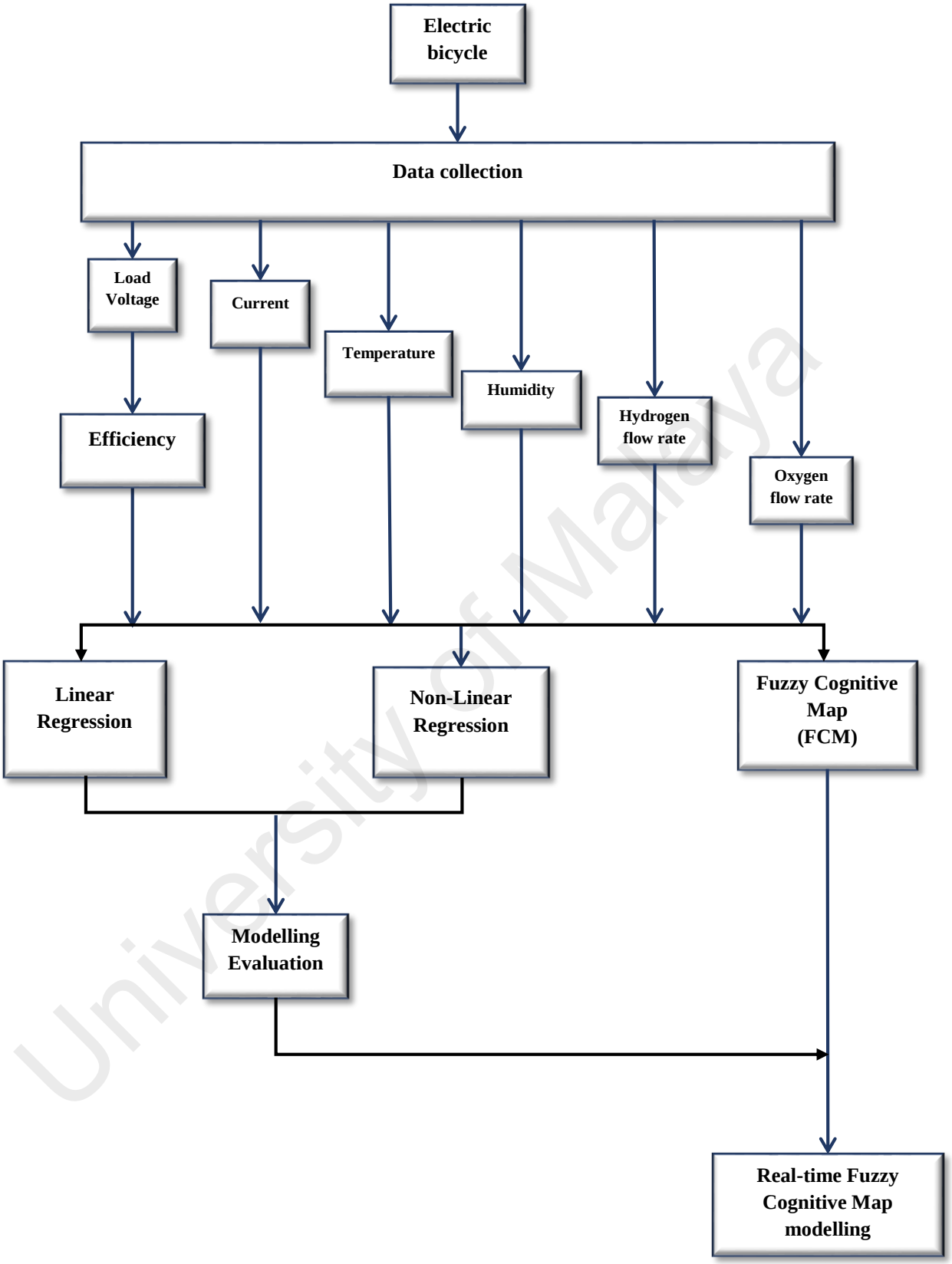

Figure 3.1: Methodology flow chart

3.2 PEM fuel cell system

Commercial electric bicycle and PEM fuel cell that have been installed in the system to provide the power are described as follows:

3.2.1 Overall System Design (Electric Bicycle)

The commercial electric-assisted bicycle that we used in this research is shown in Figure 3.2. As shown in the figure, the components of our system included a fuel cell stack forming the base of the system and integrated with other major components to generate electricity. Metal hybrid is used for storage of a large amount of hydrogen in small tank in electric bicycle. Fuel cell powered the electric motor located in tier and remote control to turn the fuel cell on and off.

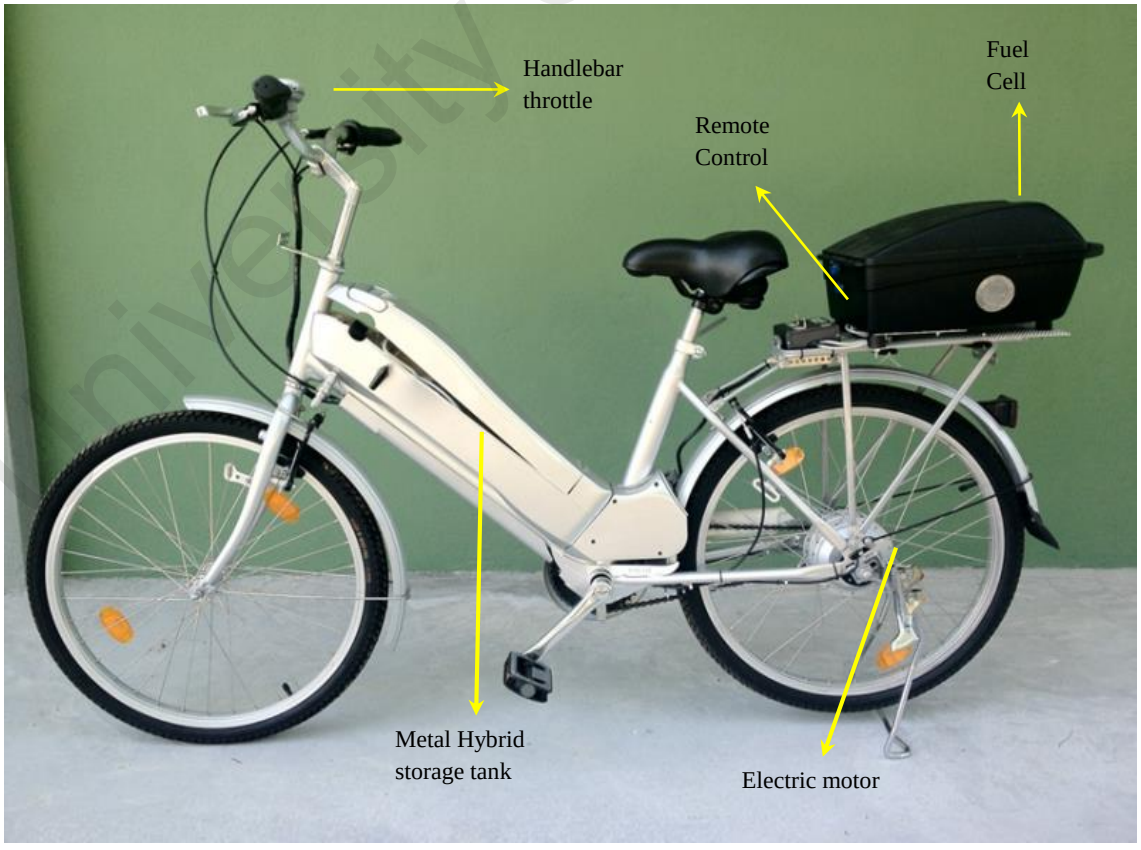

Figure 3.2: Fuel cell-powered electric bicycle

3.2.2 PEM fuel cell powered bicycle

The block diagram of the fuel cell-powered electric bicycle is shown in Figure3.3. The H_2 from a metal hydride tank and O_2 from the air blower are fed to the fuel cell, where they are combined to form water; a process that consequently produces electricity.

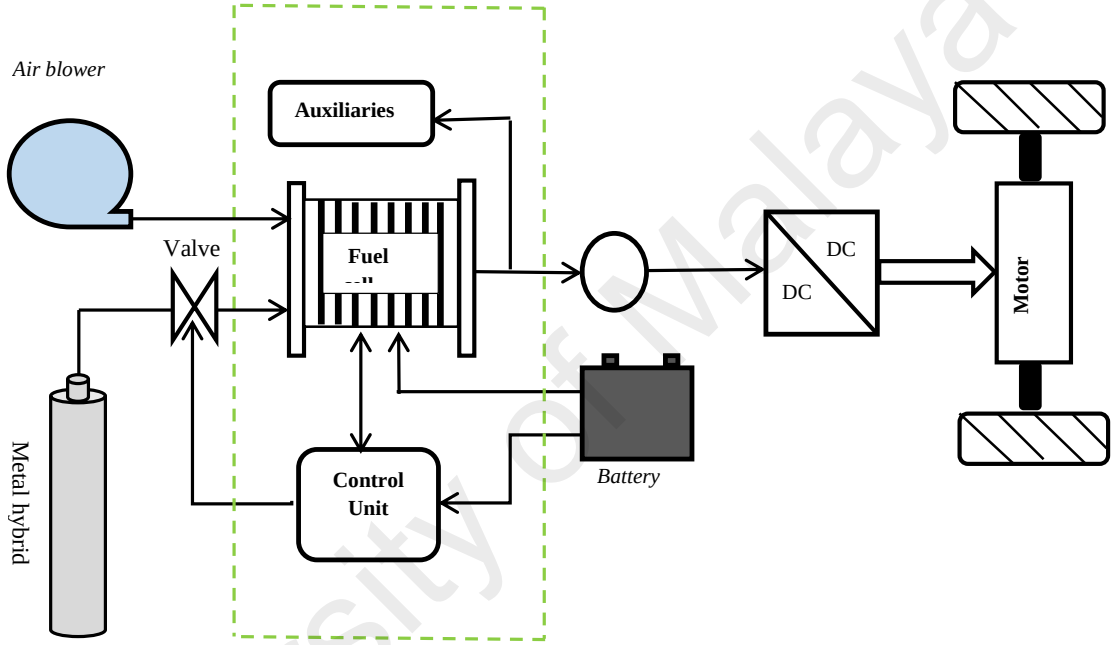

Figure3.3: Block diagram of the fuel cell-powered electric bicycle system

Figure3.4 shows a complete fuel cell system, which consists of the fuel cell, one cooling and one reaction air blower, the Electronic Control Unit (ECU), and the necessary auxiliaries to manage the hydrogen flow.

Figure3.4: Fuel Cell and auxiliary components

The entire system is controlled by an ECU designed by MES S.A., which monitors all the system's parameters and operates the system on command. The ECU features an accessible remote control outside of the main box, and the driver can switch the main power on/off and start the fuel cell on demand. The ECU operates the fuel cell during the start, normal operation, and shutdown procedures by monitoring various parameters such as the stack temperature, hydrogen pressure, stack voltage, stack current, battery voltage, and ambient condition. When the ECU detects an abnormal condition, it will alert the driver via the LED indicators placed on the remote control and handlebar throttle. If the condition for a security shut off (TRIP) is fulfilled and remains unchanged for a certain security time, the system will shut off automatically.

3.3 Data collection and analysis

The DAQ system and its software were designed by MES S.A., and used serial connection between Fuel Cell ECU and monitoring software. To connect the ECU and PC, it is recommended to use (nine-pole) communication cable with this specification: RS 232 (nine-pole), Pin to pin. The connector labelled ECU has to be connected to the appropriate nine pole connector of the ECU, the connector labelled PC to a COM port of the PC. As shown in Figure 3.5 all Fuel Cell parameters are monitored and can be logged.

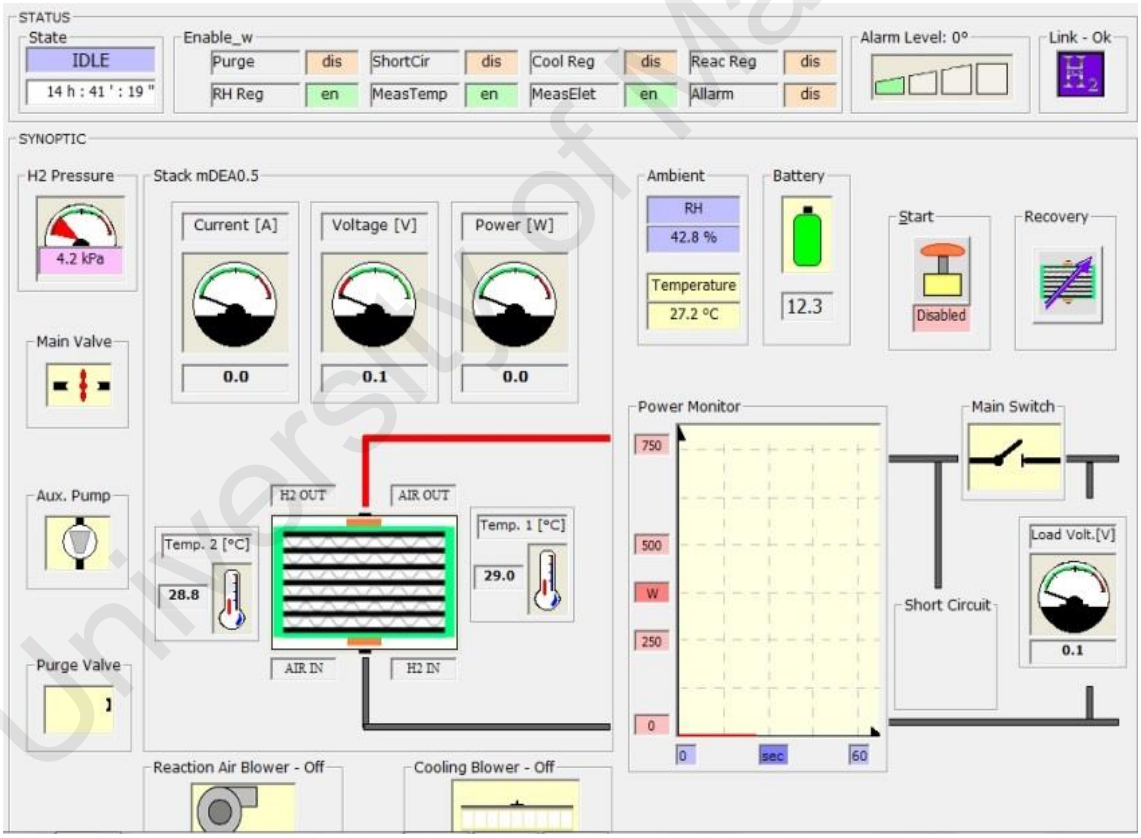

Figure 3.5: The panel of monitoring software for fuel cell system

3.3.1 Data collection

In this study, data was collected from explained stationary bicycle while the tire could spin freely on traditional Kickstand. For collecting the data, hydrogen pressure was in ranges that guarantee the operation of the fuel cell. The ECU monitors humidity and temperature by a proper sensor to maximize the fuel cell's performance.

Data record file has been created that contains the variables such as current stack, voltage stack, temperature, humidity, hydrogen flow rate, oxygen flow rate, hydrogen pressure, and ambient condition. The experimental data was logged with a sampling time of one second to a designated computer. The data collection error encountered during experimentation was outliers. An observation point which is distant from other observations is an outlier. We set the threshold of (2× standard deviation) for detection and elimination of outliers. The data which is an outlier has eliminated from collected data were 0.12% of 9527 data sets.

3.3.2 Variables selection procedure

Selecting the appropriate input and output variable for network is useful for training the network efficiently. Considering the effect of each variable on system performance provides a starting point to select the reliable variables. Since our aim is to model the system with a minimum number of inputs, the value of other variables which can be calculated by predefined equations are excluded in model design.

This project collected seven variables of electric bicycle performance information including the stack temperature, ambient humidity, stack voltage, stack current, stack power, hydrogen flow rate, and oxygen flow rate. The models use five inputs and two outputs nodes.

3.4 Efficiency of fuel cell

Calculating the efficiency for the entire system is necessary in order to improve the performance of the system. Previous studies focused more on analyzing the efficiency and performance of single cell. The efficiency properties of the fuel cell stack and each single cell are similar because all similar single cells are connected in series. Fuel cell efficiency has been computed from the fuel cell's stack operating voltage (V_{oper}) using the following equation (Feroldi & Basualdo, 2012):

$$\eta_{\mathrm{fc}}\% = \frac{100\% \times \mathrm{V_{oper}}}{1.482 \times \mathrm{n}} \tag{3.1}$$

where n in number of cells, η_{fc} is fuel cell efficiency and 1.482 V corresponds to the hydrogen higher heating value (HHV) (Feroldi & Basualdo, 2012). For hydrogen, the HHV is used when the amount of released hydrogen heat energy is measured by cooling its combustion vessel to 25 C (initial temperature of vessel). In contrast, 1.254 V is used in equation (3.1), which corresponds to the lower heating value (LHV) when the vessel cooling is halted at 150 ℃. The hydrogen LHV is used when the efficiency will be compared to internal combustion engine for transportation. However, many researcher reported fuel cell efficiencies using hydrogen HHV. Equation (3.1) cannot be used to calculate the efficiency of the entire system because this formula provides the instant

efficiency of the stack that is proportional to the stack's voltage. The system's efficiency during the experimental time is computed using the following equation:

$$\eta_{\text{fcsystem}}, \% = \frac{100\% \times \text{generated electric energy}}{\text{energy of cunsumed } H_2} \quad (3.2)$$

The mass of the consumed hydrogen stored in a metal hydride tank for our experiment is calculated using the ideal gas law because the bicycle tank had been directly charged from a buffer tank of an electrolyzer system. The energy content of the hydrogen LHV is 241.98 $kJmol^{-1}$, or 120.1 $MJkg^{-1}$. Hydrogen can release this energy via ignition heat. Hence, the energy of consumed hydrogen for lower heat values is calculated using the following equation:

$$\text{Energy of consumed } H_2, \text{kJ} = \frac{241.98 \times \Delta p \times V}{R \times T} \quad (3.3)$$

where $\Delta \boldsymbol{p}$ is the pressure drop (atm) of the electrolyzer storage tank after charging the bicycle metal hydride tank, V is the volume (L) of an electrolyzer buffer tank, T is the temperature (K) of the buffer tank, and R is ideal gas constant, 0.08206 L atm mol^{-1} K^{-1}. Because 1W.h =3.6 kJ, the numerator of the equation (3.4) can be defined as follows:

$$\text{Generated electric energy, kJ} = 3.6 \times \sum (V \times I \times \Delta h) \quad (3.4)$$

During the transfer of two electrons from water molecules in fuel cells, the ideal cell voltage or standard potential to produce water in a liquid state (25 ℃, 1 atm) is 1.23 V, while the voltage drops to nearly 1.18 V for producing water in gaseous state or at operating temperatures exceeding approximately 80 ℃. Therefore, the theoretical or maximum efficiency of fuel cell was calculated to be 83% and 94.1% for HHV and LHV, respectively, by substituting the standard voltage in Equation (3.1).

Nevertheless, the experimental efficiency is expected to be lower than the theoretical efficiency for emerging losses even without being connected to any external

load. Furthermore, the efficiency is expected to steeply decline when the load is connected because the voltage drops due to inevitable losses generated by the electrical current in a closed circuit. Furthermore, a fraction of the power generated by a primary fuel cell is used by the required auxiliary components, which include the control unit, blowing fan, cooling fan, and battery.

3.5 Data-set

The Data-set which was used for training and evaluation of the regression algorithms consisted of 720 data points from different states of system. The data included current, voltage, temperature, hydrogen flow rate, oxygen flow rate, related humidity and efficiency. Based on the advanced machine learning consideration in accurate designing of a regression model, 60% of the data was used for training, 20 % for cross-evaluation and 20% for testing the algorithm. The exact number of dataset for training the algorithm to obtain the highest accuracy in evaluation dataset was chosen based on information extracted from the learning curve. Cross-validation and training data sets have been used for optimizing the regression algorithm parameters. However, data-set was pre-processed for better performance of the models.

Five variables have been used as inputs (current, hydrogen flow rate, oxygen flow rate, temperature, related humidity) of regression models to predict voltage and efficiency as desired system outputs.

3.5.1 Data normalization

In this system, parameter values varied in the range and their standard deviations. Therefore, data was normalized to facilitate the training by providing a greater homogeneity of the input and output variables. In order to normalize the data mean has been calculated and consecutively standard variation of each variable has been computed as:

$$S = \sqrt{\frac{\sum_{i=1}^{n}(x_i - \bar{X})^2}{n-1}} \tag{3.5}$$

Where *n* is number of random samples. The z-score of value *x* is computed by:

$$z = \frac{x - \bar{X}}{S} \tag{3.6}$$

Where x is the sample data with mean $\bar{X}$ and standard deviation named S. Standardization of data or z-score calculated the distance between raw data and mean in terms of standard deviation. When the raw score is below the mean the sign of z-score is negative and is positive when the score is above (Abdi, 2007).

3.5.2 Principle component analysis (PCA)

Processing time is one of the most essential factors in introducing reliable real-time systems. Simplicity of the model as well as reducing the calculation needed are two main affected factors which can be provided by reducing the dimensionality of input variables. Principle component analysis (PCA) is a useful statistical technique for finding patterns to reduce the dimension of data set and it is a powerful tool for data analysis without losing more than 1% of data.

This section briefly describes the steps needed to perform PCA analysis on a set of data. Figure 3.6 shows the parameters that apply to our model.

Step1: Get input data-set as an $m \times n$ matrix where number of measurements is denoted by m and the number of trails by n.

Step2: Subtract the mean, which is the average across each dimension.

Step3: Compute the covariance matrix. For more details on covariance calculating see (Smith, 2002).

Step4: Calculate the eigenvectors and eigenvalues of the covariance matrix based on singular value decomposition algorithm. These calculations give us more information about the data.

Step5: Choose the component and form a feature vector, which complies to the concept of data compression and reduces dimensionality.

Step 6: Deriving the new data set, which is the final step in PCA

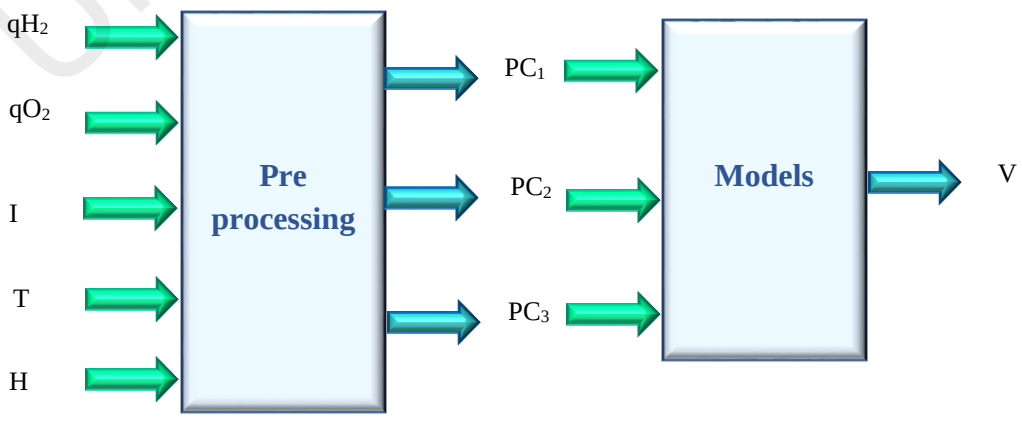

Figure 3.6: qH2: hydrogen flow, qO_2: oxygen flow, I: current load T: temperature, H: humidity

PCA has been applied on input data (current, temperature, related humidity, hydrogen flow rate and oxygen flow rate) only to reduce the complexity of calculations and to decrease the processing time.

3.6 Regression models

Researchers predict the performance of fuel cell as a function of various operating conditions by using empirical modelling. These models avoid identifying the knowledge of process parameters which is difficult to determine from fuel cell system. Empirical modelling of the system is based on setting measurable parameters and choosing appropriate inputs for predicting the behaviour of interested outputs.

For an accurate modelling of the PEM fuel cell output voltage and system efficiency, two approaches have been used in this study. First approach based on linear modelling using linear regression algorithm. Artificial neural networks has been used for non-linear modelling of the system as the second approach. In both models, related humidity (RH), current (I), oxygen flow rate (qO2), temperature (T) and hydrogen flow rate (qH2) were set as input variables and fuel cell voltage (v) and efficiency (eff) were the predicted values. Collected data was randomly divided into three groups for training (60 %), cross validation and test dataset. The remaining 40% of the data was randomly assigned into two equal groups for cross-validation and test datasets accordingly. In both regression models, advanced machine learning principles were considered for optimizing the designs based on learning curve and error processing results as shown in Figure 3.7 (Perlich, 2011). The number of training data sets was chosen based on learning curve analysis and cost function during the training procedure in order to overcome the high bias (under-fitting) and high variance (over-fitting) problems.

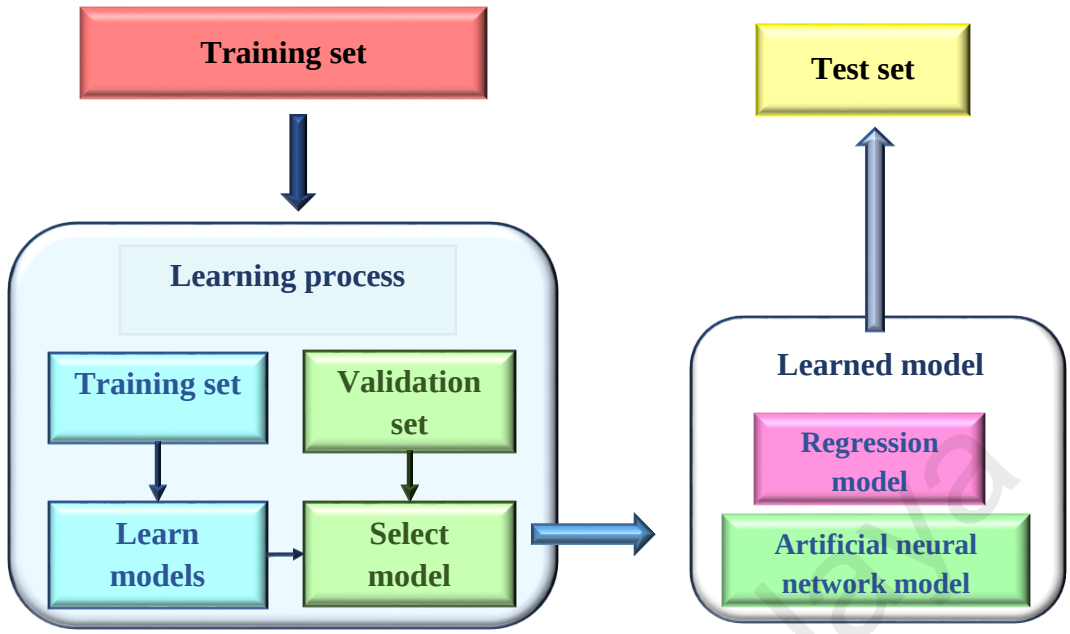

Figure 3.7: Flowchart depicts the training process of regression models. Training and validation datasets were used for model training and optimization of model parameters. Test data set was used for evaluation of final design

3.6.1 Linear Regression

Classical linear regression method is most commonly used in linear modeling the behavior of structural systems. Linear regression is a method for calculating the relation between explanatory variable and depended variable by fitting the linear equation to the observed data. Figure3.8 shows the basic linear regression model.

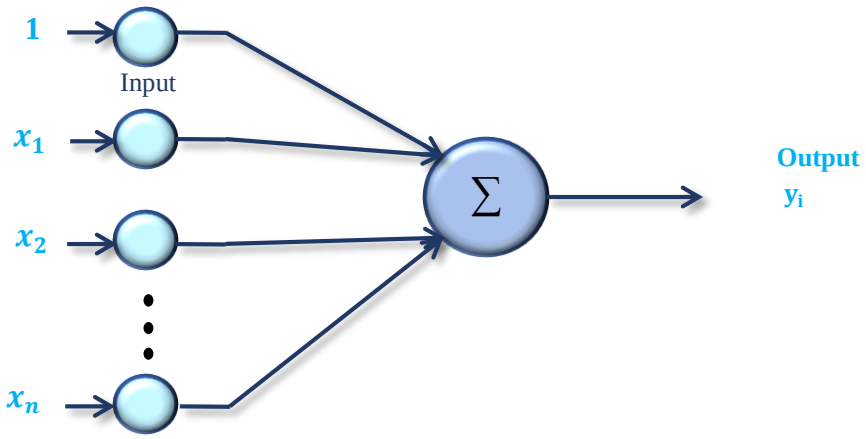

Figure3.8: Linear regression configuration

The multiple linear regression equation given n features is denoted as:

$$h\theta(x) = \theta_0 + \theta_1 x_{i1} + \theta_2 x_{i2} + \cdots + \theta_k x_{ik} \;\; for\; i = 1,2,..,n \tag{3.7}$$

where x is explanatory variable, and $h\theta(x)$ is the predicted value (hypothesis), θ_0 is the intercepts, and θ is the estimated slope coefficient of the line.

By vectorising equation (3.5) we have:

$$\begin{gathered} h\theta(x) = \theta^T x \\ \theta = [\theta_0, \theta_1, \dots, \theta_{n+1}] \\ x = [x_0, x_1, \dots, x_{n+1}] \\ \text{While} \quad x_0 = 1 \end{gathered} \tag{3.8}$$

The error term(ε) of this model is the difference between the real value (y) and the predicted value (h) of equation (3.3) which is calculated by Mean squared Error (MSE) of the difference between the predicted values and the actual value ($h\theta(x_i)$- y_i) as shown in equation (3.4) which is referred to as the cost function $J(\theta)$:

$$y - h\theta(x) = \varepsilon \tag{3.9}$$

$$J(\theta) = \frac{1}{2m}\sum_{i=1}^{m}(h\theta\,(x^{(i)}) - y^{(i)})^{2} \tag{3.10}$$

Where m is the number of iterations and $J(\theta)$ is function of the parameter vector.

The objective of linear regression is to estimate the unknown parameters while cost function is minimum. To fulfill these requirements, a fundamental algorithm called Gradient Descent (GD) is used as a promising method for estimating the interception vector θ in order to minimize the cost function (MSE).

3.6.1.1 Gradient Descent

In this project, Gradient descent algorithm was used for updating the system weights (θ vector) to calculate our hypothesis automatically. In gradient descent algorithm, each θ value is updated based on the derivation of cost function and a learning rate value (α).

The values are updated by assigning new value for θ using the previous values to achieve a lower MSE:

$$\begin{aligned} \theta_j &:= \theta_j - \alpha \frac{\partial}{\partial \theta_j} J(\theta) \\ &= \theta_j - \alpha \frac{\partial}{\partial \theta_j} \frac{1}{2m} \sum_{i=1}^{m} (h\theta\,(x^{(i)}) - y^{(i)})^2 \\ &= \theta_j - \alpha \sum_{i=1}^{m} (h\theta\,(x^{(i)}) - y^{(i)})\, x_j^i \end{aligned} \tag{3.11}$$

It is noteworthy that the updating of θ_j vector should be done simultaneously for all θ in each step for $j = 0, \ldots n$. This process would be continued until convergence of Y and $h\theta(x)$, where m is the size of training set and the value of the training set data is shown by $x^{(i)}$, $y^{(i)}$.

As shown in Figure 3.9 GD moves the weights in order to decrease the derivation of MSE function. The final values of theta are the actual weights of the prediction model.

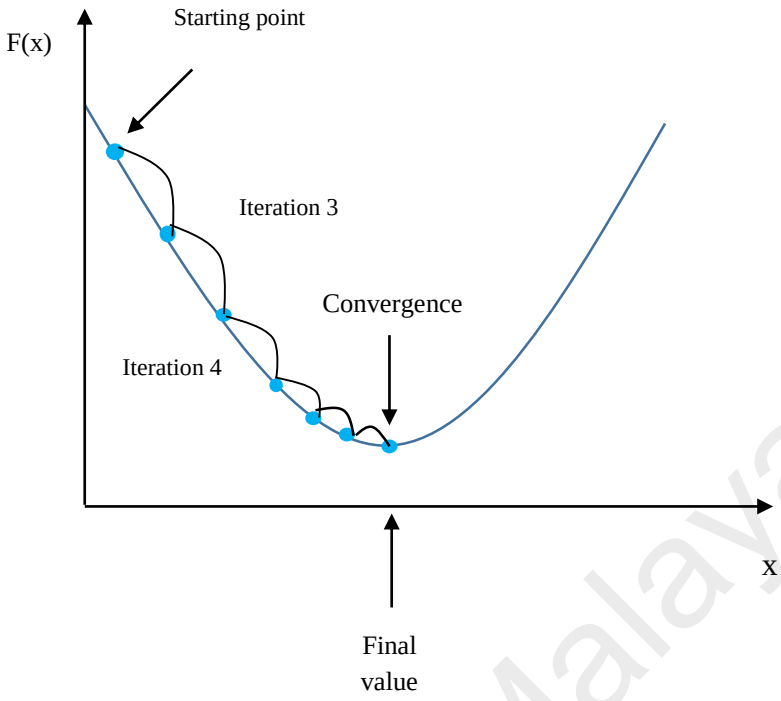

Figure 3.9: Gradient decent

3.6.1.2 Learning curve

In order to have the best possible prediction, training data was split into three parts: training set, cross validation set and testing set. As a general rule, 60% of the sample are training set and 20% for each of cross validation and test set. A learning curve is a plot of the training and cross validation mean square error versus the index of the training data set. These plots are useful to find better prediction of the system; i.e. how beneficial it will be to add more data to training set. When both training set and cross validation set are converging to a low value, there is no need to add more data to the training set.

3.6.2 Artificial Neural Network (ANN)

For non-linear modeling of the system, artificial neural network (ANN), a mathematical computation model introduced by McCulloch and Pitts in 1943, was used. In the 1950's, some development of neural network in both theory and practice occurred (Braspenning, Thuijsman, & Weijters, 1995). Ability to learn from the input data with or without teacher is one of the features of neural networks. Nonlinearity, adaptively, input output mapping and fault tolerance are other important features. In ANN, can be defined as computational tools which make the experimental knowledge to be available to be used (Zilouchian & Jamshidi, 2000).

Currently, various fields of neural network applications have been developed such as pattern recognition, time series analysis, signal processing, modelling and control. The structure of artificial neural network neuron is based on a simple mathematical model of the human brain.

3.6.2.1 The Neural Network Basic Architecture

Neural network consists of several neurons connected to perform a specific task. A processing unit, as shown in Figure3.10, is the basic component of neural network. The synaptic weight represents acquired knowledge that has been used to connect each input to a neuron.

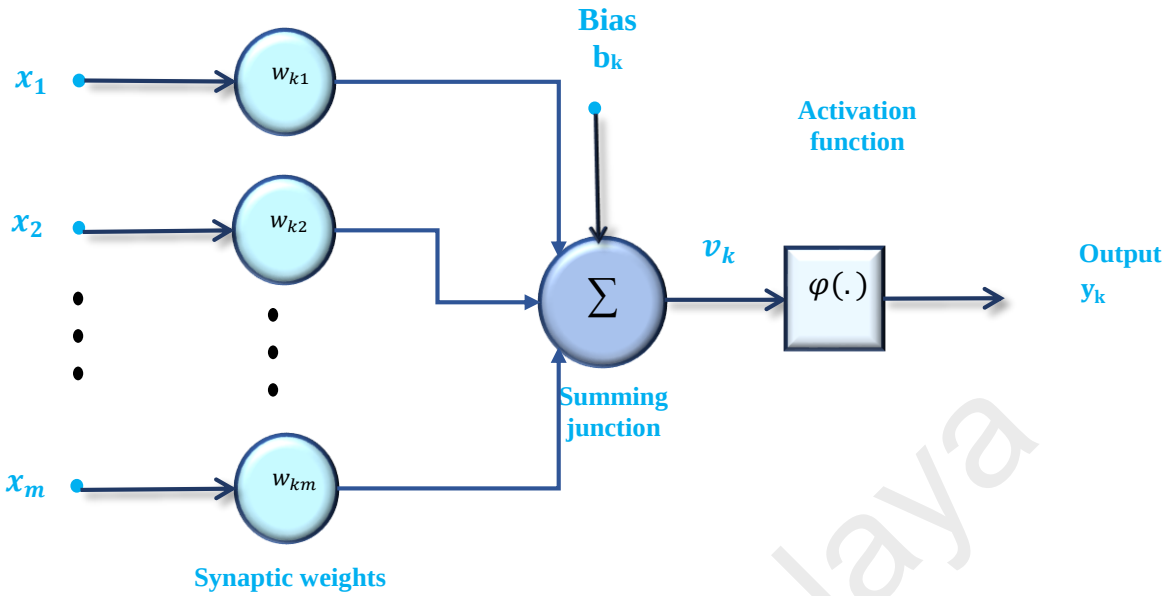

Figure3.10: Artificial Neuron configuration

A nonlinear model of neuron's output can be described as follows:

$$u_k = \sum_{j=1}^{m} w_{kj} x_j \tag{3.7}$$

Synaptic weights (w_{kj}) are multiplied by each input (x_m) in the neuron k, and the output is computed as:

$$v_k = u_k + b_k \tag{3.13}$$

The general model output of neuron shown by y_k, and $\varphi(.)$ is the activation function effected by bias for limiting the amplitude and defines the output of neuron (Sablani, Datta, Rahman, & Mujumdar, 2006).

$$y_k = \varphi(u_k + b_k) \tag{3.148}$$

3.6.2.2 Network Architecture

Learning algorithm and network architecture are two important factors for better network training performance. The fundamental neural network architecture that we use in this work is multiplayer feed-forward network.

The most popular neural network is multiplayer feed-forward network that has one or more hidden layers. For extracting higher order of the network, one or more hidden layer is added which might tend to smoothing the network output. As shown in Figure 3.11 multiplayer feed-forward networks have one input, one or more hidden layer and one output. In the input layer, neurons operate by receiving the signal from the user. Through the connections, signals are moved to the hidden layer. In networks that have more hidden layers, the input of the second hidden layer is the output of the first hidden layer and so on. To produce the network output, the signals are transmitted to the output (Sablani et al., 2006).

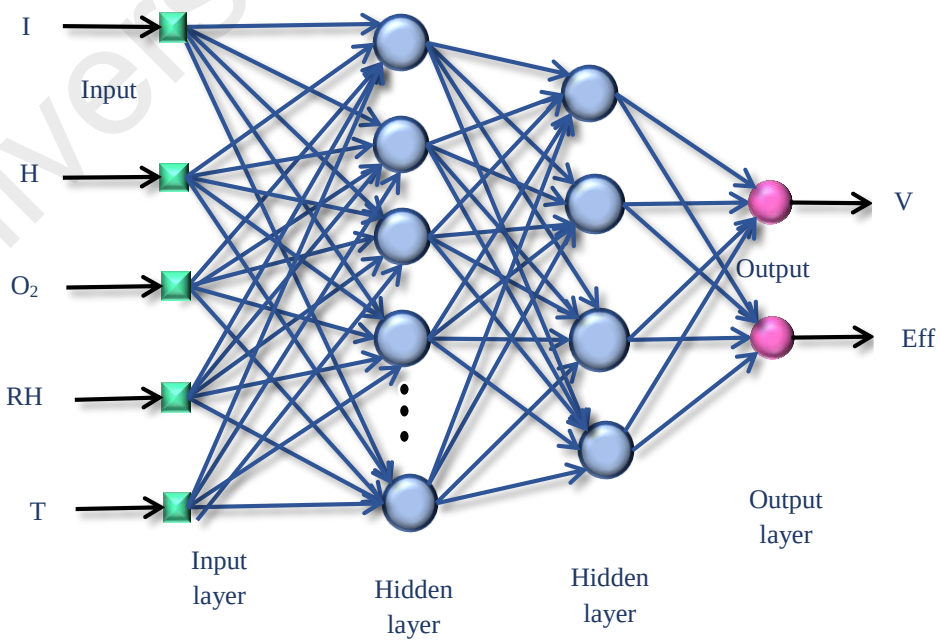

Figure 3.11: Multiplayer Feedforward Network, where I: current, H_2: hydrogen flow rate, O_2: oxygen flow rate, RH: related humidity and T: temperature as an inputs and V: voltage and EFF efficiency of system as an outputs

Levenberg-Marquardt back propagation algorithm is a variation of Newton's method, which implies a simplified form of Hessian matrix applied to train the proposed neural network model. The sum of square error is denoted by $F(x)$and combination of the weights matrix and bias is indicated by x. Hessian matrix $H(x)$ is described as follows (Gavin, 2011).

$$H(x) = \nabla^2 F(x) = 2J^T(x)J(x) \tag{3.15}$$

The gradient g(x) can be calculated as:

$$g(x) = \nabla F(x) = 2J^T(x)v(x) \tag{3.16}$$

Where $v(x)$ is a vector of network error, and $J(x)$is the Jacobian matrix

The LM-BP algorithm can be calculated by the following equation:

$$x_{k+1} = x_k - [J^T(x_k)J(x_k) + \mu_k I]^{-1} J^T(x_k)v(x_k) \tag{3.17}$$

Parameter μ_k is multiplied by some factor (θ) whenever a step increases $F(x)$. μ_k is divided by (θ) when a step is reduced $F(x)$ (the algorithm begins with μ_k set to a small value, such as $\mu_k = 0.01$and $\theta > 1$). The algorithm becomes the steepest descent while $\mu_k$is large with step $1/\mu_k$ and the algorithm becomes Gauss-Newton when $\mu_k$is small which provides rapid convergence and procedures approximating Hessian matrix. For effective agreement between the guaranteed convergence of the steepest descent method and the speed of Newton's method, LM-BP algorithm is used.

3.6.3 Fuzzy Cognitive Map:

Fuzzy cognitive map (FCM) introduced by Kosko in 1986 is a soft computing tool based on fuzzy logic (FL) and neural network (NN) methodologies (Kosko, 1986; O. Motlagh et al., 2012). FCM is classified as a neuro-fuzzy system which can easily incorporate and adapt human knowledge and represent a given system with a set of concepts and common relations between them. Inclusion of uncertainties is the one promising feature of FCM which means when less knowledge about the variable is available, no precise initial node weight is needed, and therefore FCM is more robust. Currently, various areas of the fuzzy cognitive map applications such as medicine, international relations, political science, history and engineering are being developed.

Relationship representation is the most significant improvement concern of FCMs. This means instead of using only sign, the degree of considered casual relation is associated with a number (weight) (Stach, Kurgan, & Pedrycz, 2005). The strength of relationship is described by a number from [-1, 1] interval. Promoting effect is reflected by positive values, while inhibiting effect corresponds to negative value. Value of +1 represents full positive, -1 corresponds to full negative, with neutral relation defined by 0. Other values are used for different fuzzy levels of casual effect.

As mentioned above, a FCM model is represented in the form of graphs. In a graphical representation, set of nodes (concept, C_i) and their connection edges correspond to causal effect relationships, represented by weights (W_{ij}) between them. Three possible types of causal relationships between concepts are expressed as follow: $Wij > 0$ indicates positive causality between two concepts which means increasing the value of one concept leads to increasing the value of the other concepts. $Wij < 0$ indicates negative effect

between two concepts which means increasing the value of one concept causes a decrease in another concept. Wij = 0 means there is no relationship between the two concepts.

Model can be presented by a square matrix, which is known as connection matrix. All values of edge weights between corresponding concepts are stored in rows and columns of this matrix (Stach, Kurgan, Pedrycz, et al., 2005). Figure 3.12 shows a FCM model and its connection matrix.

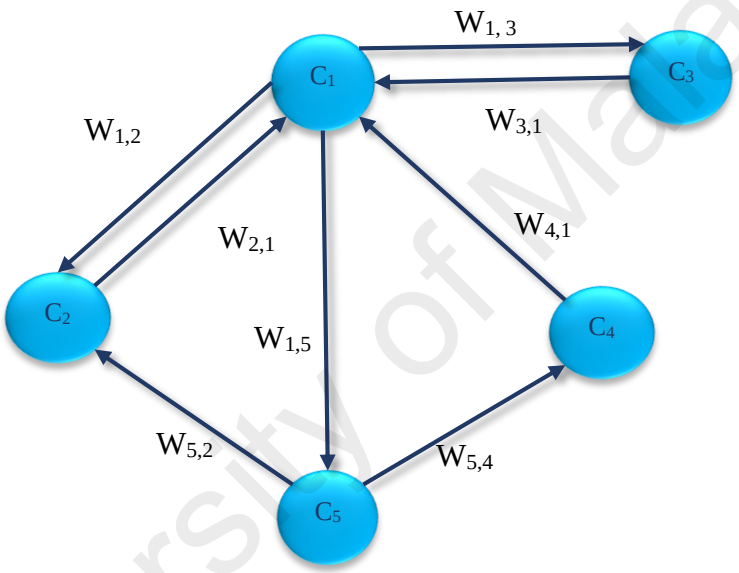

	C1	C2	C3	C4	C5
C1	0	$W_{2,1}$	$W_{1,3}$	0	$W_{1,5}$
C2	$W_{2,1}$	0	0	0	0
C3	$W_{3,1}$	0	0	0	0
C4	$W_{4,1}$	0	0	0	0
C5	0	$W_{5,2}$	0	$W_{5,4}$	0

Figure 3.12: Example of FCM graph and corresponding connection matrix

Model can be simulated when the primary values of concepts have been determined as primary state of whole system and consequently FCM has been created. Simulation of the system's dynamic is performed by functional modelling of FCM based on equation (3.18):

$$\forall\, j \in \{1, \dots, N\}, C_j(t+1) = f\left(C_j(t) + \sum_{i=1}^{N} e_{ij} C_i(t)\right) \qquad (3.18)$$

where $C_j(t)$ is activation degree of concept j^{th} at time t, e_{ij} denotes the relationship strength between concept C_i with concept C_j if $i \neq j$ and $e_{ij} = 0$ if $i = j$, and finally f is transformation function comprised of the periodic relationship between $C(t+1)$ and $C(t)$ for $t \geq 0$ (Stach, Kurgan, & Pedrycz, 2005).

Starting point of simulation consists of computing initial values of the state vector over a number of successive iterations. Present values of all nodes in specific iteration are determined by state vector. Former iteration values of nodes which influence the given node through cause-effect relationship are used to calculate the value of a given node. Iterative application of the equation (3.18) leads to calculating successive states.

The transformation function is used to preserve the weighted sum within a certain range normally set to [0, 1]. Quantitative analysis is lost by applying nonlinear transformation function, but comparison of activation levels which can be defined as active (value of 1), in active (value of 0) and active to a certain degree (value between 0 and 1). Some commonly used threshold functions are listed below:

1) Bivalent

$$f(x) = \begin{cases} 0, & x \leq 1 \\ 1, & x > 0 \end{cases} \tag{3.19}$$

2) Trivalent

$$f(x) = \begin{cases} -1, & x \leq -0.5 \\ 0, & 0.5 < x < 0.5 \\ 1, & x \geq 0.5 \end{cases} \tag{3.20}$$

3) Logistic signal

$$f(x) = \frac{1}{1 + e^{-cx}} \tag{3.21}$$

Where c is a real positive number and x is the value $C_j(t)$ on the equilibrium point. To reduce the unbounded weighted sum to a certain range, the threshold function can be used.

3.6.3.1 Learning algorithm

Learning algorithms can train the FCM which means determining the weights for best-fit decision-making. The most important algorithms for training FCM are classified into Hebbian-based, Population-based and Hybrid algorithms.

3.6.3.1.1 Hebbian learning algorithm

Hebbian based method updates the FCM weights based on Hebbian law and available data. More successful weight matrices are then produced. Hebbian learning algorithm increases the efficiency, flexibility and dynamic behavior of FCM model. For training FCM the most efficient Hebbian based methods are the following:

3.6.3.1.2 Nonlinear Hebbian learning (NHL)

The NHL is based on the nonlinear Hebbian learning raw for training the FCM. NHL is based on the assumption that at each iteration, all the concepts are triggered and synchronously update their value. Initial FCM and values of concepts are taken by learning algorithm, and until the desired map is defined, weights keep on being updated. The values of other weights which remain zero do not change. During the learning process the nodes which are directly connected are updated according to their physical incorporation. For the entire learning process, the weight values retain their initial sign and direction as suggested by experts.

For finding the weights of neuron Oja learning rule is introduced which can be expressed as follows:

$$e_{ij}(k) = e_{ij}(k-1) + \eta C_j(C_i - sgn(e_{ij})C_j e_{ij}(k-1)) \qquad (3.22)$$

Where $C_i \; and \; C_j$ are the current activation values of concept $i^{th} \; and \; j^{th}$ calculated for each iteration, $e_{ij}(k)$ is the value of the weights between concepts $i^{th} \; and \; j^{th}$ and η is the learning coefficient.

Hebbian learning principle is based on the premise that weights update e_{ij} and the product of the C_i and C_j concept activation are proportional. However, this may lead to infinite growth of the weight values. Oja learning rule uses *forgetting term* to avoid this effect that is reduced by iteration. In this method, the forgetting term is proportional to weight values and square of the value of target concepts (fore_{ij}, C_j is the concept).

This method has two conditions. The first one is the Desired Output Concepts (DOC) which utilizes information on desired value of some concepts and usually has predefined desired values. For each specific problem, when all desired concepts reach or become close enough to the desired activation level, the learning may be completed. The second condition takes into consideration the variation of the subsequent values of the DOCs and is held if all of them change less than a predefined very small constant *e*. Algorithm stops the learning process when *e* is larger than the variation in DOCs.

3.6.3.1.3 Data-driven nonlinear Hebbian learning (DD-NHL)

The DD-NHL is based on an improved version of NHL principle and applied on the historical data to train the model. For training fuzzy cognitive map, seven steps of generic NHL and proposed novel approach of learning FCM which is called DD-NHL(Stach et al., 2008) are described:

Non-linear Hebbian algorithm:

Step 1: $C(0)$ $known\ as\ value\ of\ concepts$ and $E(0)$ as the connection matrix and restriction imposed on desired value of DOCs in form of $C_j^{Min} \leq C_j \leq C_j^{Max}$

Step 2: For each iteration step *k*

Step 3: according to equation (3.22) update the weights

Step 4: according to equation (3.18) for each concept calculate $C(k)$

Step 5: Evaluate termination condition using $C(k)$ from step 4, $E(k)$and $E(k-1)$

Step 6: When both termination conditions are fulfilled go to step 2

Step 7: Return the final connection matrix W_{FINAL}

Two conditions from step 6 can be defined as follows:

Condition1: (minimize the cost function *F)* for each $f = \sqrt{\sum_{DOC_j} \left\| C_j(k) - T_j \right\|^2}$ where T_j is the mean target value of the concept C_j mean: $T_j = \frac{C_j^{Max} - C_j^{Min}}{2}$

Determining the set of weights is the objective of the training process that minimizes function *F*.

Condition 2: (after limited number of steps, terminate the algorithm)

Step 1: Calculate the maximum difference e_{max} between $e_{ij}(k)$ and $e_{ij}(k-1)$

Step 2: Return "True" if the absolute value of e_{max} is less than ε, otherwise return "False".

Now assume that for the given system the historical data are available. Matrix D is formed, where d_{ij} is related to the value of i^{th} concept at the j^{th} time point. In other words, value of concepts is defined as time series. Size of matrix *D* is $K \times N$ where the number of available data points is denoted by K and the number of concepts in modeled system is defined by N. Figure 3.13 shows the flowchart of NHL algorithm.

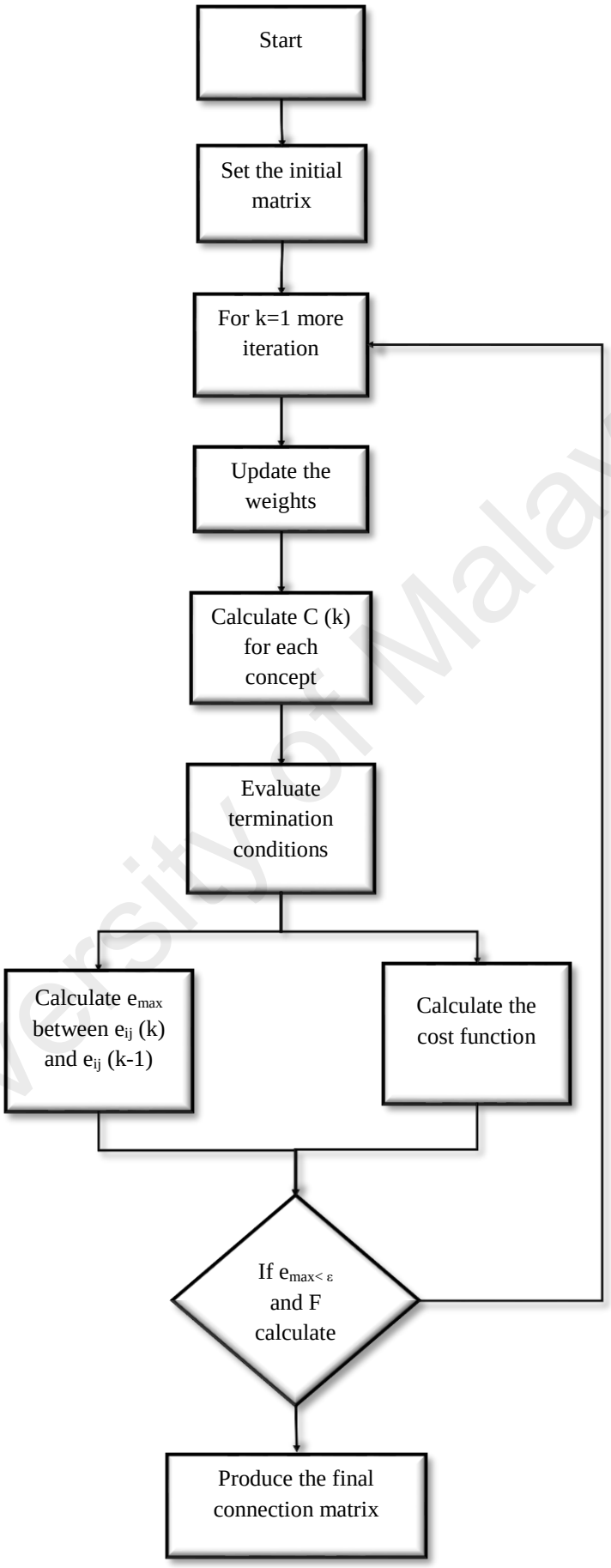

Figure 3.13: Flowchart of NHL

Available historical data in *step 4* are used by data-driven nonlinear Hebbian learning (DD-NHL) which is improved as the follows:

Step 4: Define $C(k)$ in accordance with the next row of matrix *D.*

Therefore, based on available data used in each iteration step, the matrix is updated. Same data points are utilized when all data points are exploited and the termination conditions are not satisfied. Essentially, Oja learning rules are used in DD-NHL, but for a given system it takes advantage of the data available instead of creating the data used for training only from the current model. Initial connection matrix is still needed in DD-NHL but randomly generated initial map can be used instead of on expert generated map.

Until the stable state is obtained, from primary state vector, current FCM is simulated after each iteration of updating the weights. Then, the value of DOCs from this state and the desired value of DOCs, are compared. When the answer is found, this technique guarantees it would meet all the learning conditions. Figure 3.14 displays the flowchart of DD-NHL algorithm. Thus, condition 1 is defined as follows:

Condition 1: (checking condition imposed on DOCs)

Step 1: Until the fixed state is reached simulate the current FCM defined by $E(k)$ starting from the initial condition $C(0)$.

Step 2: For each C_j that has been defined as DOC_j, check whether the fixed value $C_j(n)$ meets the constraint $C_j^{Min} \leq C_j(n) \leq C_j^{Max}$

Step 3: Return "False" if there is at least one C_j that does not meet the limitation from step 2.

Step 4: otherwise return "True".

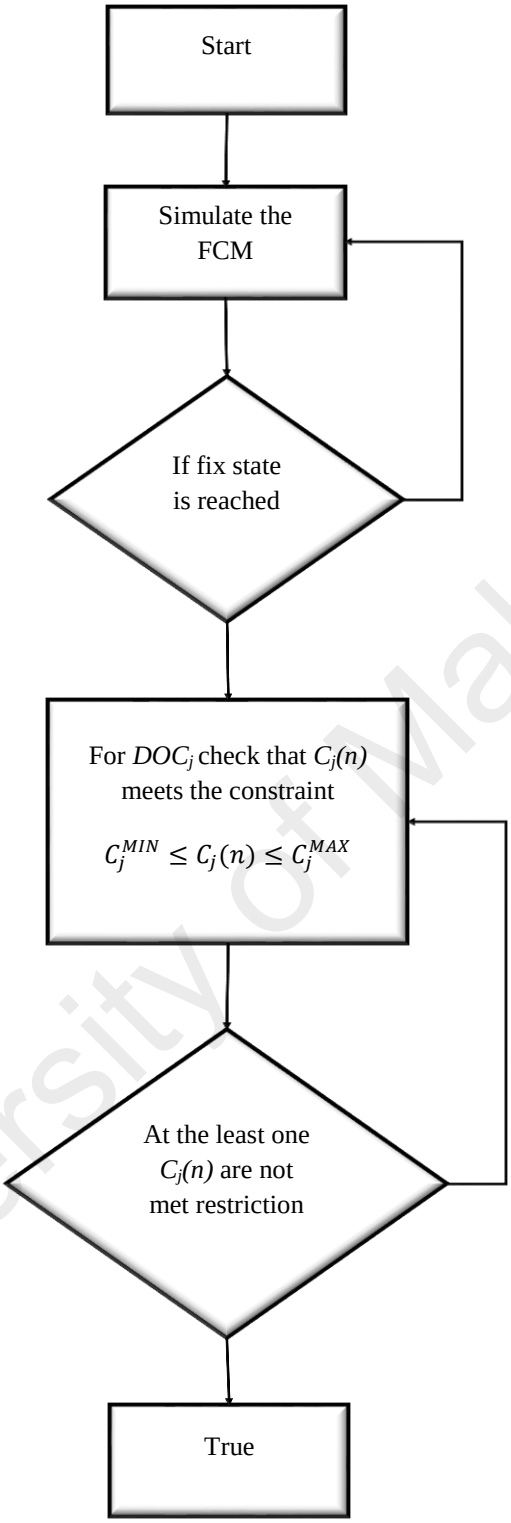

Figure 3.14: Flow chart of DD-NHL

3.6.3.2 Rule base fuzzy cognitive maps (RB-FCMs)

RB-FCM added feedback and mechanism to deal with casual relations to the standard rule based fuzzy system. As shown in Figure 3.15 RBFCM consists of fuzzy nodes (concepts) and fuzzy role bases (relations). Several membership functions (MF) are related to each concept that represent the possible values of concepts or their changes. Relations such as similarity, opposition, implication, classical fuzzy reasoning, etc. can be represented by fuzzy rules. RB-FCM are iterative which means previous values of each concept are used to compute its current value. RB-FCM allows the answer to "what if" question using not just casual maps but cognitive map.

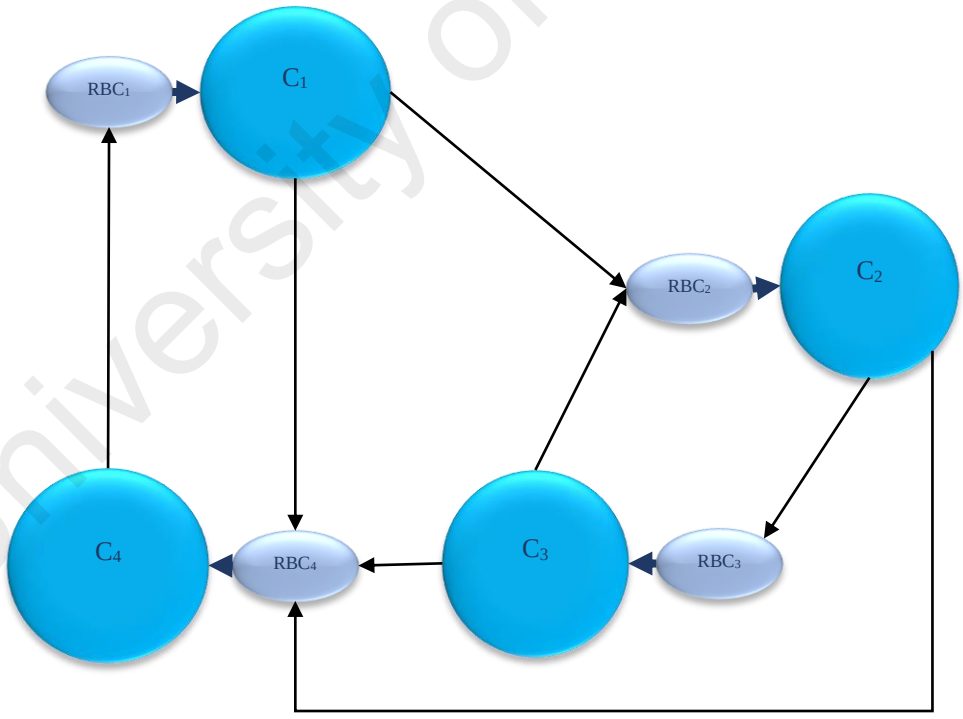

Figure 3.15: Rule based fuzzy cognitive map structure

3.6.3.3 Linguistic variables influence for FCM weights

This methodology presented here makes fuzzy cognitive map structure closer to fuzzy logic. The influence of concept C_i on concept C_j which has been determined by experts as negative or positive and with linguistic variables describe the grade of influence such as "strong", "weak" and etc. The interval of linguistic variable, is [-1, 1] and its term set T (influence) is suggested as: negatively very strong, negatively strong, negatively medium, negatively weak, zero, positively weak, positively medium, positively strong, positively very strong.

Figure 3.16 shows the membership function characterized by fuzzy sets. Semantic rule *M* can be defined as follows:

- *M* (negatively very strong): membership function μ_{nvs} describe fuzzy sets for "an influence below to -75%".

- *M* (negatively strong): membership function μ_{ns} describe fuzzy sets for "an influence close to -75%".

- *M* (negatively medium): membership function μ_{nm} describe fuzzy sets for "an influence close to -50%".

- *M* (negatively weak): membership function μ_{nw} describe fuzzy sets for "an influence close to -25%".

- *M* (zero): membership function μ_z describe fuzzy sets for "an influence close to 0".

- *M* (positively weak): membership function μ_{pw} describe fuzzy sets for "an influence close to 25%".

- *M* (positively medium): membership function μ_{pm} describe fuzzy sets for "an influence close to 50%".

- *M* (positively strong): membership function μ_{ps} describe fuzzy sets for "an influence close to 75%".

- *M* (positively very strong): membership function μ_{pvs} describe fuzzy sets for "an influence above to 75%".

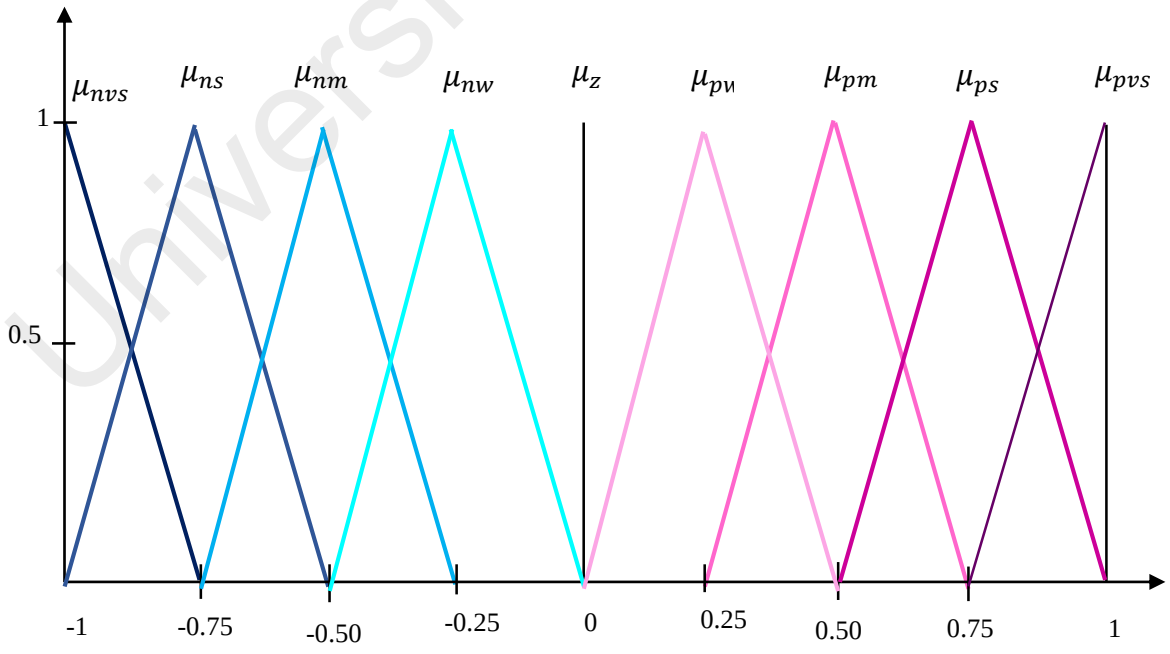

Figure 3.16: Membership function for influence of the linguistic variables

Each interconnection defined by linguistic variables are combined and the interval of overall linguistic variables is transformed to [-1, 1]. A numerical weight for each interconnection will be the outcome of the defuzzifier where the Centre of Gravity method is used to produce these weights. Figure 3.17 display flowchart of linguistic variable influence for FCM.

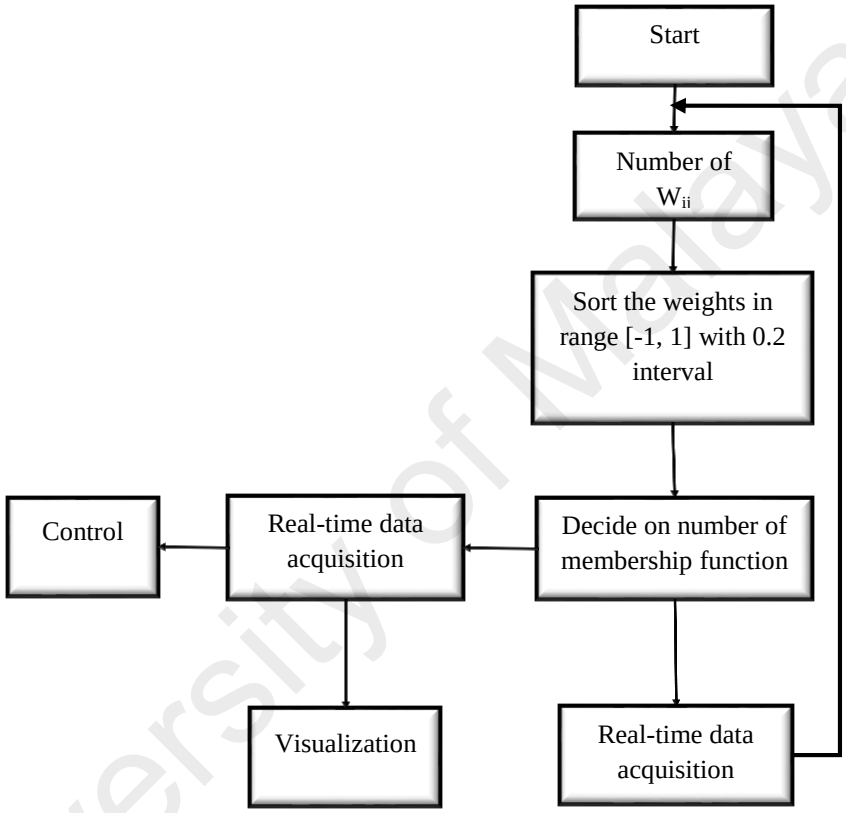

Figure 3.17: Flowchart of linguistic variable influence for FCM

This chapter has provided an in-depth and detailed of linear regression and artificial neural network modelling. Network architecture and learning algorithms of both modelling approaches are described. In addition, the fuzzy cognitive map algorithm is presented. The fuzzy membership function and linguistic variables of FCM are explained as well.

Chapter 4 : RESULTS AND DISCUSSION

4.1 Introduction

This study aims to develop a model and control strategy for electric bicycle powered by PEM fuel cell to improve the efficiency and performance of system. In the first phase of the study, efficiency of electric bicycle was computed as the main indicator for PEM fuel cell system performance. In the second phase of the study the modelling and performance analysis of PEM fuel cell electric bicycle system has been carried out. This includes the study and utilizing linear and nonlinear regressions for predicting overall PEM fuel cell efficiency and output voltage based on some fundamental variables namely current, temperature, humidity, hydrogen flow rate and oxygen flow rate. Finally, fuzzy cognitive maps were used for the first time in this field to design a dynamic FCM model for convenient control of system and real-time casualty calculation model among the system concepts (current, temperature, humidity, hydrogen flow rate, oxygen flow rate, voltage and efficiency). The validation of the applied cognitive model has been ensured by comparison with a set of experimental data extracted from electric bicycle system regarding electrical performance. In the following section each stage of result representation will be explored in detail.

4.2 Data collection

Data set was collected from electric bicycle powered by PEM fuel cell using DAQ system and are logged with sampling time of 1s to a designated computer. The installed fuel cell is a 250-W PEM fuel cell, which contains a 22 cell air-cooled stack that provides a nominal stack voltage and current at 14 V and 20 A. It generates a peak power of 250 W to a 25-kg bicycle with a rated consumption of 3.5 normal litters of H_2 per minute. The specifications of the fuel cell is listed in Table 4-1.

Table 4-1: Nominal Fuel cell specifications

Parameter	Supplier	Finding
Number of single cells	22	22
Maximum total power output (W)	About 250	About 180
Output voltage (V)	13-20	13-20
Nominal stack current (A)	20 (max 28)	18
Weight of the stack (kg)	0.7	0.7
Overall dimensions of the Fuel Cell system (blowers Inc.) (mm^3)	approx.230×220×150	approx.230×220×150
Ambient temperature range (°C)	>0 up to +35	>0 up to +35
Ambient relative humidity range (%) (recommended)	30-80	50
Hydrogen supply nominal pressure (bar)	0.65	0.65
Hydrogen supply minimum flow rate guaranteed (Nl/min)	3.5	3.5
Maximum purged hydrogen flow rate (Nl/min)	0.07	0.07

A 150-W electric motor drives the bicycle via the regulated voltage from DC/DC converter, which is connected to a 13.2-20.2 V unregulated output voltage of the fuel cell. The DC/DC convertor is 300-W convertor from Zahn Elect with efficiency of 92% (at Vin=12 V, I out=8.4 A) and recommended input voltage of 10-20 V.

The motor is activated by a handle bar mounted throttle, just like on most motorcycles or scooters. In the other words, this vehicle is to be operated on a power-on demand basis; the electric motor is only engaged and operated manually using a throttle, while the pedalling can be coupled with the motor in tough conditions, such as cycling uphill.

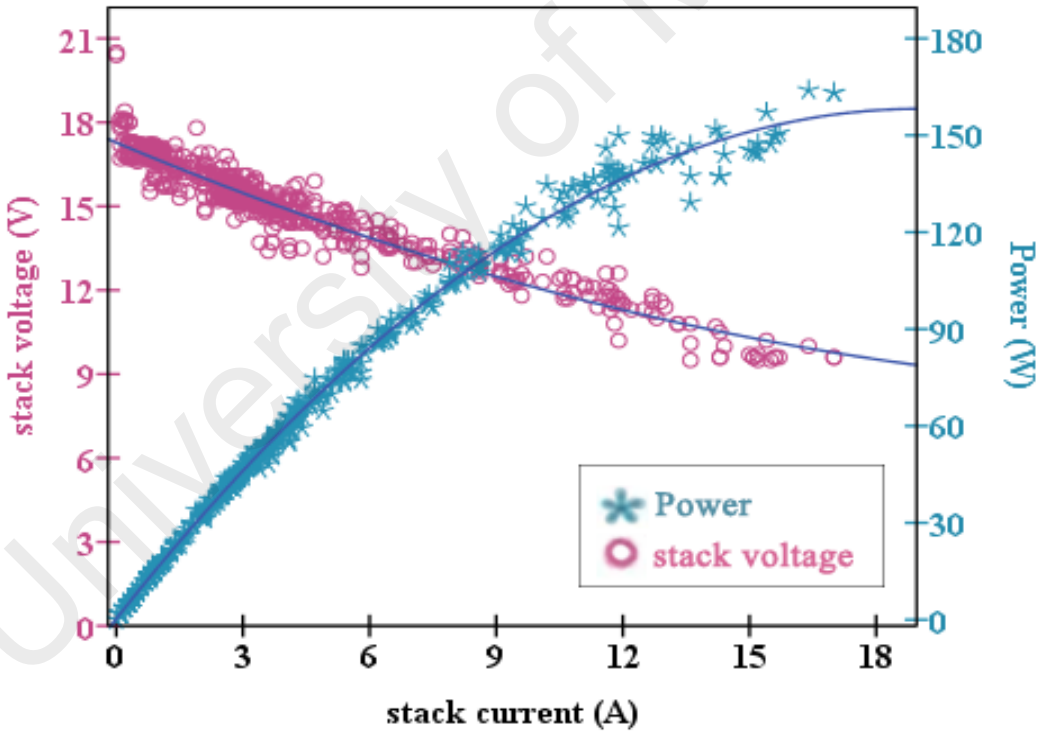

Figure 4.1: Plot of the voltage–current and power-current curves of Fuel Cell stack at temperature average of 37.6 °C

For a better visualization and operation dimensions of the system an example of V-I and P-I curves of PEM fuel cell system are shown in Figure 4.1 which have been obtained at approximately in constant fuel cell temperature 37.6 ℃ and relative humidity averaging 48.8%. This plot shows the changes in constant temperature and humidity condition which illustrates the typical V-I behaviour; the voltage monotonically decreases as the current increased. As the V-I curve shows, the pattern after the sharp voltage drop of the start-up experiences a steady linear decline when the current is increased.

While the load circuit is open, the current is close to zero, and the stack voltage is estimated to at least be close to the theoretical value. However, the voltage is often considerably less when a fuel cell is utilized. The following key points are evident from the graph of the cell voltage versus the current:

- The open circuit voltage is less than the theoretical value
- A sharp initial voltage decrease is anticipated
- The voltage then decreases less rapidly and more linearly

In addition, the stack at higher power production or current density releases more heat if the system design is imperfect; the overheating that occurs during tough working situations can disturb the normal operation of system.

Figure 4.2 shows that the ECU can perfectly control the temperature of stack and keep it almost constant. The humidity curve illustrates the humidity ratio of the input air.

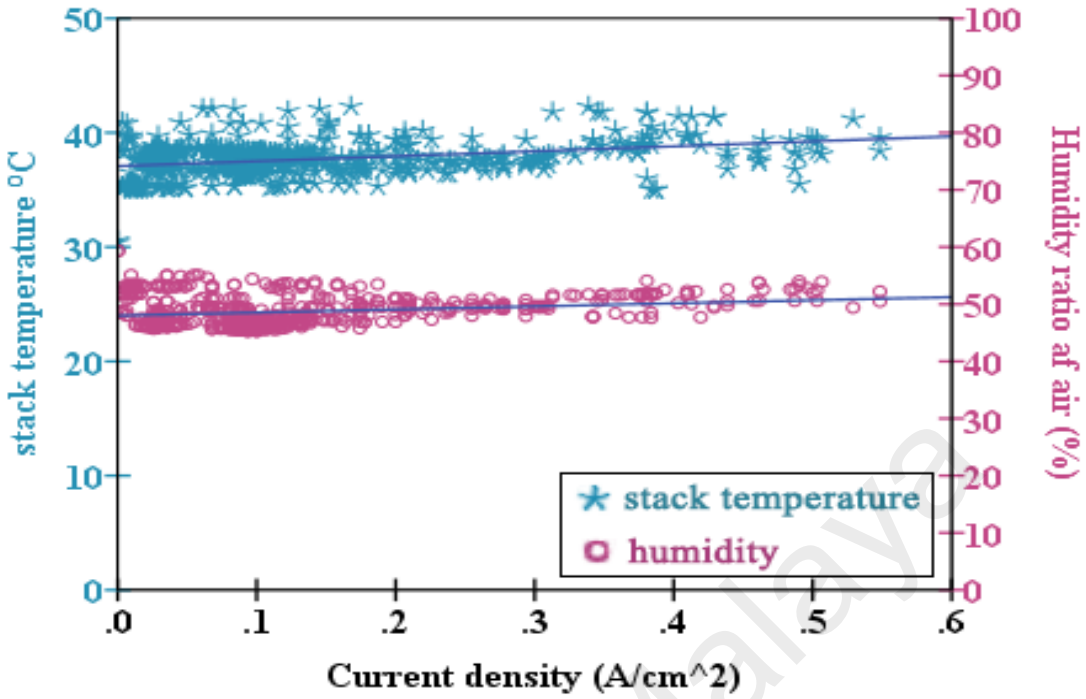

Figure 4.2: Plot of Stack temperature and air humidity ratio versus current density of Fuel Cell

4.3 System efficiency

To study the behaviour and compute the efficiency of such system, we decided to study, test, and analyse the features of an electric-assisted bicycle that is powered by a PEM fuel cell as a common and suitable type of power source for transportation systems.

The efficiency–power curve of a fuel cell stack is shown in Figure 4.3. It is plotted using equation 3.1 for hydrogen HHV. As expected, a maximum efficiency of the fuel cell's stack is available in the low power or current range, as the highest stack voltage is expected at an open circuit. Accordingly, while the stack power or current is increased, the efficiency will decrease. As previously mentioned, this characteristic is the opposite of the efficiency curve over power in an internal combustion engine, rendering the fuel cell superior in terms of city transportation, where at most only a small fraction of nominal power is required.

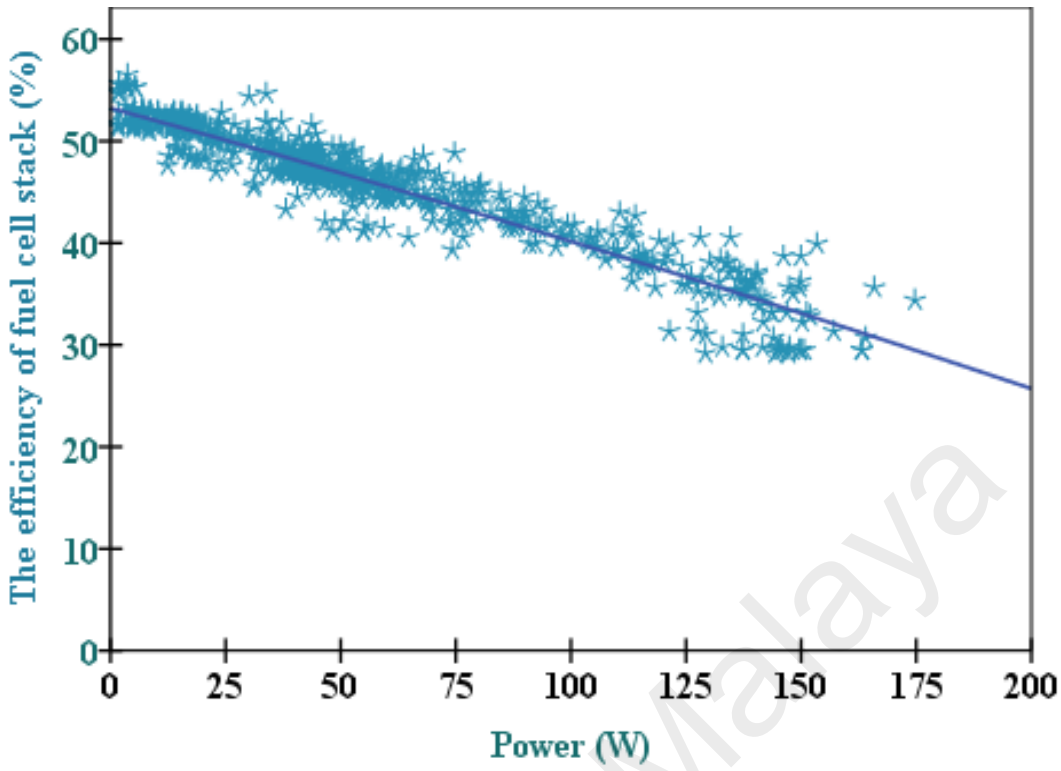

Figure 4.3: Plot of FC stack efficiency versus FC stack output power for relatively average temperature 37.6 ℃ over experiment period

In the next step, efficiency of the whole system was analysed. As explained in chapter 3, the ratio between the energy output and input forms the basis of calculation of efficiency in any energy transformation system. This ratio in fuel cell is between the output electrical power and the hydrogen energy that is consumed. The consumed hydrogen energy for this experiment is calculated by Equation **(**3.3), as follows:

Energy of consumed H_2 =241.98×4.96×20/ (308.65×0.08206) =947.75 kJ

Where for 3.92 mol of hydrogen, the pressure of 20-liter electrolyzer buffer tank was dropped from 19.91 bar to 14.88 bar. Thus, 947.75 kJ was used by the fuel cell as the system input, and the electric motor used the FC power output. The output electric power of the system is calculated by measuring the power consumption of the bicycle's electric

motor over time, which is 335.82 kJ, over approximately 159 minutes of experimental period. Hence, the overall system efficiency for this experiment is calculated using Equation (3.2):

$$\text{The overall system efficiency} = 100 \times 335.82/947.75 = 35.43\ \%$$

Figure 4.4 shows the Sankey diagram, which visualizes the different energy flows and power losses in an analysed electric-bicycle system. As shown in the picture the entire amount of hydrogen energy is 947.75 kJ and only 335.82 KJ is used for motor electric power.

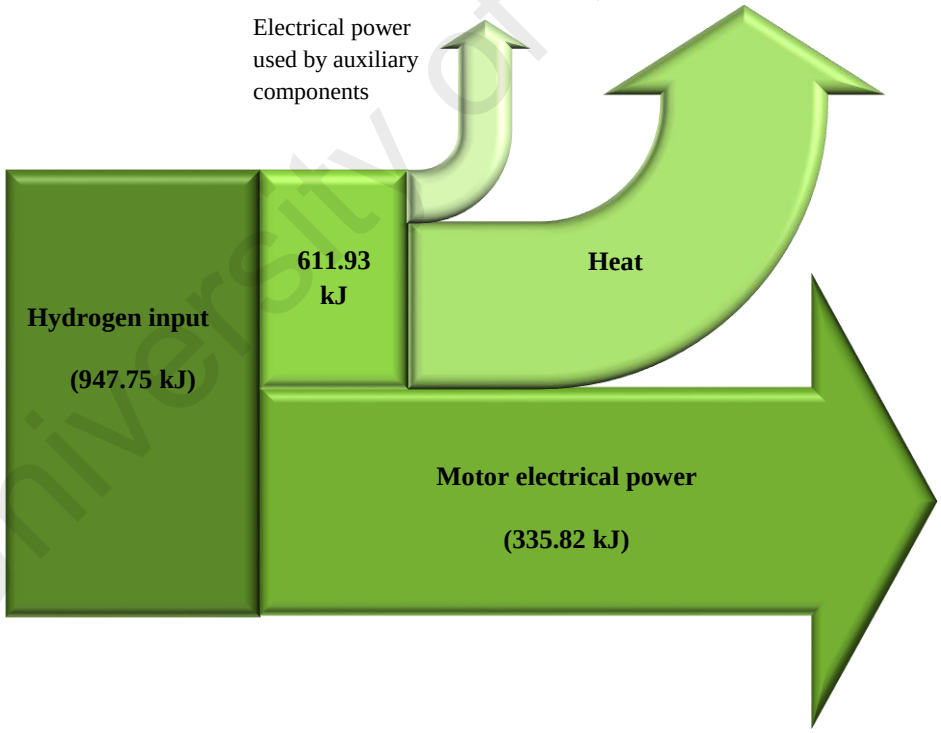

Figure 4.4: Flow diagram for PEM fuel cell powered electric bicycle. This diagram illustrates the various energy flows in system

However, the following important point should be considered that the efficiency of the fuel cell stack is not constant and depends on the stack voltage (bicycle usage condition). Thus, this value can change for different experimental conditions for the same bicycle. For this experiment, we have attempted to keep the bicycle at the cruise condition (constant speed) with a fuel cell power average of 35.29 W, and fuel cell stack efficiency average of 48.45%. The specifications of our efficiency study are listed in Table 4-2.

Table 4-2: Fuel cell powered electric bicycle parameter measurements from data demonstrated in Figure 4.5 (efficiency indicted by eff)

Parameters	Experiment duration	Hydrogen consumption[a]	Load energy consumption[b]	System eff[c]	Max– Min of FC eff[d]	Mean of FC eff [e]	Mean of FC power[f]
Value	9515 s	3.917 mol (947.75 kJ)	335.82 kJ	35.43%	63.88% 42.69%	48.45 %	35.29 W

[a] From Equation (3.3)

[b] Consumption electric power obtained from the sum of 9515 load power values that logged each second.

[c] Efficiency of fuel cell powered electric bicycle base on experimental data using Equation (3.2).

[d] The maximum and minimum of fuel cell stack efficiency during this experiment.

[e] Average of FC stack efficiency over 9515 individual efficiency values calculated for each second of experimental time.

[f] The mean was calculated from 9515 individual data points shown in Figure 4.5

Figure 4.5 shows the plot of the fuel cell power output throughout the efficiency experiment. As the curve shows, we attempted to keep the output power constant for small fractions of the nominal fuel cell power as needed at the cruise condition. The logged power data in this curve show a bold line at the bottom of the power line. The power differences between these higher points on top of this line and the points on the line are due to auxiliaries, such as 10-W cooling blower, which the ECU altered to maintain its

speed and compensate for the temperature of the fuel cell at the designated working temperature. When the fan is working at a minimum rate, the load power and other constant auxiliaries form the bold line in the curve, and the other variable components form the approximately 15-W line.

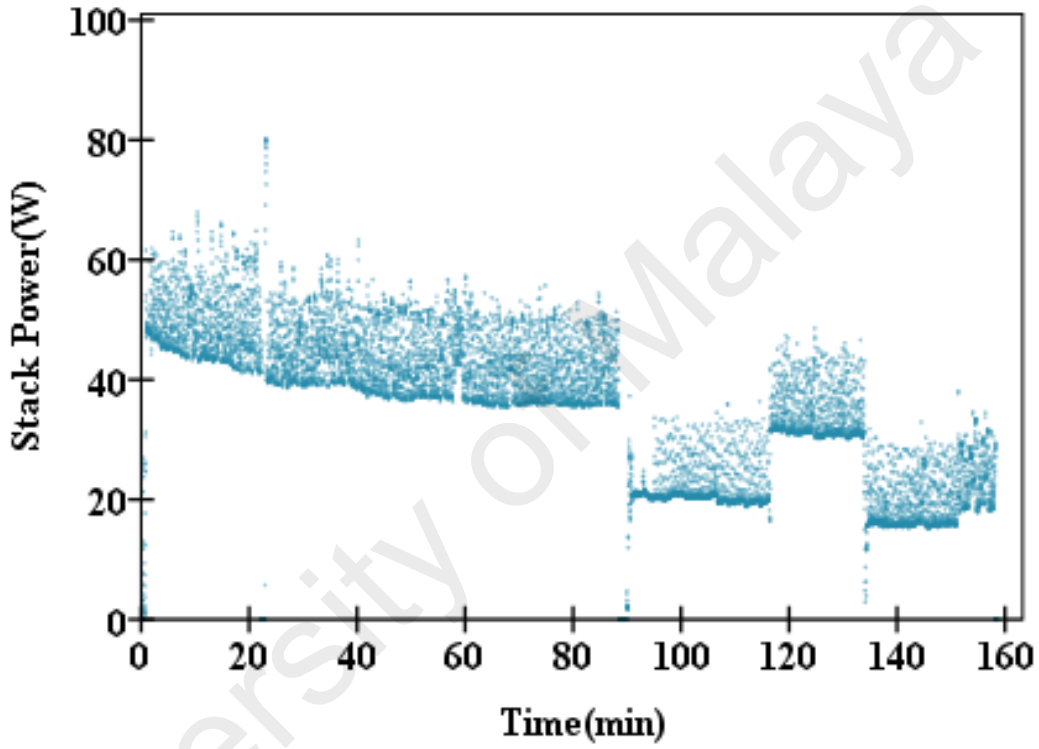

Figure 4.5: Plot of fuel cell stack power measured during efficiency experiment

During the experiment, it was observed that the ECU always automatically shuts down the system prior to reaching the full output power, which is important to the performance. Data analysis shows that the fuel cell stack voltage is below the minimum value (12 V) before reaching the maximum power due to insufficient hydrogen flow at stack; therefore, the ECU automatically shuts down the system to protect the fuel cell.

As mentioned, the temperature of Metal Hydride tank decreases during de-charging, the canister's surface temperature dropped from 27 ℃ to 0 ℃ in less than 15 min and this

affects the maximum hydrogen flow rate, which could potentially provide energy for fuel cell. In other words, when the fuel cell of bicycle works for a while, Metal Hydride tank cannot supply the minimum 3.5 Nl/ min of hydrogen in the time of high power demand of bicycle. Consequently, the voltage of fuel cell drops under the limitation and ECU shuts down the stack. Empirical model provides useful and reasonable accurate input-output relations for finding better performance of system and prevents any danger in real life for considering critical situations and investigating the system in various conditions. In this section the results of modelling are considered.

4.4 System modelling

Empirical models provide useful and reasonable accurate input-output relations in order to better investigate the system in various conditions to avoid any danger in real life considering the critical situation. In this study, both linear and nonlinear regression models were used for prediction of voltage and efficiency of system. In this section, the results of each of these designs are reported.

For the purpose of system modelling, 720 data points of following variables have been used. The data set collected from 25-kg electric bicycle powered by PEM fuel cell for prediction of electric bicycle system included load current, temperature, humidity, hydrogen flow rate, oxygen flow rate as regression model inputs and voltage and efficiency as outputs. Classical Linear regression with gradient descent algorithm was used for linear modelling, while a 3-layer feed forward artificial neural network with Levenberg-Marquardt algorithm used for training.

4.4.1 Linear regression model

Based on the machine learning principles, 60 % of dataset has been used for training while another 40% was divided equally into both cross-validation and test datasets. Gradient descent algorithm is applied for training the data. Cross validation dataset is used for model evaluation from splitting data set into training set for training the classifier and validation set for evaluating the model and estimating the error rate of trained classifier.

Cost function of training data set for both voltage and efficiency is shown in Figure 4.6 which shows the Mean Squared Error (MSE) over 300 data points for training for voltage and efficiency observed as 0.0302 and 0.106 respectively. To evaluate the performance of PEM fuel cell linear regression model against experimental result, and in order to find this performance numerically, mean squared error is necessary to be calculated by the equation (4.1):

$$MSE = \frac{1}{n}\sum_{i=1}^{n}(A - T)^2 \tag{4.1}$$

Where *A* denotes the simulated data vector for every output parameter, *T* represents the real experimental value.

a)

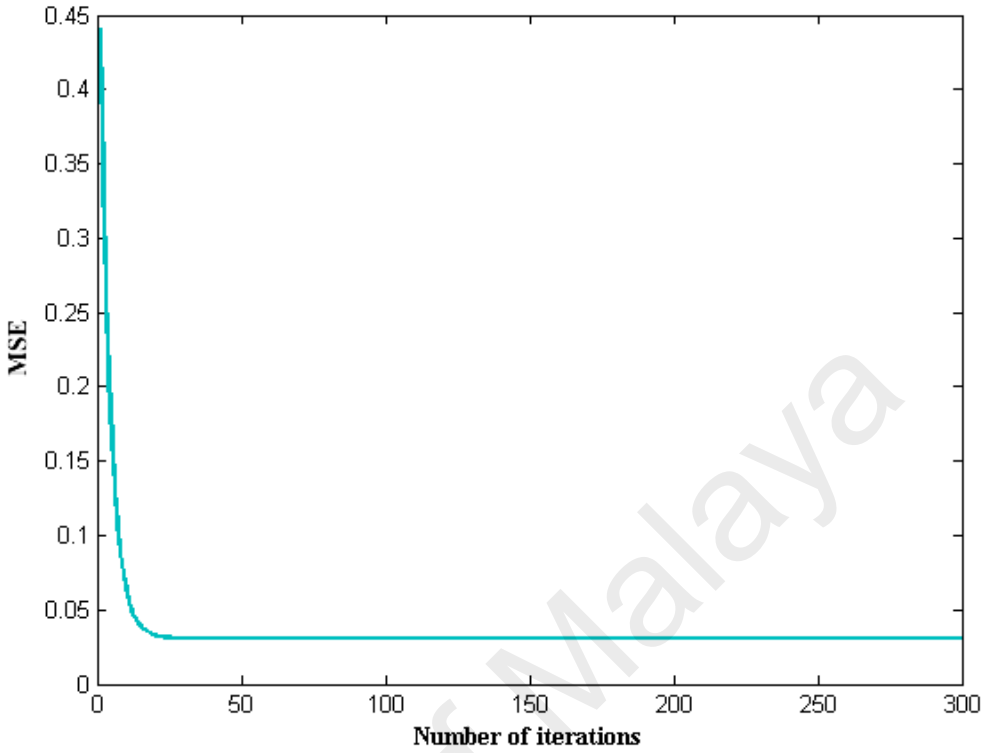

b)

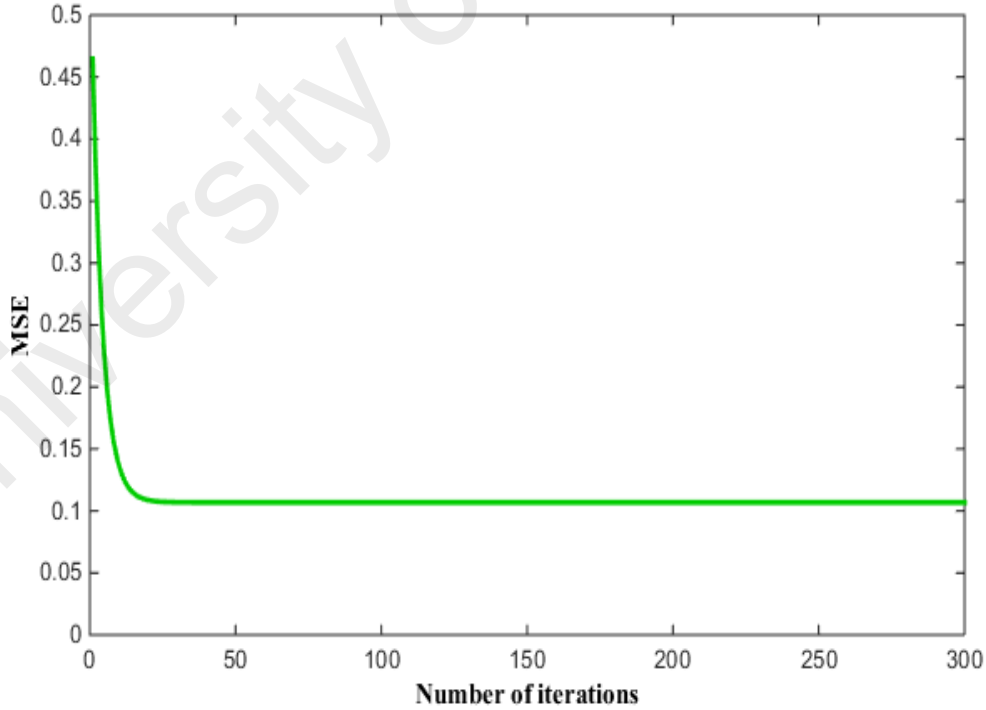

Figure 4.6: MSE for training the data a) voltage b) efficiency

In this study, principles of machine learning were considered for an optimized regression model design; therefore, learning curve based on training and cross-validation sets have been manipulated to process the error of the model and modification of model parameters using MSE. This evaluation was explained in chapter 3 and the best number of data points for model training was set to 300 in order to make sure there is no overtraining.

The performance of the linear regression model for the output voltage and efficiency value are shown in Figure 4.7. The convergence of training and cross validation error for 300 data points in the learning curve plots confirmed the optimal number of training needed for this model. Cross validation has been used for model evaluation by splitting the data set into training set for training the classifier and validation set for evaluating the model and estimating the error rate of the trained classifier.

a)

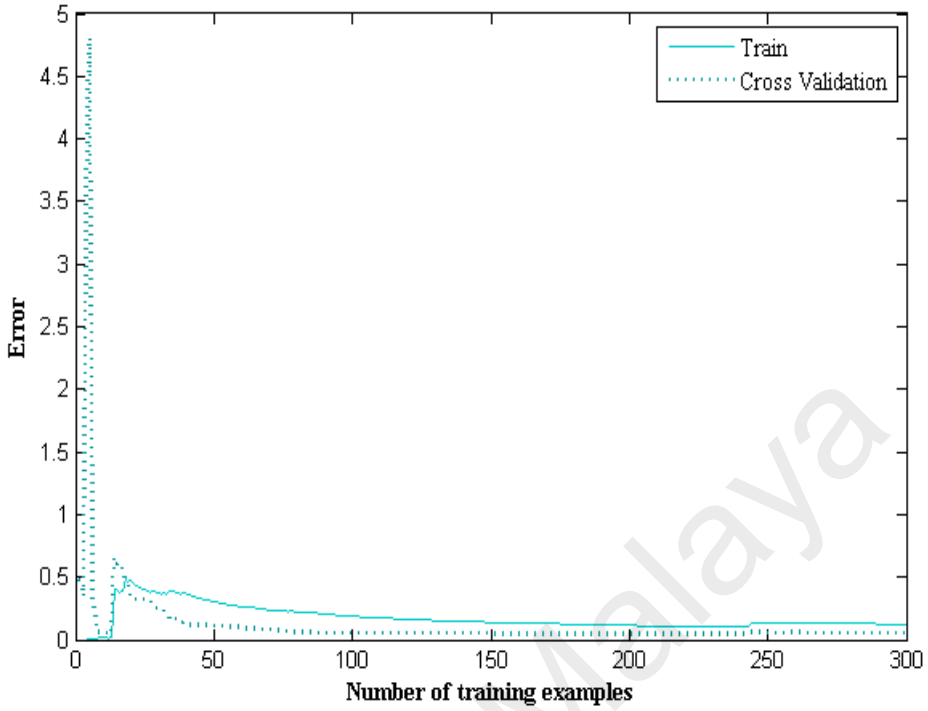

b)

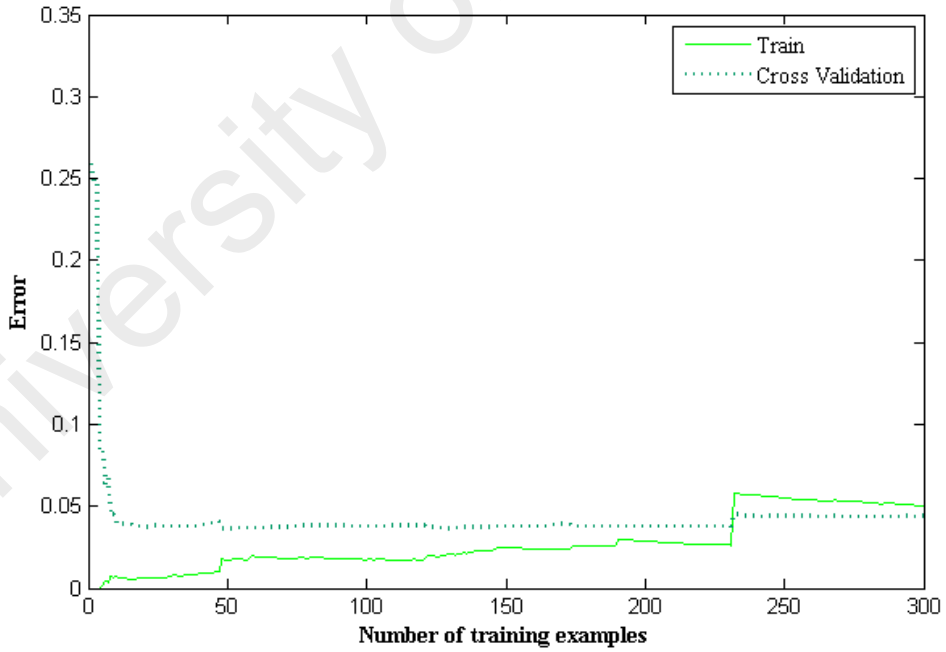

Figure 4.7: Training of linear regression model for output a) voltage value b) efficiency value

To train the linear regression efficiently, selecting the number of variables as inputs and outputs is useful. Evaluation of system performance based on selecting the fewest dominate input variables can provide the fastest training, reduce unnecessary complications and improve instant recall. In our particular system, as shown in Figure 4.8, 3 inputs were selected to the appropriate for modelling to avoid long run-time to achieve results.

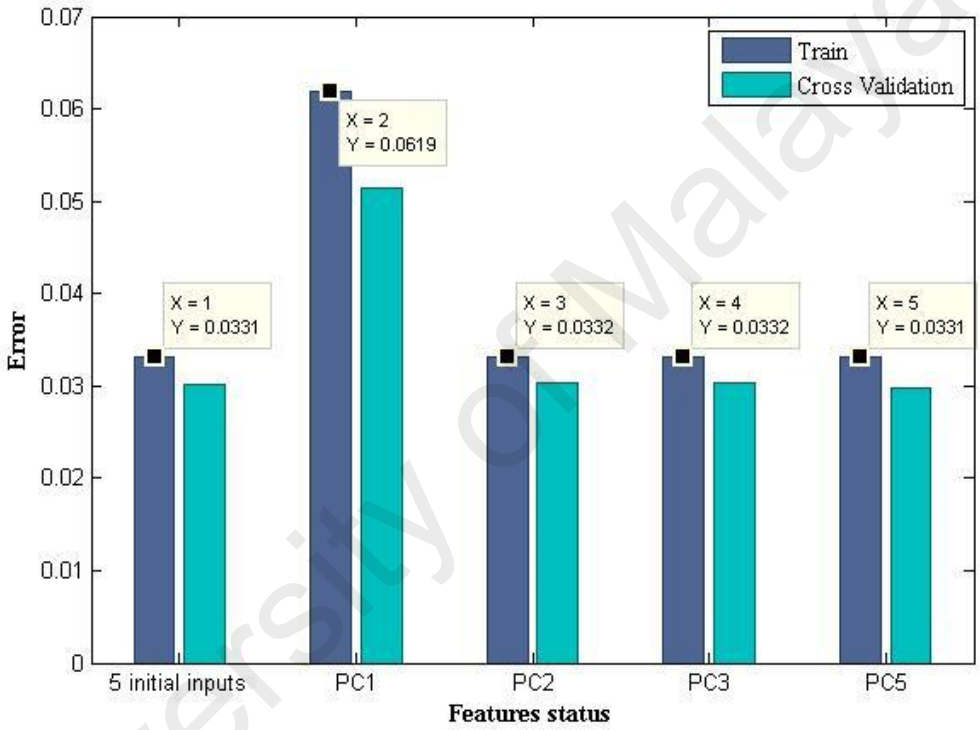

Figure 4.8: Evaluation of system performance based on input features

Once the model parameters were defined, a new random set of data were used for final design and evaluation of regression model using test dataset. Once satisfactory output has been provided by linear regression on the validation data set, cross validation was carried out on the test set. After the final test, linear regression model used be ready to predict V-I performance for different range of conditions.

Figure 4.9 displays Mean Square Error (MSE) of training, cross validation and testing for voltage and efficiency as an output separately. The errors associated with each distribution for voltage and efficiency are shown in Table 4-3.

Table 4-3: Men Square Error (MSE) for train, cross validation and test in linear regression LR

	MSE	
Process	**Voltage output**	**Efficiency output**
Train	0.0286	0.0311
Cross validation	0.03310	0.0482
Test	0.106	0.319

a)

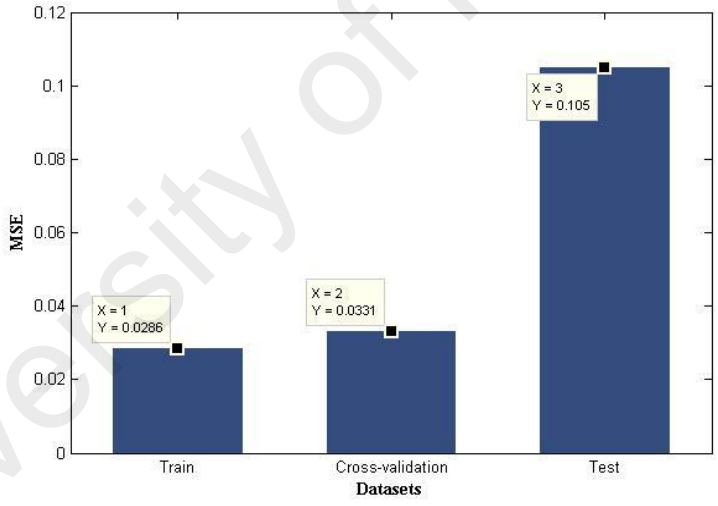

b)

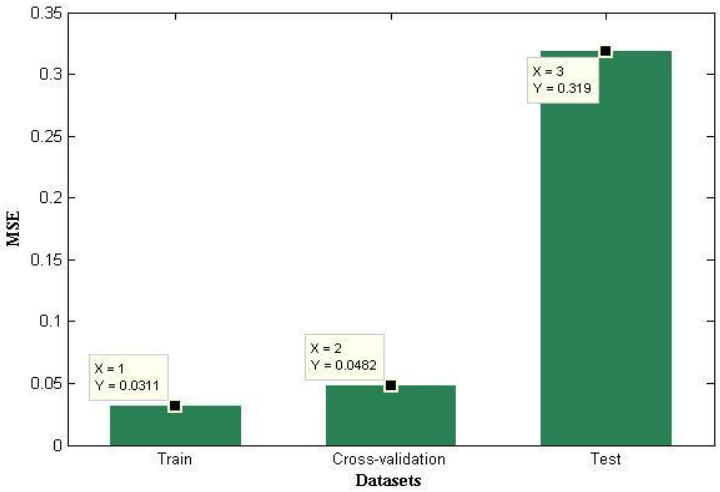

Figure 4.9: MSE for training, cross validation and testing a) voltage b) efficiency

Designed linear regression model was used for prediction of voltage and efficiency of test data and Figure 4.10 represents the sequence of simulated and real output data voltage and efficiency for PEM fuel cell.

a)

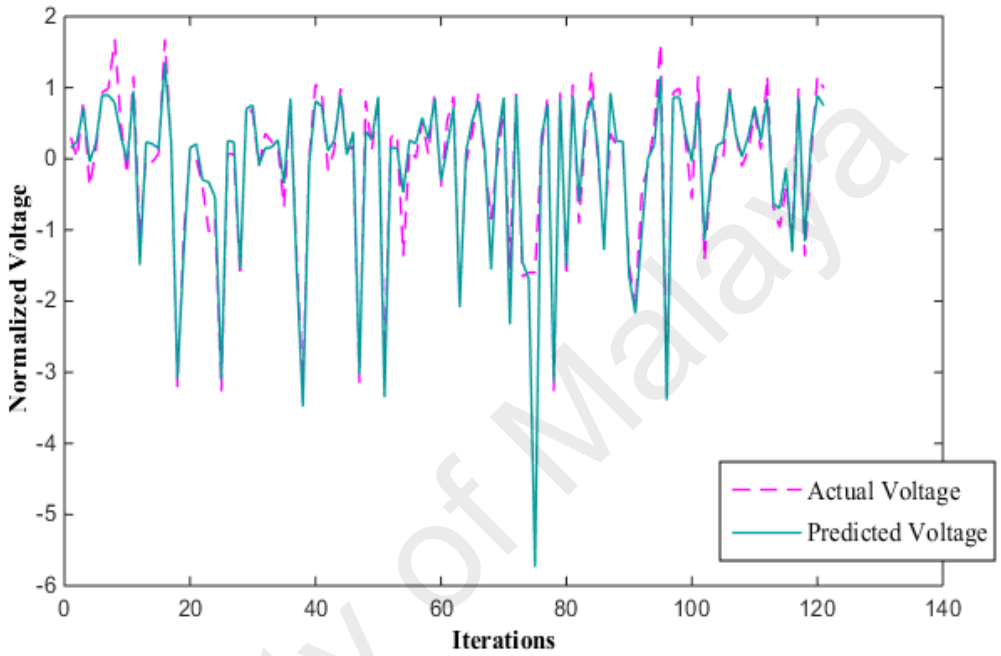

b)

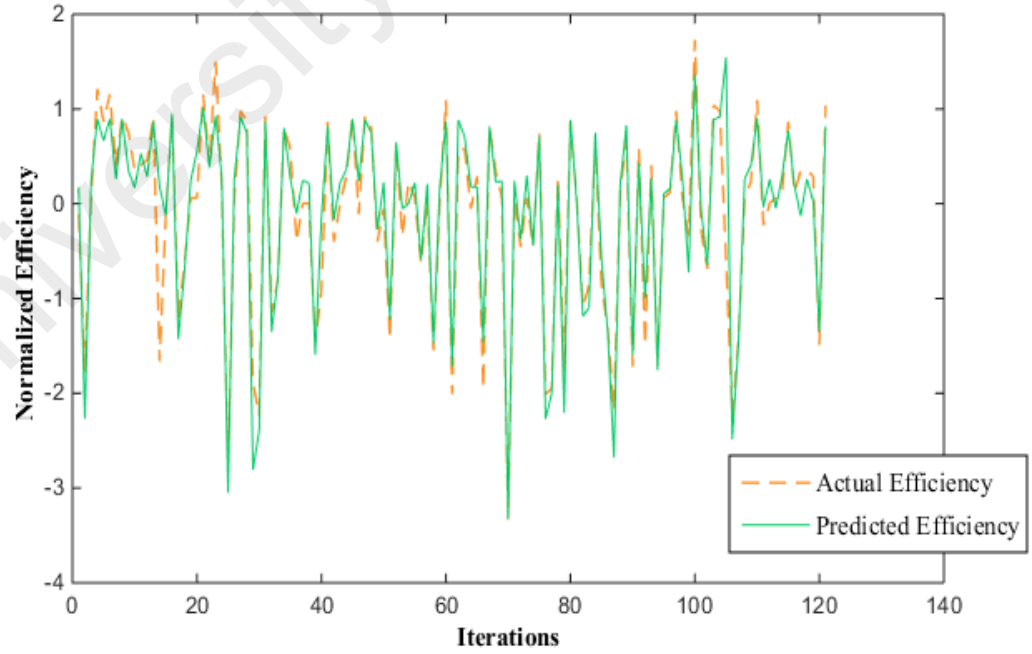

Figure 4.10: Comparison of predicted result and experimental data, a) voltage simulation b) efficiency simulation by LR

Figure 4.11a) demonstrates the polarization curve predicted by the proposed linear regression model. Representing the system behaviour with the smallest number of sensors in electric bicycle as perfectly as possible by the proposed model, is one of the main objectives here. In addition, Figure 4.11 b) represents the efficiency versus power curve prediction.

a)

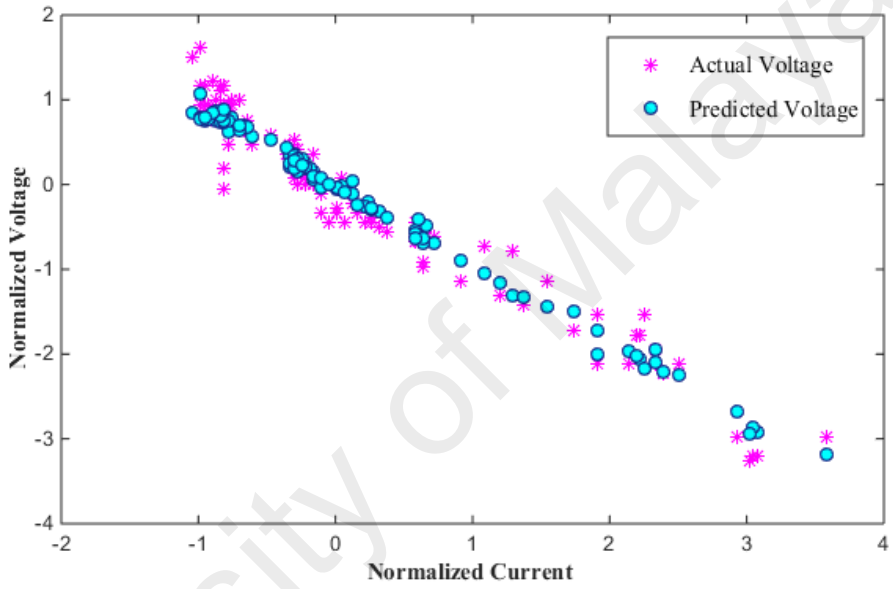

b)

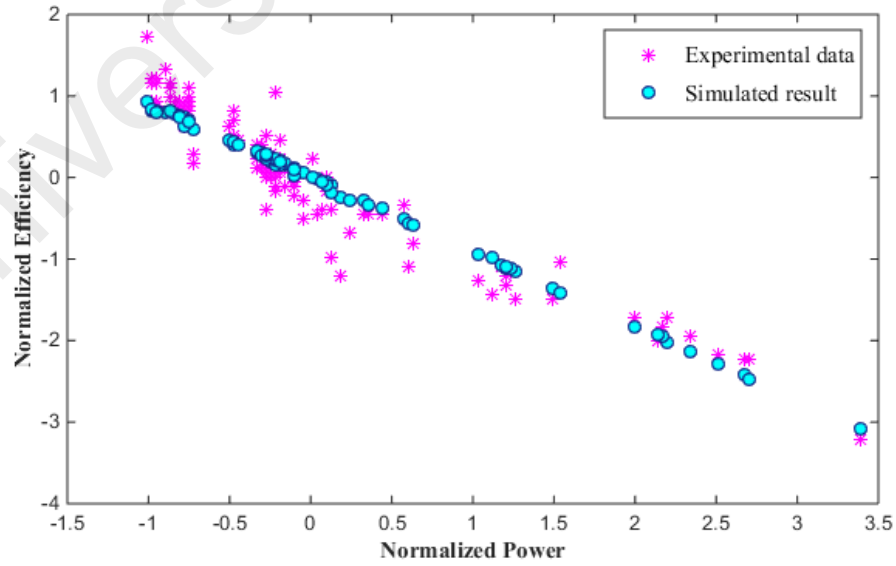

Figure 4.11: Predict the **a)** polarization curve and **b)** efficiency versus power by linear regression (LR) and compare with experimental data of PEM fuel cell.

4.4.2 Artificial neural networks model

Non-linear relations among numerous inner fuel cell parameters cause nonlinearity functions for the whole system. Therefore, in order to have a non-linear regression model for this electric bicycle, artificial neural network (ANN) have been adopted. We investigated linear regression model and neural network model to determine which one tends to provide better prediction in terms of accuracy and speed. Before designing the network, a few dominate input and output variables are recognized.

To accelerate the performance prediction, it is important that training data set goes through the normalization procedure and to be well distributed in operating range. For training the NN, the inputs and outputs had to be normalized to be within a [-1, 1] for better convergence of the model. Input features were reduced using the same principle of linear regression by using first 3 principle components. Network was trained with Levenberg-Marquardt back propagation (LM-BP) to produce the proper output. Scheme neural network are shown in Figure 4.12.

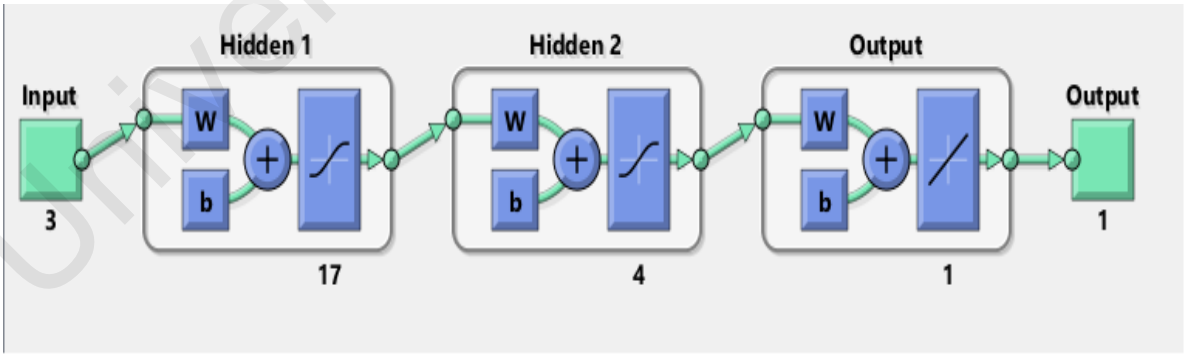

Figure 4.12: Scheme of function fitting NN model

For selecting the best structure of neural network model, possible different hidden layers and neuron structures have been designed and evaluated based on the MSE value of the cross-validation set. Table 4-4 indicates that LM-BP with two layer 17-4 neurons provided the best prediction in terms of accuracy and speed. Therefore, similar neuron networks may perform better than complicated ones.

Number of epochs and the average error of prediction indicated by cost function, which is calculated by equation below, determine the training speed:

$$\mathrm{cost}_{\mathrm{function}} = \frac{1}{\mathrm{N}} \sum_{i=1}^{N} (\mathrm{DC}_{\mathrm{i}}^{\mathrm{estimated}} - \mathrm{DC}_{\mathrm{i}}^{\mathrm{real}})^2 \tag{4.2}$$

$$\mathrm{cost}_{\mathrm{function}} = \frac{1}{\mathrm{N}.(\mathrm{K}-1)} \sum_{\mathrm{K}=1}^{\mathrm{K}-1} \sum_{\mathrm{j}=1}^{\mathrm{N}} (\mathrm{DC}_{\mathrm{i}}^{\mathrm{estimated}} - \mathrm{DC}_{\mathrm{i}}^{\mathrm{real}})^2 \tag{4.3}$$

Where *N* is the sample number. The error has been calculated by comparing real values against estimated values for voltage and efficiency in the validation set.

Table 4-4: Prediction result for different network architectures

Hidden layer	Epoch	MSE	Processing Time
3	10	0.074	00:00:17
3-3	74	0.055	00:00:18
10	70	0.044	00:00:01
10-10	12	0.071	00:00:00
20	12	0.035	00:00:00
20-10	11	0.134	00:00:01

Figure 4.13 displays the performance of the training, testing and validation processes for output voltage variable. Critical convergence for best validation performance is set to 10^{-2}. After training the model for 10 epochs for voltage output and 16 epochs for efficiency output, the mean square error for voltage and efficiency is observed to be 0.0118 and 0.0314 respectively. Table 4-5 demonstrates the best neural network model performance with the higher correlation coefficient which has 17-4 hidden neurons.

a)

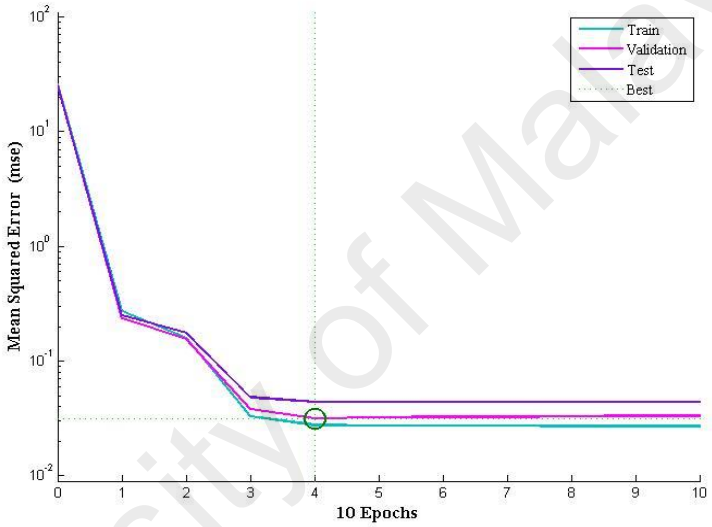

b

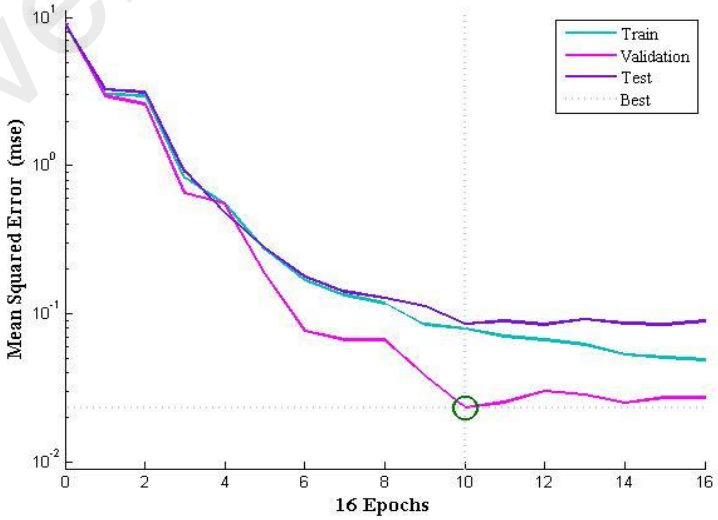

Figure 4.13: Best validation performance of neural network model for output a) voltage and b) efficiency value

Table 4-5: Performance of the best PEM fuel cell neural network model

	Variable	Mean square error	Correlation coefficient
Test	**Load Voltage**	0.0118	0.993
	Efficiency	0.0314	0.982

Figure 4.14 displays the error histogram of the output variables. As shown, the majority of error rates are in the interval of [-0.1, 0.2] and the error signal for training, testing and validation is stretched out to the value of 0.8 for voltage and 0.9 for efficiency outputs and the main portion lies between [-0.3, 0.4] and [-0.3, 0.4] for voltage and efficiency output respectively.

a

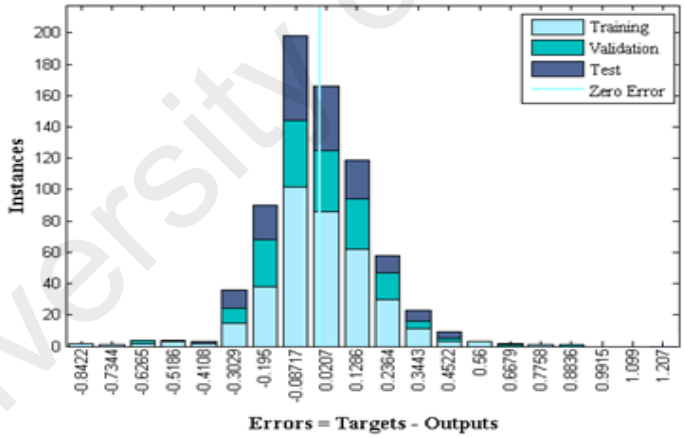

b)

Figure 4.14: Histogram of error for a) voltage output b) efficiency output

For investigating the correlation between experimental data and predicted data from ANN model, linear regression model of training, testing and validation set for every output has been calculated. The training session for output voltage presented better correlation rate which is R= 0.989 as shown in Figure 4.15 a) where the output efficiency obtained the minimum correlation rate which is R= 0.977 (Figure 4.15 b))

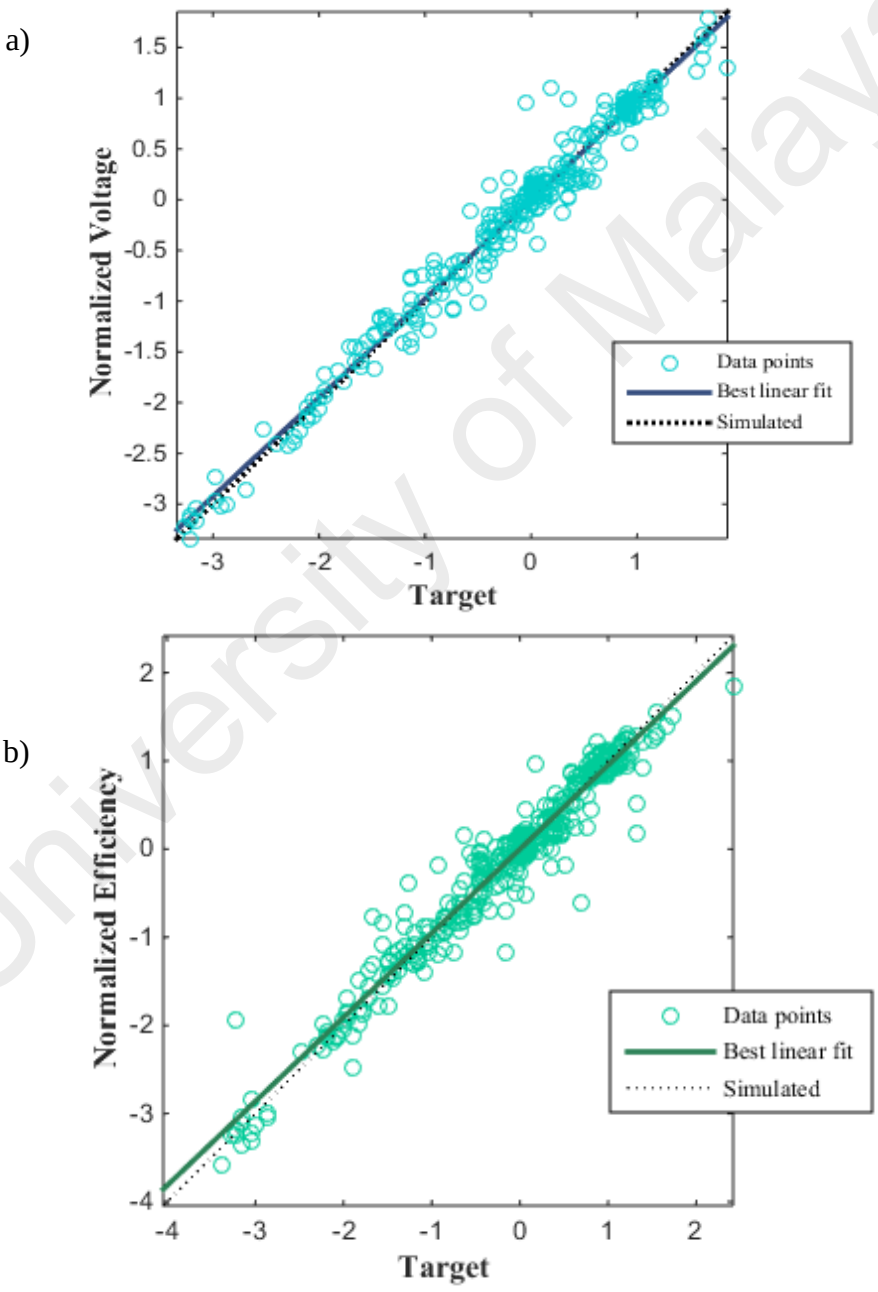

Figure 4.15: Rates of correlation of output variables a) voltage b) efficiency by linear regression for training

In order to provide accurate regression model, sufficient number of iterations should be used in training phase. As shown in Figure 4.16 this procedure demonstrated great behaviour. Figure 4.16 displays voltage variable obtained correlation rate of R= 0.993 and also shows that for efficiency variable R= 0.978

a)

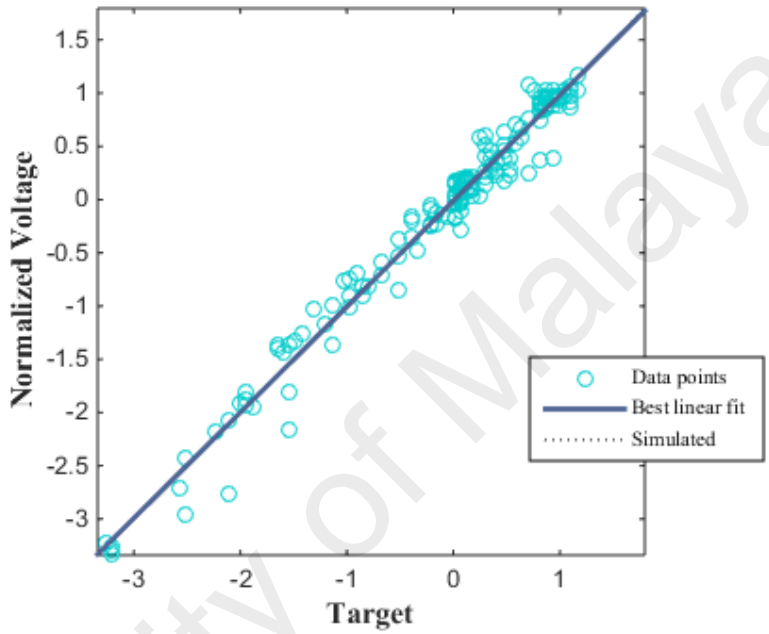

b)

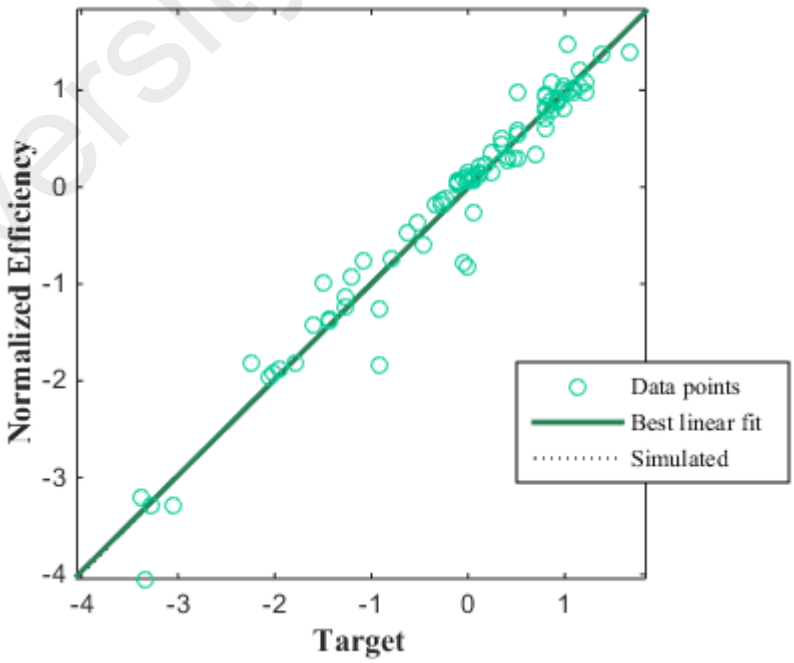

Figure 4.16: Correlation rate for testing patterns of outputs variable a) voltage b) efficiency

In order to detect and compare predicted results against experimental results, current sequence, temperature, humidity, hydrogen flow rate and oxygen flow rate were propagated through the neural network model. Figure 4.17 displays outstanding modelling performance of the neural network prediction, where estimated validation pattern by data, show great linear fit to real data. Figure 4.17 a) demonstrates the acceptable validation correlation rate of voltage in this procedure for R= 0.986 and Figure 4.17 b) displays suitable performance of efficiency variable for R= 0.976.

a)

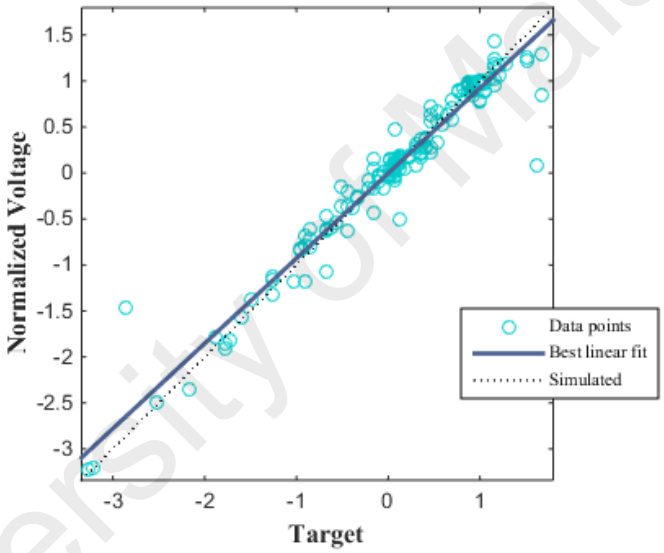

b)

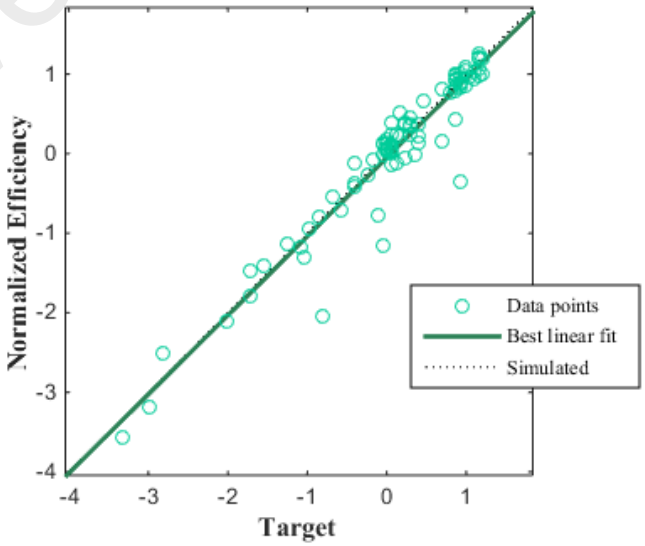

Figure 4.17: Correlation rate of output variable a) voltage b) efficiency for validation

The result shows us the proposed ANN has proper performance for prediction, however testing them by using another set of experimental data is essential. Table 4-6 describes for training, testing and validation process when the best fitting line is obtained for correlation rate.

Table 4-6: Best linear fit for output variable for training, testing and validation

Process	Voltage best linear fit	Efficiency best linear fit
Training	R= 1.001 T + 0.12	R=0.997 T+ 0.0022
Testing	R=0.986 T - 0.0503	R=0.987 T- 0.021
Validation	R= 1.00 T – 0.008	R= 0.998 T- 0.047

Figure 4.18 represents the real and predicted value of output data voltage and efficiency from ANN to experimental results. The results were obtained by using mentioned inputs to illustrate the accuracy of estimation of the neural network modelling. The values of inputs are not shown in the figure.

Figure 4.18a) shows the simulation results are in a good agreement with the experimental results. As we can see, voltage drops gradually when current increases. We found that at high voltage which is close to the open circuit voltage, large error accrues. Inadequate amount of experimental data which is followed by rapidly decreasing voltage in the polarization area is the main reason for this error. To achieve better prediction, a possible way is to make more data measurements during the experiment.

Same phenomena occurs in Figure 4.18 b). As shown, for efficiency output, when power demand increases its slope decreases. Calculating the simulation error is necessary in order to numerically set the performance of prediction.

It is important to check the degree of compliance of predicted data with the experimental data. Hence, simulation result of polarization curve or V-I characteristics are validated with experimental data of electric bicycle powered by PEM fuel cell model.

a)

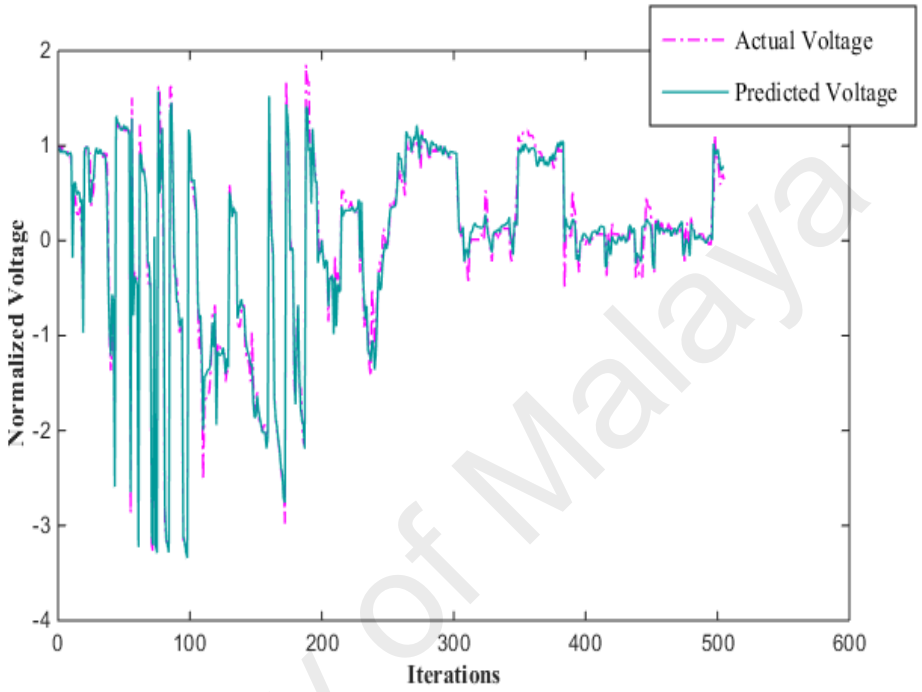

b)

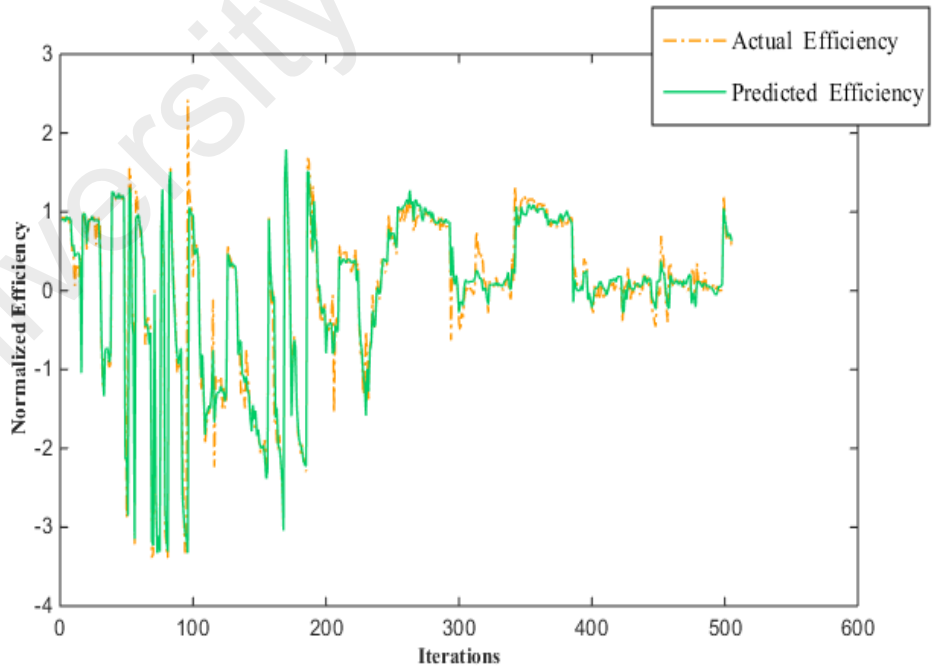

Figure 4.18: Comparison of predicted result and experimental data, a) voltage simulation b) efficiency simulation by NN

The comparison is demonstrated in Figure 4.19. The dataset used for this curve prediction is the same as what we used in section 4.2. It is seen that as the current is increased, the output voltage is decreased. The operated voltage is less than theoretical due to various losses. It must be noted that the value of individual voltage losses inside the PEM fuel cell cannot be computed by neural network model. Only general change in voltage losses can be determined by the system's model. We observe from the graph that ANN gives fairly good prediction on voltage and current curves.

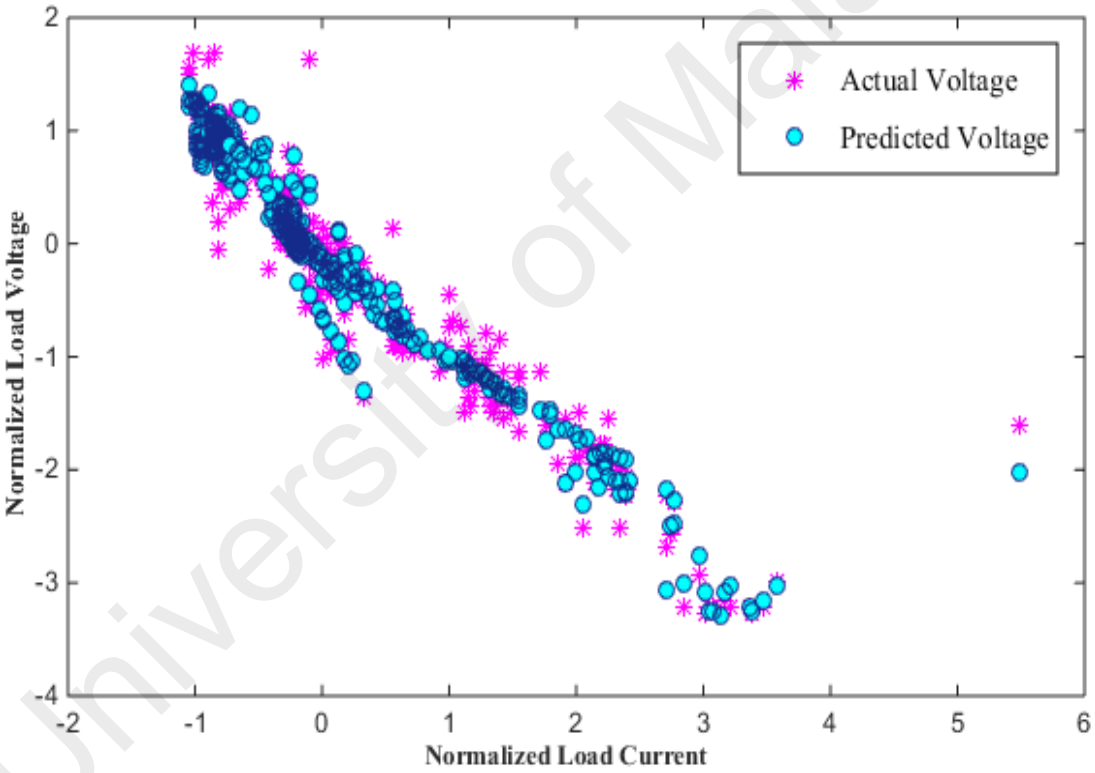

Figure 4.19: Prediction of the polarization curve by NN and comparison with experimental data of PEM fuel cell

Figure 4.20 shows the simulation of efficiency versus power characteristics by neural network. It can be noticed that maximum power is predicted close to the (17A) fuel cell current which is similar to the experimental data.

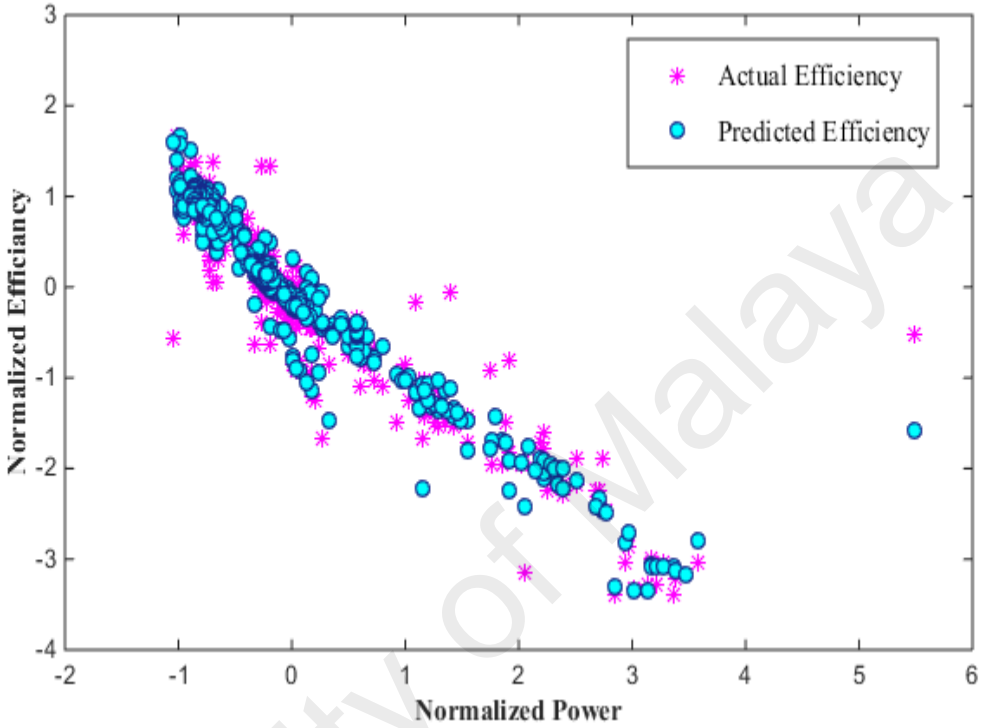

Figure 4.20: Prediction of efficiency versus power curve by NN and comparison with experimental data of PEM fuel cell

As it can be seen in Table 4.7 comparison of the mean square error (MSE) for voltage and efficiency as an output for regression and artificial neural networks are displayed and ANN has had much better results.

Table 4.7 : Comparison MSE in artificial neural network (ANN) and linear regression (LR) model

	ANN		LR	
MSE	**Voltage**	**Efficiency**	**Voltage**	**Efficiency**
Train	0.0203	0.0334	0.0286	0.0311
Cross validation	0.0118	0.0443	0.03310	0.0482
Test	0.0203	0.0334	0.106	0.319

4.5 Fuzzy Cognitive Map

As demonstrated earlier in chapter 2 and 3, fuzzy cognitive map (FCM) is a type of network for describing the behaviour of systems in terms of concepts and effect between concepts. In this study, measured variables were the concepts of FCM (Figure 4.21) which consist of 7 concepts (C_1=current, C_2=temperature, C_3=related humidity, C_4=hydrogen flow rate, C_5= oxygen flow rate, C_6=voltage, C_7=efficiency). We described the features of the system which are crucial for modelling and represented each one by a concept.

The characteristics of PEM fuel cell system are demonstrated by the concepts effects. The influence of the concepts on each other are represented by weights W_{ij} among them. In general, the key factor of PEM fuel cell system are represented by concepts that can also be characteristics of the variables, inputs, outputs, events, states and trend of our system. The weights between concepts are shown in matrix W (Table 4-8) as the initial FCM of the PEMFC. As explained in chapter 3, any inner slope of self-effect of concepts was considered as zero which caused the diagonal values of W matrix to be equal to zero.

The initial design of FCM with all weights consists of 42 connections among the concepts. However, due to complexity the initial FCM is not shown in this thesis. Source nodes are denoted by the rows of the matrix and destination nodes are denoted by the columns. The concepts that influence other concepts are “Transmitter” and the concepts influenced by other concepts are “Receiver”.

Table 4-8: FCM connection matrix between 7 concepts of PEM fuel cell system

	I	**T**	**RH**	**H_2**	**O_2**	**V**	**Eff**
I	0	$W_{1,2}$	$W_{1,3}$	$W_{1,4}$	$W_{1,5}$	$W_{1,6}$	$W_{1,7}$
T	$W_{2,1}$	0	$W_{2,3}$	$W_{2,4}$	$W_{2,5}$	$W_{2,6}$	$W_{2,7}$
RH	$W_{3,1}$	$W_{3,2}$	0	$W_{3,4}$	$W_{3,5}$	$W_{3,6}$	$W_{3,7}$
H_2	$W_{4,1}$	$W_{4,2}$	$W_{4,3}$	0	$W_{4,5}$	$W_{4,6}$	$W_{4,7}$
O_2	$W_{5,1}$	$W_{5,2}$	$W_{5,3}$	$W_{5,4}$	0	$W_{5,6}$	$W_{5,7}$
V	$W_{6,1}$	$W_{6,2}$	$W_{6,3}$	$W_{6,4}$	$W_{6,5}$	0	$W_{6,7}$
Eff	$W_{7,1}$	$W_{7,2}$	$W_{7,3}$	$W_{7,4}$	$W_{7,5}$	$W_{7,6}$	0

We describe the relation between concepts by using a fuzzy value for each interconnection, so weights take values in the interval [-1, 1]. As we mentioned in chapter3, in FCM structure with three possible types of interaction between concepts C_i and C_j can be expressed as follows:

- $Wij > 0$ specifies positive causality between two concepts which means increase in the value of concept C_i causes an increase in the value of concept C_j and decrease in the value of concept C_i causes a decrease in the value of concept C_j.
- $Wij < 0$ indicates negative causality between two concepts that means increase in the value of concept C_i causes a decrease in the value of concept C_j and vice versa.
- $W_{ij} = 0$ indicates no relationship between two concepts.

Based on the flowchart of FCM training procedure in chapter 3, the initial interconnections were chosen based on the system behaviour. This FCM is designed to be used for dynamic modelling and control of the PEMFC; therefore, some of the weights where chosen to be zero. For instance, the effect of PEM fuel cell efficiency and stack output voltage have no direct effect on input hydrogen, oxygen as input variables or temperature and humidity as experiment conditions. FCM of PEM fuel cell is shown in Figure 4.21, and Table 4-9 indicates the concept and relation between them in real time modelling of PEM fuel cell system.

Table 4-9: FCM connection matrix between 7 concepts of PEM fuel cell system in real time modelling

	I	**T**	**RH**	**H_2**	**O_2**	**V**	**Eff**
I	0	$W_{2,1}$	0	0	0	$W_{1,6}$	$W_{1,7}$
T	$W_{2,1}$	0	$W_{2,3}$	$W_{2,4}$	$W_{2,5}$	$W_{2,6}$	$W_{2,7}$
RH	$W_{3,1}$	$W_{3,2}$	0	$W_{3,4}$	$W_{3,5}$	$W_{3,6}$	$W_{3,7}$
H_2	$W_{4,1}$	0	0	0	0	$W_{4,6}$	$W_{4,7}$
O_2	$W_{5,1}$	0	0	0	0	$W_{5,6}$	$W_{5,7}$
V	0	0	0	0	0	0	$W_{6,7}$
Eff	0	0	0	0	0	0	0

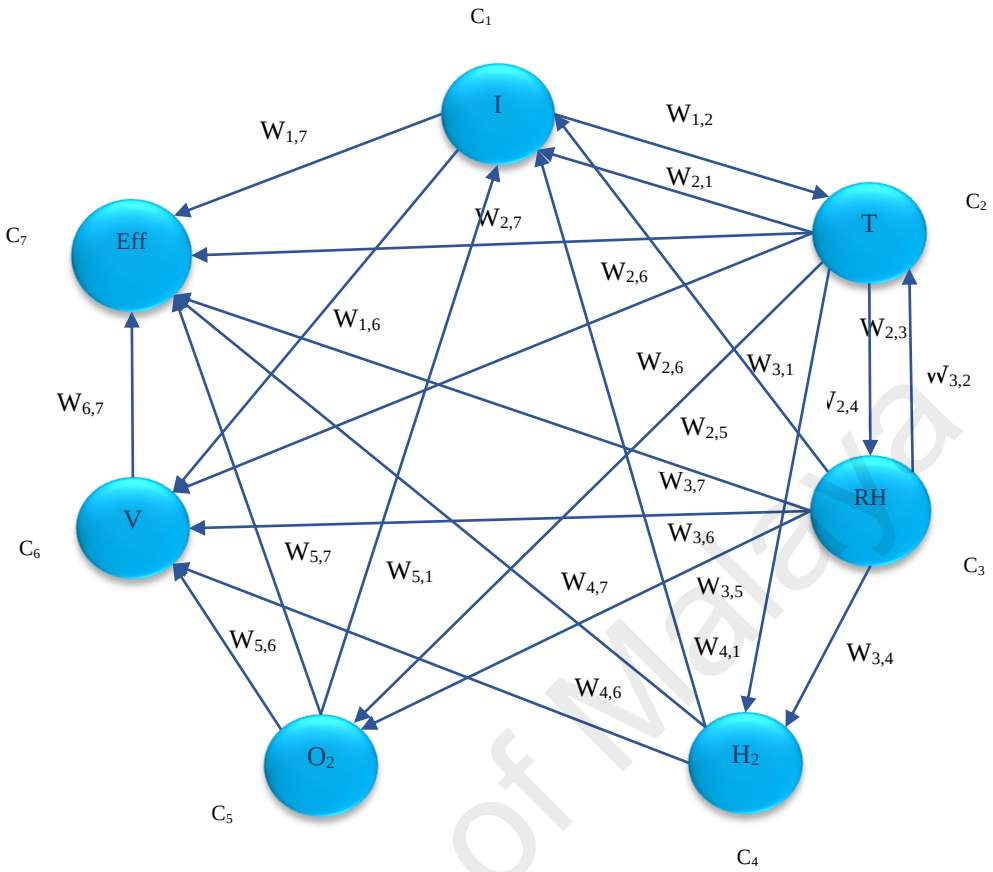

Figure 4.21: FCM scheme of PEM fuel cell system, I: current, T: temperature, RH: related humidity, H2: hydrogen flow rate, O2: oxygen flow rate, V: voltage and Eff: efficiency

4.5.1 FCM Training Process

In this study, FCM has been used as a newly applied method for dynamic modelling of the system, which can generate the next state of the whole system's concepts. This is the first dynamic model of a PEMFC, which predicts all variables (concepts) of the system. To date, FCM has been used in many engineering applications, and as one of the novelties of this study, FCM has been used for modelling PEMFC. It is notable that there have been different algorithms designed for training FCM. However, majority of these methods are based on an initial weight setting of FCM by an expert.

This initial weight setting is one of the main drawbacks of FCMs which limits its usage in areas where a system expert in needed to set the values. Therefore, in this study a newly established learning algorithm (DDNHL) was used as a state-of-art FCM training algorithm. DDNHL was developed based on non-linear Hebbian learning method and it benefits the FCM training by using previous data-points for finding the weights based on random initial weight setting. Therefore, the main drawback of FCM- requiring an expert for initial weight setting is resolved and FCM can be trained based on random initial weights. A detailed explanation of the training algorithm was explained in chapter 3. We used 1000 data points for training FCM based on DD-NHL algorithm (Figure 4.21). The final weight matrix is shown in Table 4-10:

Table 4-10: FCM connection matrix between 7 concepts of PEM fuel cell system in real time modelling

	I	**T**	**RH**	**H_2**	**O_2**	**V**	**Eff**
I	0	-0.5	0	0	0	-0.88	-0.81
T	-0.43	0	-0.62	-0.43	-0.44	0.27	0.28
RH	0.9	-0.98	0	0.98	0.98	-0.9	-0.9
H_2	1	0	0.22	0	0	-0.89	-0.8
O_2	1	0	0	0	0	-0.87	-0.81
V	0	0	0	0	0	0	-0.84
Eff	0	0	0	0	0	0	0

Based on the results of this step and in order to simplify the FCM of our system, residual causalities and system concepts that are less effective were omitted from the final design and Figure 4.22 was suggested for a new weight training. This simplification increases the speed of FCM performance for each state prediction. The fuzzy cognitive model for electric bicycle contains four concept including:

Concept 1 (C_1): represents hydrogen flow rate (H_2)

Concept 2 (C_2): represents temperature

Concept 3 (C_3): represents related humidity

Concept 4 (C_4): represents efficiency of the system

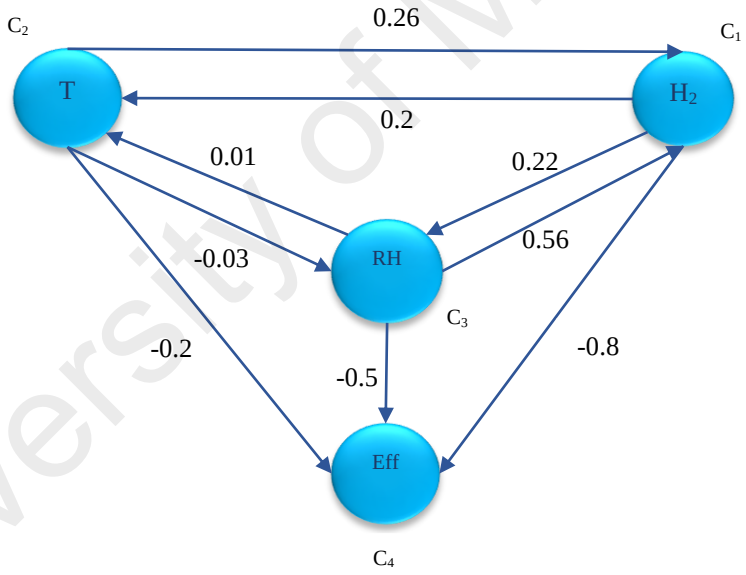

Figure 4.22: Final FCM design of system.

The state-of-the-art learning method that exist in the literature is used for the investigation of the quality of trained models. DD-NHL has been implemented to train this FCM model. The simulation error was computed as follows:

$$simulation\_error = \frac{1}{N.(K-1)} \sum_{K=1}^{K-1} \sum_{j=1}^{N} \left| DC_i^{estimated} - DC_i^{real} \right| \qquad (4.2)$$

Where $DC_i^{estimated}$ and DC_i^{real} are the estimated and real value of decision concepts (DC), K is the number of available iterations to compare and $N$is the number of concepts (E. I. Papageorgiou, 2013). By equation (4.3) the cost function is calculated:

$$cost\_function = \frac{1}{N.(K-1)} \sum_{K=1}^{K-1} \sum_{j=1}^{N} (DC_i^{estimated} - DC_i^{real})^2 \qquad (4.3)$$

In this condition our model can calculate the prediction error (which is the summation of MSE for all concepts), while using it for improving its accuracy. The cost function in FCM model as can be seen in Figure 4.23 is 0.0357.

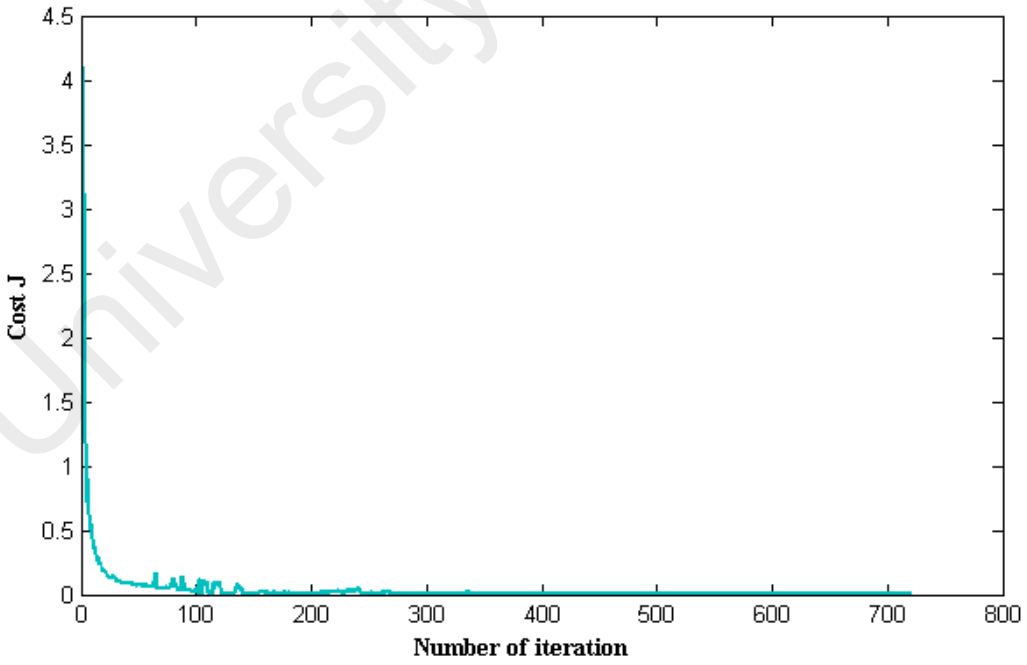

Figure 4.23: MSE for training the data in FCM

The final values of W matrix is shown In Table ***4-11***, and the cost function is depicted in Figure 4.23. This FCM MSE value is lower than the MSE for efficiency and output voltage models that guarantee the highest accuracy on system modelling using FCM.

Table 4-11: FCM connection matrix between four concepts of PEMFC

	H_2	**T**	**RH**	**Eff**
H_2	0	0.2	0.22	-0.8
T	0.26	0	-0.03	-0.2
RH	0.56	0.01	0	-0.5
Eff	0	0	0	0

4.5.2 RB-FCM

Prediction model for precision PEM fuel cell system is developed by proposed FCM approach that can be implemented for decision-making to control the system. Figure 4.24 shows the corresponding membership function for the four selected parameters (temperature, related humidity, hydrogen flow rate, and system efficiency). Table 4-12 describes the set of linguistic variables that every concepts can take.

Table 4-12: Type of value of FCM Concepts

	Type of value				
Parameter	**Very low**	**low**	**Medium**	**High**	**Very high**
Hydrogen flow rate	<-0.2	-0.2, 0	0, 025	0.25, 0.5	>0.5
Temperature	<-0.4	-0.4, -0.20	-0.20, 0.20	0.2, 0.6	>0.6
Related humidity	<-0.4	-0.4, -0.15	-0.15, 0.25	0.25, 0.55	>0.55
Efficiency of system	<-2	-2, -1	-1, 0	0, 1.5	>1.5

a)

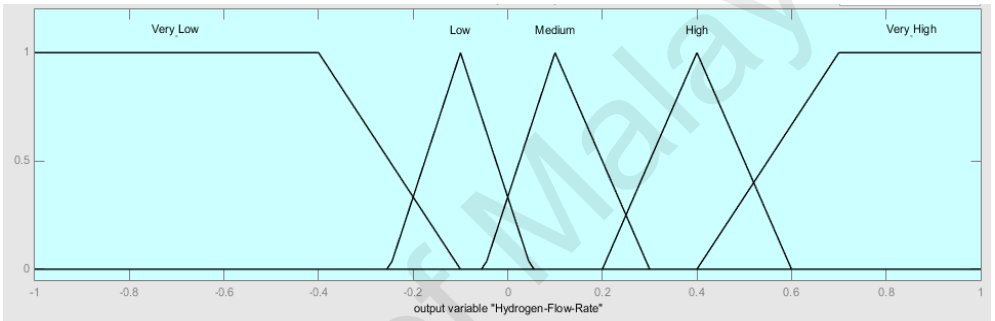

b)

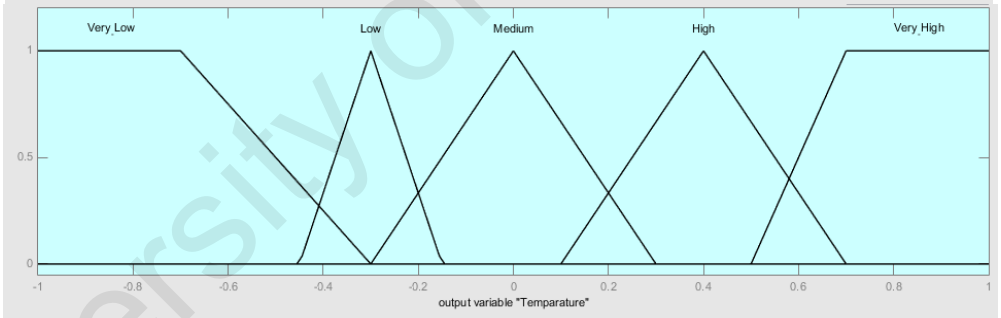

c)

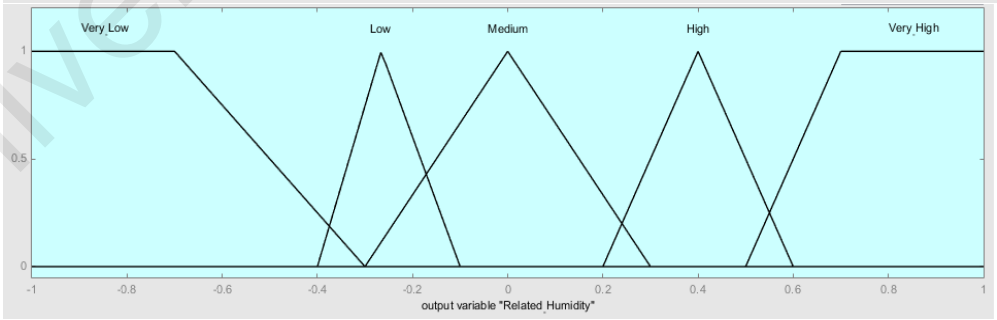

d)

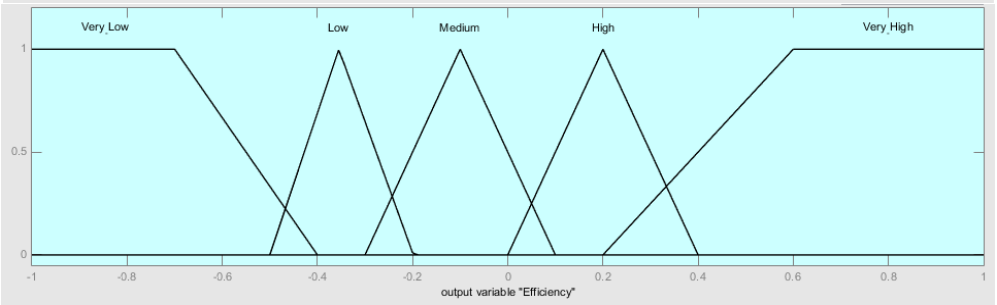

Figure 4.24: Membership function for a) hydrogen flow rate b) Temperature c) Related Humidity d) Efficiency

As explained in chapter 3, we use a rule-based FCM in this study which converts the quantitative matrix weight into qualitative values which can be understood and interpreted by any user. This benefits the system for a real time control and modification. Using these fuzzy rules, the final weight matrix was converted to rule based FCM (RB-FCM). Therefore, each concept value and the causality (influence matrix) should be converted to fuzzy values. Figure 4.24 shows the fuzzy values for each concept. It is notable that all the values of concept were normalized between [-1, 1] and based on the density function of each concept, the fuzzy memberships were defined. In Figure 4.25the membership function of influence matrix (W) is shown.

The influence of concept C_i to concept C_j is determined as negative or positive and linguistic variables describe the grade of influence such as "strong", "weak" and etc. The interval of linguistic variable is [-1, 1] and its term set T (influence) are suggested as: negatively very strong, negatively strong, negatively medium, negatively weak, zero, positively weak, positively medium, positively strong, and positively very strong. Rule *M* can be defined as follows:

- *M* (negatively very strong): μ_{nvs} for "an influence below -0.85".
- *M* (negatively strong): μ_{ns} for "an influence between -0.65 to 0.85".
- *M* (negatively medium): μ_{nm} for "an influence in interval -0.45 to -0.65".
- *M* (negatively weak): μ_{nw} for "an influence between -0.25 to – 0.45".
- *M* (zero): μ_z for "an influence between -0.2to 0.2".

- *M* (positively weak): μ_{pw} d for “an influence between 0.2 to 0.45”.

- *M* (positively medium): μ_{pm} d for “an influence between 0.45 to 0.65”.

- *M* (positively strong): μ_{ps} s for “an influence between 0.65 to 0.85”.

- *M* (positively very strong): μ_{pvs} for “an influence above to 0.85”.

Using these fuzzy rules, the final weight matrix was converted to rule-based FCM (RB-FCM).

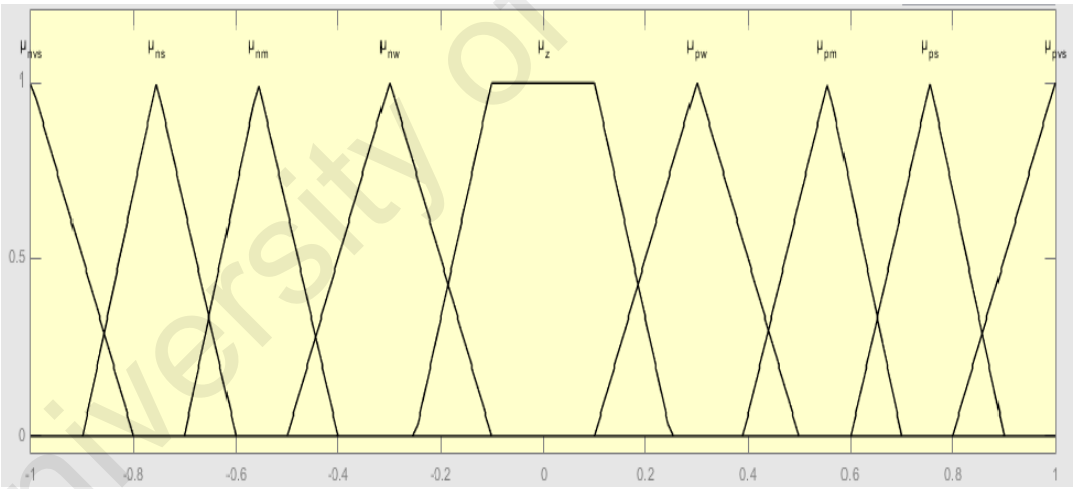

Figure 4.25: Membership function for influence matrix in electric bicycle system

Figure 4.26 indicates Rule- Based FCM model. Relationship between a numbers of nodes is determined by RB-FCM. For computing the new state of one node, fuzzy rules and Defuzzification process were used.

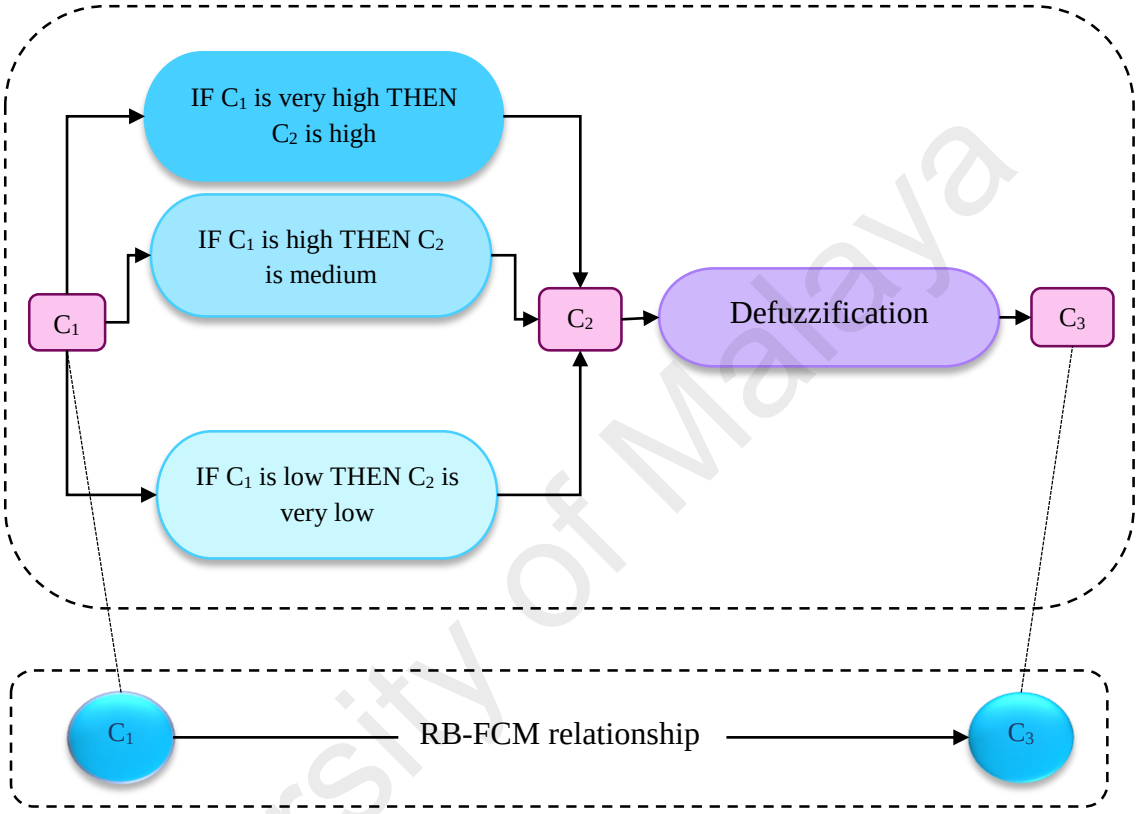

Figure 4.26: Sample of RB-FCM relationship

In this section, a practical example of modelling the electric bicycle will be examined. As mentioned before, the definition of concepts which describe the system and relation between concepts are the most important components in developing FCM.

For electric bicycle system a fuzzy cognitive map with four concepts that gives a good description of system is developed.

Concept 1 Hydrogen flow rate

Concept 2 Temperature

Concept 3 Related humidity

Concept 4 Efficiency

These concepts are connected with each other. First, we decided about connection between two concepts. Then, we decided the sign of connection, and at last, the weights between connections were determined. Each event or connection between concepts has weights that range in the interval [-1, 1]. The value of each concept has a range between [-1, 1].

Now the connection between concepts are as follow:

Event 1 concept1 (hydrogen flow rate) connects with concept2 (temperature).

Event2 concept1 (hydrogen flow rate) relates with concept3 (related humidity).

Event3 concept1 (hydrogen flow rate) connects with concept4 (efficiency).

Event4 concept2 (temperature) related with concept1 (hydrogen flow rate).

Event5 concept2 (temperature) connects with concept3 (related humidity).

Event6 concept3 (related humidity) related with concept1 (hydrogen flow rate).

Event7 concept3 (related humidity) connects with concept2 (temperature).

In this work, the relation among concepts has been described and to justify the cause and effect of the relation between concepts, we have used IF-THEN rules, and also for each interconnection, we have come up with the linguistic weight. The relation between two concepts emerge as the weights of interconnection, are described by IF-THEN rules. An example of fuzzy rule is as follows, where A, B, C are the linguistic variables:

If an **A** change occurs in the value of concept C_i *then* a **B** change is caused in the value of concept C_j. Thus, influence of concept C_i to concept C_j is **C**.

For every interconnection, we can propose linguistic rules; for the relationship between two concepts, linguistic value can be concluded from the rules. Therefore, a fuzzy rule has described the causal relationship that gives the degree of causality among concepts and so the corresponding weights is derived. As an example, the relation between two concepts will be examined (Figure 4.27).

If-then rule: If a very low change in value of concept C_i then a very high change in value of concept C_j is caused.

Conclusion: The influence of C_i to C_j is positively very high and so value of W_{ij} is positively very strong.

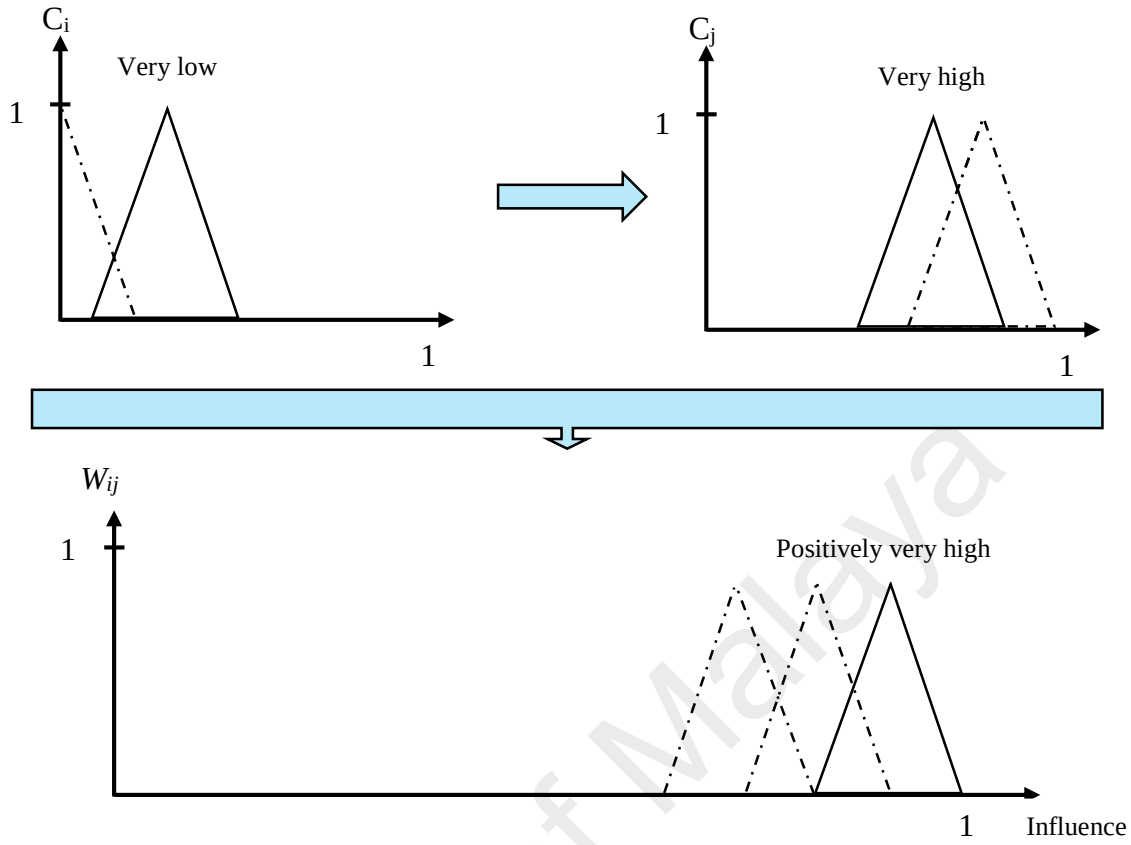

Figure 4.27: Example of fuzzy rule for an interconnection

To describe the relation between concepts RB-FCM used linguistic fuzzy rules and they are not limited to casual relations. Now fuzzy *if _then* rules for each membership function in the input concepts are defined by RB_FCM.

Rule 1: *IF* value of concept C_1 (hydrogen flow rate) is **very high** *THEN* value of concept C_4 (efficiency) is **low**.

Inference: The influence of C_1 to C_4 is **negatively strong**, so value of W_{ij} is **negatively strong**.

Rule 2: *IF* value of concept C2 (temperature) is **low** *THEN* value of concept C_4 (efficiency) is **medium**.

Inference: The influence of C_2 to C_4 is **negatively weak**, so value of W_{ij} is **negatively weak**.

Rule 3: *IF* value of concept C_3 (related humidity) is **high** *THEN* value of concept C_4 (efficiency) is **low**.

Inference: The influence of C_3 to C_4 is **negatively medium**, so value of W_{ij} is **negatively medium**.

Rule 4: *IF* value of concept C_1 (hydrogen flow rate) is **very low** *THEN* value of concept C_3 (related humidity) is **low**.

Inference: The influence of C_1 to C_3 is **positively weak**, so value of W_{ij} is **positively weak**.

According to the results achieved from voltage and efficiency equation shown in chapter3 in the final system design, where it can be used for online control, voltage as a system output was removed from FCM due to linearly correlation with efficiency and we just put the concepts that can be controlled on alternative designs. It is noteworthy that the design on Figure 4.21 also can be used, since capability of control system is feasible only by some of the variables in the system which are suitable for real-time control such as temperature, related humidity, hydrogen flow rate and efficiency (Figure 4.22). In fuzzy cognitive map which describe the system, designer can easily decide to add or remove connections. Moreover, for improving the system description and analyses of the system performance in different conditions, concept can be added or removed, without the reconstruction in whole model of the system. Since the initial design of the system is done by extracting information from the system itself, this system can be controlled by any operator without expert knowledge.

Chapter 5 : CONCLUSION AND FUTURE WORK

5.1 Conclusion

In this thesis, we described and experimentally tested a commercial electric bicycle powered by a PEM fuel cell to investigate its performance and efficiency in real-life operations. The polarization curve was obtained by using logged experimental data. The stack voltage rapidly declined during the start-up of the system due to the losses, which have strongly influenced later stages. The stack voltage also subtly reduces while the current increases. This finding proves that improving the stack behaviour during start up ameliorates the efficiency in future fuel cells. Furthermore, the overall system efficiency was measured throughout normal daily life operations. The results demonstrate that similar to internal combustion engines, the efficiency of the fuel cell is not a single value and directly depends on the output power of the system.

However, the efficiency-power curves of fuel cells and internal combustion engines showed opposite behaviours. The fuel cell-powered systems are more efficient at lower output powers, which is the exact inverse of the behaviour of internal combustion engines. The overall system efficiency was calculated to be approximately 35% for close to cruising operations, while the stack efficiency varied 43-64% which is significantly higher than that of an internal-combustion engine and also in compare to other similar research which efficiency of 18.8-38% was recorded to be acceptable.

Consequently, any improvement in the system's performance to amend the efficiency could lead to the growth of the fuel cell systems in transportation. For instance, adding a regenerative break system to future designs can significantly increase the system's

efficiency, which could also save up to 28% of energy in a similar project involving electric buses.

This study has evaluated modelling and controlling the PEM fuel cell system using soft computing methodology including linear regression (LR) and artificial neural network (ANN) methods. For model a PEM fuel cell system using related humidity (RH), current (I), oxygen flow rate (qO2), temperature (T) and hydrogen flow rate (qH2) as the input factors and fuel cell voltage (V) and efficiency (E) as the model output. Although linear regression model has good results in predicting stack voltage, it was shown that neural networks are more accurate and reliable for predicting fuel cell performance. Neural networks are faster than other methods, including linear regression because they are global approximators that operate without the need for any formula. In our research work, for estimation of fuel cell stack voltage, an ANN model was used to predict the commercial electric bicycle powered by PEM fuel cell that was trained by the Levenberg–Marquardt back Propagation (LM-BP) algorithm.

The proposed model is easy to use and computationally fast. Result of the analysis shows that the neural network algorithm fits the validation sample better than the linear regression model. In addition, using the neural network technique the nonlinear variances fit automatically, while linear regression techniques require an explicit design.

In the last part of this study, a new soft computing approach based on fuzzy cognitive map (FCM) was proposed for the first time to describe the behaviour of electric bicycle system powered by fuel cell. For automated learning of FCM from data, data driven nonlinear hebbian learning (DD-NHL) is proposed. Then fuzzy rules explain the cause and effect between concepts. Displaying the whole system behaviour by analytical model is extremely difficult. Thus, it is more useful and attractive to consider system behaviour in graphical way to show the causal relationship between concepts. One of the

superior capabilities of FCM is rule-based fuzzy cognitive map (RB-FCM) potential. Since RB-FCM were developed to allow us to predict and analyse the cognitive map involved in negotiation process. The main feature of RB-FCM are improving immunity and stability to initial state, and flexible casual relation.

5.2 Contributions

This work has novel approaches in the following aspects:

- We are experimentally compute the actual electric bicycle system's efficiency
- Regression models were optimized for predicting the output variables (voltage and efficiency).
- FCM as a novel combination of fuzzy logic (FL) and neural network (NN) approaches was utilized for the first time in this field. The novelty of this model make it possible to predict the whole system variables.
- This approach can be further developed to allow control this system in different condition

5.3 Future work

Based on the research work in my dissertation regarding a two-wheel fuel cell system have motivated me to a further research in modelling and nonlinear controlling design related to fuel cell system and other renewable energy systems. The potential for future work on fuel cell vehicle design will be proposed in the following directions:

- Any improvement in the system's performance to amend the efficiency could lead to the growth of the fuel cell systems in transportation. For instance, adding a regenerative break system to future designs can significantly increase the system's

efficiency, which could also save up to 28% of energy in a similar project involving electric buses.

- A prediction algorithm with more variables can be considered in future work to increase the accuracy of the model.
- This thesis has presented some rules for decision-making to control the electric bicycle; in terms of higher-level optimization of electric bicycle efficiency and increase the lifetime of component. The corresponding controller can be designed in future.

References

Abdi, H. (2007). Z-scores. *Encyclopedia of measurement and statistics. Thousand Oaks, CA: Sage*.

Acampora, G., & Loia, V. (2009). *A dynamical cognitive multi-agent system for enhancing ambient intelligence scenarios.* Paper presented at the Fuzzy Systems, 2009. FUZZ-IEEE 2009. IEEE International Conference on.

Acampora, G., Loia, V., & Vitiello, A. (2011). Distributing emotional services in ambient intelligence through cognitive agents. *Service Oriented Computing and Applications, 5*(1), 17-35.

Aguilar, J. (2003). A dynamic fuzzy-cognitive-map approach based on random neural networks. *International Journal of Computational Cognition, 1*(4), 91-107.

Andreou, A., Mateou, N. H., & Zombanakis, G. A. (2003). The Cyprus puzzle and the Greek-Turkish arms race: Forecasting developments using genetically evolved fuzzy cognitive maps. *Defence and Peace Economics, 14*(4), 293-310.

Andreou, A. S., Mateou, N. H., & Zombanakis, G. A. (2005). Soft computing for crisis management and political decision making: the use of genetically evolved fuzzy cognitive maps. *Soft Computing, 9*(3), 194-210.

Asl, S. S., Rowshanzamir, S., & Eikani, M. (2010). Modelling and simulation of the steady-state and dynamic behaviour of a PEM fuel cell. *Energy, 35*(4), 1633-1646.

Azmy, A. M., & Erlich, I. (2005). Online optimal management of PEM fuel cells using neural networks. *Ieee Transactions on Power Delivery, 20*(2), 1051-1058. doi: 10.1109/tpwrd.2004.833893

Azmy, A. M., & Erlich, I. (2005). Online optimal management of PEMFuel cells using neural networks. *Power Delivery, IEEE Transactions on, 20*(2), 1051-1058.

Bagotsky, V. S. (2012). Phosphoric Acid Fuel Cells. *Fuel Cells: Problems and Solutions, Second Edition*, 99-106.

Barbir, F. (2012). *PEM fuel cells: theory and practice*: Academic Press.

Barbir, F., & Gomez, T. (1996). Efficiency and economics of proton exchange membrane (PEM) fuel cells. *International Journal of Hydrogen Energy, 21*(10), 891-901.

Barbir, F., & Gomez, T. (1997). Efficiency and economics of proton exchange membrane (PEM) fuel cells. *International Journal of Hydrogen Energy, 22*(10-11), 1027-1037. doi: Doi 10.1016/S0360-3199(96)00175-9

Baschuk, J. J., & Li, X. G. (2005). A general formulation for a mathematical PEM fuel cell model. *Journal of Power Sources, 142*(1-2), 134-153. doi: 10.1016/j.jpowsour.2004.09.027

Baschuk, J. J., & Li, X. H. (2000). Modelling of polymer electrolyte membrane fuel cells with variable degrees of water flooding. *Journal of Power Sources, 86*(1-2), 181-196. doi: 10.1016/s0378-7753(99)00426-7

Beeson, P., Modayil, J., & Kuipers, B. (2009). Factoring the mapping problem: Mobile robot map-building in the Hybrid Spatial Semantic Hierarachy. *The International Journal of Robotics Research*.

Bhagavatula, Y. S., Bhagavatula, M. T., & Dhathathreyan, K. (2012). Application of artificial neural network in performance prediction of PEM fuel cell. *International Journal of Energy Research, 36*(13), 1215-1225.

Bischoff, M., & Huppmann, G. (2002). Operating experience with a 250 kWel molten carbonate fuel cell (MCFC) power plant. *Journal of Power Sources, 105*(2), 216-221. doi: http://dx.doi.org/10.1016/S0378-7753(01)00942-9

Blomen, L. J., & Mugerwa, M. N. (2013). *Fuel cell systems*: Springer Science & Business Media.

Boscaino, V., Miceli, R., & Capponi, G. (2013). MATLAB-based simulator of a 5 kW fuel cell for power electronics design. *International Journal of Hydrogen Energy, 38*(19), 7924-7934. doi: 10.1016/j.ijhydene.2013.04.123

Bossel, U., Schönbein, C. F., & Grove, W. R. (2000). *The Birth of the Fuel Cell: 1835-1845. Including the First Publication of the Complete Correspondence from 1839 to 1868 Between Christian Friedrich Schoenbein (discoverer of the Fuel Cell Effect) and William Robert Grove (inventor of the Fuel Cell)*.

Boutalis, Y., Kottas, T. L., & Christodoulou, M. (2009). Adaptive estimation of fuzzy cognitive maps with proven stability and parameter convergence. *Fuzzy Systems, IEEE Transactions on, 17*(4), 874-889.

Brandon, C., & Hommann, K. (1996). *The Cost of Inaction: Valuing the Economy-wide Cost of Environmental Degration in India*: UNU, Institute of Advanced Studies.

Braspenning, P. J., Thuijsman, F., & Weijters, A. J. M. M. (1995). *Artificial neural networks: an introduction to ANN theory and practice* (Vol. 931): Springer Science & Business Media.

Buchholz, M., & Krebs, V. (2007). Dynamic modelling of a polymer electrolyte membrane fuel cell stack by nonlinear system identification. *Fuel Cells, 7*(5), 392-401.

Cai, Y., Miao, C., Tan, A.-H., Shen, Z., & Li, B. (2010). Creating an immersive game world with evolutionary fuzzy cognitive maps. *IEEE computer graphics and applications*(2), 58-70.

Carvalho, J. P. (2010). *On the semantics and the use of fuzzy cognitive maps in social sciences.* Paper presented at the Fuzzy Systems (FUZZ), 2010 IEEE International Conference on.

Carvalho, J. P., & Tomè, J. A. (1999). Rule based fuzzy cognitive maps-fuzzy causal relations. *Computational Intelligence for Modelling, Control and Automation, Edited by M. Mohammadian*.

Ceraolo, M., Miulli, C., & Pozio, A. (2003). Modelling static and dynamic behaviour of proton exchange membrane fuel cells on the basis of electro-chemical description. *Journal of Power Sources, 113*(1), 131-144. doi: 10.1016/s0378-7753(02)00565-7

Chang, K.-Y., & Teng, Y.-W. (2012). THE OPTIMAL DESIGN FOR PEMFC MODELING BASED ON BPNN AND TAGUCHI METHOD. *International Journal of Green Energy, 9*(2), 139-159. doi: 10.1080/15435075.2011.622018

Chang, W.-Y. (2013). Equivalent Circuit Parameters Estimation for PEM Fuel Cell Using RBF Neural Network and Enhanced Particle Swarm Optimization. *Mathematical Problems in Engineering*. doi: 10.1155/2013/672681

Chávez-Ramírez, A. U., Muñoz-Guerrero, R., Duron-Torres, S., Ferraro, M., Brunaccini, G., Sergi, F., . . . Arriaga, L. (2010). High power fuel cell simulator based on artificial neural network. *International Journal of Hydrogen Energy, 35*(21), 12125-12133.

Chavez-Ramirez, A. U., Munoz-Guerrero, R., Duron-Torres, S. M., Ferraro, M., Brunaccini, G., Sergi, F., . . . Arriaga, L. G. (2010). High power fuel cell simulator based on artificial neural network. *International Journal of Hydrogen Energy, 35*(21), 12125-12133. doi: 10.1016/j.ijhydene.2009.09.071

Chen, H.-W., Hsaio, H.-C., & Wu, S.-J. (1992). Current Situation and Prospects of Motorcycle Pollution Control in Taiwan, Republic of China: SAE Technical Paper.

Cheng, S.-J., Miao, J.-M., & Wu, S.-J. (2013). Use of metamodeling optimal approach promotes the performance of proton exchange membrane fuel cell (PEMFC). *Applied Energy, 105*, 161-169.

Chunying, Z., Lu, L., Dong, O., & Ruitao, L. (2011). Research of rough cognitive map model *Advanced Research on Electronic Commerce, Web Application, and Communication* (pp. 224-229): Springer.

Contreras, A., Posso, F., & Guervos, E. (2010). Modelling and simulation of the utilization of a PEM fuel cell in the rural sector of Venezuela. *Applied Energy, 87*(4), 1376-1385. doi: 10.1016/j.apenergy.2009.05.040

Cook, B. (2002). Introduction to fuel cells and hydrogen technology. *Engineering Science & Education Journal, 11*(6), 205-216.

Dickerson, J., & Kosko, B. (1993). *Virtual worlds as fuzzy cognitive maps.* Paper presented at the Virtual Reality Annual International Symposium, 1993., 1993 IEEE.

Dicks, A. L. (2004). Molten carbonate fuel cells. *Current Opinion in Solid State and Materials Science, 8*(5), 379-383.

Dockery, D. W., Pope, C. A., Xu, X., Spengler, J. D., Ware, J. H., Fay, M. E., . . . Speizer, F. E. (1993). An association between air pollution and mortality in six US cities. *New England journal of medicine, 329*(24), 1753-1759.

Dyer, C. K. (2002). Fuel cells for portable applications. *Journal of Power Sources, 106*(1), 31-34.

Faiz, A., Weaver, C. S., & Walsh, M. P. (1996). *Air pollution from motor vehicles: standards and technologies for controlling emissions*: World Bank Publications.

Ferng, Y., Tzang, Y., Pei, B., Sun, C., & Su, A. (2004). Analytical and experimental investigations of a proton exchange membrane fuel cell. *International Journal of Hydrogen Energy, 29*(4), 381-391.

Feroldi, D., & Basualdo, M. (2012). Description of PEM fuel cells system *PEM Fuel Cells with Bio-Ethanol Processor Systems* (pp. 49-72): Springer.

Fuerte, A., Valenzuela, R. X., & Daza, L. (2007). Preparation and characterisation of SOFC anodic materials based on Ce–Cu. *Journal of Power Sources, 169*(1), 47-52. doi: http://dx.doi.org/10.1016/j.jpowsour.2007.03.033

Funes, E., Allouche, Y., Beltrán, G., & Jiménez, A. (2015). A Review: Artificial Neural Networks as Tool for Control Food Industry Process. *Journal of Sensor Technology, 5*(01), 28.

Furfaro, R., Kargel, J. S., Lunine, J. I., Fink, W., & Bishop, M. P. (2010). Identification of cryovolcanism on Titan using fuzzy cognitive maps. *Planetary and Space Science, 58*(5), 761-779.

Furht, B., & Marques, O. (2003). *Handbook of video databases: design and applications*: CRC press.

Garche, J., Dyer, C. K., Moseley, P. T., Ogumi, Z., Rand, D. A., & Scrosati, B. (2013). *Encyclopedia of electrochemical power sources*: Newnes.

Gavin, H. (2011). The Levenberg-Marquardt method for nonlinear least squares curve-fitting problems. *Department of Civil and Environmental Engineering, Duke University*, 1-15.

Georgopoulos, V. C., Malandraki, G. A., & Stylios, C. D. (2003). A fuzzy cognitive map approach to differential diagnosis of specific language impairment. *Artificial Intelligence in Medicine, 29*(3), 261-278. doi: http://dx.doi.org/10.1016/S0933-3657(02)00076-3

Gong, W., & Cai, Z. (2014). Parameter optimization of PEMFC model with improved multi-strategy adaptive differential evolution. *Engineering Applications of Artificial Intelligence, 27*, 28-40. doi: 10.1016/j.engappai.2013.07.016

Gonzalez, J. L., Aguilar, L. T., & Castillo, O. (2009). A cognitive map and fuzzy inference engine model for online design and self fine-tuning of fuzzy logic controllers. *International Journal of Intelligent Systems, 24*(11), 1134-1173.

Haji, S. (2011). Analytical modeling of PEM fuel cell i-V curve. *Renewable Energy, 36*(2), 451-458. doi: 10.1016/j.renene.2010.07.007

Hammou, A., & Guindet, J. (1997). Solid oxide fuel cells. *The CRC Handbook of Solid State Electrochemistry, CRC Press. Inc*, 407.

Hamnett, A. (1997). Mechanism and electrocatalysis in the direct methanol fuel cell. *Catalysis Today, 38*(4), 445-457.

Hasikos, J., Sarimveis, H., Zervas, P., & Markatos, N. (2009). Operational optimization and real-time control of fuel-cell systems. *Journal of Power Sources, 193*(1), 258-268.

Hasikos, J., Sarimveis, H., Zervas, P. L., & Markatos, N. C. (2009). Operational optimization and real-time control of fuel-cell systems. *Journal of Power Sources, 193*(1), 258-268. doi: 10.1016/j.jpowsour.2009.01.048

Hatti, M., Tioursi, M., & Nouibat, W. (2006). *Neural Network Approach for Semi-Empirical Modelling of PEM Fuel-Cell.* Paper presented at the Industrial Electronics, 2006 IEEE International Symposium on.

Hou, Y., Zhuang, M., & Wan, G. (2007). The analysis for the efficiency properties of the fuel cell engine. *Renewable Energy, 32*(7), 1175-1186.

Hu, P., Cao, G.-Y., Zhu, X.-J., & Li, J. (2010). Modeling of a proton exchange membrane fuel cell based on the hybrid particle swarm optimization with Levenberg–Marquardt neural network. *Simulation Modelling Practice and Theory, 18*(5), 574-588.

Huerga, A. V. (2002). *A balanced differential learning algorithm in fuzzy cognitive maps.* Paper presented at the Proceedings of the 16th International Workshop on Qualitative Reasoning.

Isaac, M. E., Dawoe, E., & Sieciechowicz, K. (2009). Assessing local knowledge use in agroforestry management with cognitive maps. *Environmental Management, 43*(6), 1321-1329.

Ismail, M. S., Ingham, D. B., Hughes, K. J., Ma, L., & Pourkashanian, M. (2014). An efficient mathematical model for air-breathing PEM fuel cells. *Applied Energy, 135*, 490-503. doi: 10.1016/j.apenergy.2014.08.113

Jang, J.-Y., Cheng, C.-H., Liao, W.-T., Huang, Y.-X., & Tsai, Y.-C. (2012). Experimental and numerical study of proton exchange membrane fuel cell with spiral flow channels. *Applied Energy, 99*, 67-79. doi: 10.1016/j.apenergy.2012.04.011

Jemei, S., Hissel, D., Péra, M.-C., & Kauffmann, J.-M. (2002). *Black-box modeling of proton exchange membrane fuel cell generators.* Paper presented at the IECON 02 [Industrial Electronics Society, IEEE 2002 28th Annual Conference of the].

Jemeı, S., Hissel, D., Péra, M.-C., & Kauffmann, J.-M. (2003). On-board fuel cell power supply modeling on the basis of neural network methodology. *Journal of Power Sources, 124*(2), 479-486.

Jemei, S., Hissel, D., Pera, M.-C., & Kauffmann, J. M. (2008). A new modeling approach of embedded fuel-cell power generators based on artificial neural network. *Ieee Transactions on Industrial Electronics, 55*(1), 437-447. doi: 10.1109/tie.2007.896480

Jemeï, S., Hissel, D., Péra, M.-C., & Kauffmann, J. M. (2008). A new modeling approach of embedded fuel-cell power generators based on artificial neural network. *Industrial Electronics, IEEE Transactions on, 55*(1), 437-447.

Jose, A., & Contreras, J. (2010). The FCM Designer Tool. In M. Glykas (Ed.), *Fuzzy Cognitive Maps* (Vol. 247, pp. 71-87): Springer Berlin Heidelberg.

Kafetzis, A., McRoberts, N., & Mouratiadou, I. (2010). Using fuzzy cognitive maps to support the analysis of stakeholders' views of water resource use and water quality policy *Fuzzy Cognitive Maps* (pp. 383-402): Springer.

Kammen, D. M. (2002). The role of fuel cells in the renewable roadmap to energy independence. *Testimony for the United States House Subcommittee on Energy, Washington, DC*.

Kasahara, K., Morioka, M., Yoshida, H., & Shingai, H. (2000). PAFC operating performance verified by Japanese gas utilities. *Journal of Power Sources, 86*(1–2), 298-301. doi: http://dx.doi.org/10.1016/S0378-7753(99)00409-7

Kazim, A. (2002). A novel approach on the determination of the minimal operating efficiency of a PEM fuel cell. *Renewable Energy, 26*(3), 479-488.

Kazim, A. (2004). Exergy analysis of a PEM fuel cell at variable operating conditions. *Energy Conversion and Management, 45*(11), 1949-1961.

Kazim, A. (2005). Exergoeconomic analysis of a PEM fuel cell at various operating conditions. *Energy Conversion and Management, 46*(7), 1073-1081.

Kheirandish, A., Kazemi, M. S., & Dahari, M. (2014). Dynamic performance assessment of the efficiency of fuel cell-powered bicycle: An experimental approach. *International Journal of Hydrogen Energy, 39*(25), 13276-13284.

Kok, K. (2009). The potential of Fuzzy Cognitive Maps for semi-quantitative scenario development, with an example from Brazil. *Global Environmental Change, 19*(1), 122-133.

Kong, X., & Khambadkone, A. M. (2009). Modeling of a PEM fuel-cell stack for dynamic and steady-state operation using ANN-based submodels. *Industrial Electronics, IEEE Transactions on, 56*(12), 4903-4914.

Kong, X., Yeau, W., & Khambadkone, A. M. (2006). *Ann modelling of nonlinear subsystem of a pemfc stack for dynamic and steady state operation.* Paper presented at the IEEE Industrial Electronics, IECON 2006-32nd Annual Conference on.

Kordesch, K., & Simader, G. (1996). *Fuel cells and their applications*: VCH.

Kosko, B. (1986). Fuzzy cognitive maps. *International Journal of man-machine studies, 24*(1), 65-75.

Kosko, B. (1996). *Fuzzy engineering*: Prentice-Hall, Inc.

Kottas, T., Boutalis, Y., Diamantis, V., Kosmidou, O., & Aivasidis, A. (2006). *A fuzzy cognitive network based control scheme for an anaerobic digestion process.* Paper presented at the Control and Automation, 2006. MED'06. 14th Mediterranean Conference on.

Kottas, T. L., Boutalis, Y. S., & Christodoulou, M. A. (2007). Fuzzy cognitive network: A general framework. *Intelligent Decision Technologies, 1*(4), 183-196.

Kottas, T. L., Boutalis, Y. S., & Christodoulou, M. A. (2010). Fuzzy cognitive networks: Adaptive network estimation and control paradigms *Fuzzy Cognitive Maps* (pp. 89-134): Springer.

Kottas, T. L., Karlis, A. D., & Boutalis, Y. S. (2010). Fuzzy cognitive networks for maximum power point tracking in photovoltaic arrays *Fuzzy Cognitive Maps* (pp. 231-257): Springer.

Koulouriotis, D., Diakoulakis, I., & Emiris, D. (2001). *Learning fuzzy cognitive maps using evolution strategies: a novel schema for modeling and simulating high-level behavior.* Paper presented at the Evolutionary Computation, 2001. Proceedings of the 2001 Congress on.

Lai, X., Zhou, Y., & Zhang, W. (2009). *Software usability improvement: modeling, training and relativity analysis.* Paper presented at the Second International Symposium on Information Science and Engineering.

Larminie, J. (2003). *Fuel Cell Systems Explained* (2nd ed.).

Larminie, J., Dicks, A., & McDonald, M. S. (2003). *Fuel cell systems explained* (Vol. 2): J. Wiley Chichester, UK.

Lee, W.-Y., Park, G.-G., Yang, T.-H., Yoon, Y.-G., & Kim, C.-S. (2004). Empirical modeling of polymer electrolyte membrane fuel cell performance using artificial neural networks. *International Journal of Hydrogen Energy, 29*(9), 961-966.

Levenberg, K. (1944). A method for the solution of certain non–linear problems in least squares.

Li, Q., Chen, W., Liu, Z., Guo, A., & Huang, J. (2014). Nonlinear multivariable modeling of locomotive proton exchange membrane fuel cell system. *International Journal of Hydrogen Energy, 39*(25), 13777-13786.

Li, X., Ji, H., Zheng, R., Li, Y., & Yu, F. R. (2009). *A novel team-centric peer selection scheme for distributed wireless P2P networks.* Paper presented at the Wireless Communications and Networking Conference, 2009. WCNC 2009. IEEE.

Lin, B. Y. S., Kirk, D. W., & Thorpe, S. J. (2006). Performance of alkaline fuel cells: A possible future energy system? *Journal of Power Sources, 161*(1), 474-483. doi: http://dx.doi.org/10.1016/j.jpowsour.2006.03.052

Liu, D., & Case, S. (2006). Durability study of proton exchange membrane fuel cells under dynamic testing conditions with cyclic current profile. *Journal of Power Sources, 162*(1), 521-531. doi: http://dx.doi.org/10.1016/j.jpowsour.2006.07.007

Marquardt, D. W. (1963). An algorithm for least-squares estimation of nonlinear parameters. *Journal of the Society for Industrial & Applied Mathematics, 11*(2), 431-441.

Marr, C., & Li, X. G. (1999). Composition and performance modelling of catalyst layer in a proton exchange membrane fuel cell. *Journal of Power Sources, 77*(1), 17-27. doi: 10.1016/s0378-7753(98)00161-x

McLean, G., Niet, T., Prince-Richard, S., & Djilali, N. (2002). An assessment of alkaline fuel cell technology. *International Journal of Hydrogen Energy, 27*(5), 507-526.

Meidanshahi, V., & Karimi, G. (2012). Dynamic modeling, optimization and control of power density in a PEM fuel cell. *Applied Energy, 93*, 98-105. doi: 10.1016/j.apenergy.2011.04.048

Meiler, M., Hofer, E., Nuhic, A., & Schmid, O. (2012). An Empirical Stationary Fuel Cell Model Using Limited Experimental Data for Identification. *Journal of Fuel Cell Science and Technology, 9*(6), 061001.

Miao, J.-M., Cheng, S.-J., & Wu, S.-J. (2011). Metamodel based design optimization approach in promoting the performance of proton exchange membrane fuel cells. *International Journal of Hydrogen Energy, 36*(23), 15283-15294.

Miao, Y., Liu, Z.-Q., Siew, C. K., & Miao, C. Y. (2001). Dynamical cognitive network-an extension of fuzzy cognitive map. *Fuzzy Systems, IEEE Transactions on, 9*(5), 760-770.

Motlagh, O., Tang, S. H., Ismail, N., & Ramli, A. R. (2012). An expert fuzzy cognitive map for reactive navigation of mobile robots. *Fuzzy sets and systems, 201*, 105-121. doi: http://dx.doi.org/10.1016/j.fss.2011.12.013

Motlagh, O., Tang, S. H., Khaksar, W., & Ismail, N. (2012). An alternative approach to FCM activation for modeling dynamic systems. *Applied Artificial Intelligence, 26*(8), 733-742.

Napoli, G., Ferraro, M., Sergi, F., Brunaccini, G., & Antonucci, V. (2013). Data driven models for a PEM fuel cell stack performance prediction. *International Journal of Hydrogen Energy, 38*(26), 11628-11638.

Niu, Q., Zhang, H., & Li, K. (2014). An improved TLBO with elite strategy for parameters identification of PEM fuel cell and solar cell models. *International Journal of Hydrogen Energy, 39*(8), 3837-3854.

Oezbek, M., Wang, S., Marx, M., & Soeffker, D. (2013). Modeling and control of a PEM fuel cell system: A practical study based on experimental defined component behavior. *Journal of Process Control, 23*(3), 282-293. doi: 10.1016/j.jprocont.2012.11.009

Ogaji, S., Singh, R., Pilidis, P., & Diacakis, M. (2006). Modelling fuel cell performance using artificial intelligence. *Journal of Power Sources, 154*(1), 192-197.

Ou, S., & Achenie, L. E. (2005). A hybrid neural network model for PEM fuel cells. *Journal of Power Sources, 140*(2), 319-330.

Ou, S., & Achenie, L. E. K. (2005). A hybrid neural network model for PEM fuel cells. *Journal of Power Sources, 140*(2), 319-330. doi: 10.1016/j.jpowsour.2004.08.047

Pandian, M. S., Anwari, M., Husodo, B. Y., & Hiendro, A. (2010). *Efficiency and economics analysis of Proton Exchange Membrane fuel cell.* Paper presented at the IPEC, 2010 Conference Proceedings.

Papageorgiou, E. (2011). *Review study on fuzzy cognitive maps and their applications during the last decade.* Paper presented at the Fuzzy Systems (FUZZ), 2011 IEEE International Conference on.

Papageorgiou, E., & Groumpos, P. (2004). A weight adaptation method for fuzzy cognitive maps to a process control problem *Computational Science-ICCS 2004* (pp. 515-522): Springer.

Papageorgiou, E., & Groumpos, P. (2005). A new hybrid learning algorithm for fuzzy cognitive maps learning. *Applied Soft Computing, 5*(4), 409-431.

Papageorgiou, E., Papandrianos, N., Karagianni, G., Kyriazopoulos, G. C., & Sfyras, D. (2009). *A fuzzy cognitive map based tool for prediction of infectious diseases.* Paper presented at the Fuzzy Systems, 2009. FUZZ-IEEE 2009. IEEE International Conference on.

Papageorgiou, E., Spyridonos, P., Stylios, C., Ravazoula, P., Groumpos, P., & Nikiforidis, G. (2003). *A Fuzzy Cognitive Map model for grading urinary bladder tumors.* Paper presented at the 5th Int. Conf. in Neural Networks & Experts Systems in Medicine & Healthcare 1st Int. Conf. in Computational Intelligence in Medicine & Healthcare, NNESMED/CIMED Conference.

Papageorgiou, E., Spyridonos, P., Stylios, C. D., Ravazoula, P., Groumpos, P. P., & Nikiforidis, G. (2006). Advanced soft computing diagnosis method for tumour grading. *Artificial Intelligence in Medicine, 36*(1), 59-70.

Papageorgiou, E., Stylios, C., & Groumpos, P. (2008). The soft computing technique of fuzzy cognitive maps for decision making in radiotherapy. *Intelligent and Adaptive Systems in Medicine*, 106-127.

Papageorgiou, E., Stylios, C. D., & Groumpos, P. P. (2004). Active Hebbian learning algorithm to train fuzzy cognitive maps. *International journal of approximate reasoning, 37*(3), 219-249.

Papageorgiou, E. I. (2013). *Fuzzy Cognitive Maps for Applied Sciences and Engineering: From Fundamentals to Extensions and Learning Algorithms* (Vol. 54): Springer Science & Business Media.

Papageorgiou, E. I., Papadimitriou, C., & Karkanis, S. (2009). *Management of uncomplicated urinary tract infections using fuzzy cognitive maps.* Paper presented at the Information Technology and Applications in Biomedicine, 2009. ITAB 2009. 9th International Conference on.

Papageorgiou, E. I., Stylios, C., & Groumpos, P. P. (2006). Unsupervised learning techniques for fine-tuning fuzzy cognitive map causal links. *International Journal of Human-Computer Studies, 64*(8), 727-743.

Park, K. S., & Kim, S. H. (1995). Fuzzy cognitive maps considering time relationships. *International Journal of Human-Computer Studies, 42*(2), 157-168.

Peng, L., & Lai, X. (2010). Effect of assembly error of bipolar plate on the contact pressure distribution and stress failure of membrane electrode assembly in proton exchange membrane fuel cell. *Journal of Power Sources, 195*(13), 4213-4221.

Perlich, C. (2011). Learning Curves in Machine Learning *Encyclopedia of Machine Learning* (pp. 577-580): Springer.

Powell, M. J. (1977). Restart procedures for the conjugate gradient method. *Mathematical programming, 12*(1), 241-254.

Puranik, S. V., Keyhani, A., & Khorrami, F. (2010). Neural Network Modeling of Proton Exchange Membrane Fuel Cell. *Ieee Transactions on Energy Conversion, 25*(2), 474-483. doi: 10.1109/tec.2009.2035691

Puranik, S. V., Keyhani, A., & Khorrami, F. (2010). Neural network modeling of proton exchange membrane fuel cell. *Energy conversion, IEEE Transactions on, 25*(2), 474-483.

Purkrushpan, J., & Peng, H. (2004). Control of Fuel Cell Power Systems: Principle, Modeling. *Analysis and Feedback Design, Germany: Springer*.

Rajaram, T., & Das, A. (2010). Modeling of interactions among sustainability components of an agro-ecosystem using local knowledge through cognitive mapping and fuzzy inference system. *Expert Systems with Applications, 37*(2), 1734-1744.

Ramsey, D. S., & Norbury, G. L. (2009). Predicting the unexpected: using a qualitative model of a New Zealand dryland ecosystem to anticipate pest management outcomes. *Austral Ecology, 34*(4), 409-421.

Ren, Z. (2007). Learning Fuzzy Cognitive Maps by a Hybrid Method Using Nonlinear Hebbian Learning and Extended Great Deluge Algorithm.

Rezazadeh, S., Mehrabi, M., Pashaee, T., & Mirzaee, I. (2012). Using adaptive neuro-fuzzy inference system (ANFIS) for proton exchange membrane fuel cell (PEMFC) performance modeling. *Journal of Mechanical Science and Technology, 26*(11), 3701-3709.

Rifkin, J. (2003). *The hydrogen economy: The creation of the worldwide energy web and the redistribution of power on earth*: Penguin.

Rouss, V., Lesage, P., Bégot, S., Candusso, D., Charon, W., Harel, F., . . . Yde-Andersen, S. (2008). Mechanical behaviour of a fuel cell stack under vibrating conditions linked to aircraft applications part I: Experimental. *International Journal of Hydrogen Energy, 33*(22), 6755-6765.

Rowe, A., & Li, X. (2001). Mathematical modeling of proton exchange membrane fuel cells. *Journal of Power Sources, 102*(1–2), 82-96. doi: http://dx.doi.org/10.1016/S0378-7753(01)00798-4

Ruan, D., Hardeman, F., & Mkrtchyan, L. (2011). *Using belief degree-distributed fuzzy cognitive maps in nuclear safety culture assessment.* Paper presented at the Fuzzy Information Processing Society (NAFIPS), 2011 Annual Meeting of the North American.

Rumelhart, D. E., Hinton, G. E., & Williams, R. J. (1985). Learning internal representations by error propagation: DTIC Document.

Rumelhart, D. E., Hinton, G. E., & Williams, R. J. (1988). Learning representations by back-propagating errors. *Cognitive modeling, 5*, 3.

Sablani, S. S., Datta, A. K., Rahman, M. S., & Mujumdar, A. S. (2006). *Handbook of food and bioprocess modeling techniques*: CRC Press.

Saenrung, A., Abtahi, A., & Zilouchian, A. (2007). Neural network model for a commercial PEM fuel cell system. *Journal of Power Sources, 172*(2), 749-759. doi: 10.1016/j.jpowsour.2007.05.039

Salameh, Z. (2014). *Renewable energy system design*: Academic Press.

Salemme, L., Menna, L., & Simeone, M. (2009). Analysis of the energy efficiency of innovative ATR-based PEM fuel cell system with hydrogen membrane separation. *International Journal of Hydrogen Energy, 34*(15), 6384-6392.

Salmeron, J. L. (2010). Modelling grey uncertainty with fuzzy grey cognitive maps. *Expert Systems with Applications, 37*(12), 7581-7588.

Samsun, R. C., Pasel, J., Janssen, H., Lehnert, W., Peters, R., & Stolten, D. (2014). Design and test of a 5 kW(e) high-temperature polymer electrolyte fuel cell system operated with diesel and kerosene. *Applied Energy, 114*, 238-249. doi: 10.1016/j.apenergy.2013.09.054

Silva, R., Gouriveau, R., Jemei, S., Hissel, D., Boulon, L., Agbossou, K., & Steiner, N. Y. (2014). Proton exchange membrane fuel cell degradation prediction based on Adaptive Neuro-Fuzzy Inference Systems. *International Journal of Hydrogen Energy, 39*(21), 11128-11144.

Smith, L. I. (2002). A tutorial on principal components analysis. *Cornell University, USA, 51*, 52.

Stach, W., Kurgan, L., & Pedrycz, W. (2005). A survey of fuzzy cognitive map learning methods. *Issues in soft computing: theory and applications*, 71-84.

Stach, W., Kurgan, L., & Pedrycz, W. (2008). *Data-driven nonlinear Hebbian learning method for fuzzy cognitive maps.* Paper presented at the Fuzzy Systems, 2008. FUZZ-IEEE 2008.(IEEE World Congress on Computational Intelligence). IEEE International Conference on.

Stach, W., Kurgan, L., Pedrycz, W., & Reformat, M. (2005). Genetic learning of fuzzy cognitive maps. *Fuzzy sets and systems, 153*(3), 371-401.

Stylios, C. D., & Georgopoulos, V. C. (2008). Fuzzy cognitive maps structure for medical decision support systems *Forging New Frontiers: Fuzzy Pioneers II* (pp. 151-174): Springer.

Stylios, C. D., & Groumpos, P. P. (2004). Modeling complex systems using fuzzy cognitive maps. *Systems, Man and Cybernetics, Part A: Systems and Humans, IEEE Transactions on, 34*(1), 155-162.

Tan, C. O., & Özesmi, U. (2006). A generic shallow lake ecosystem model based on collective expert knowledge. *Hydrobiologia, 563*(1), 125-142.

Tiss, F., Chouikh, R., & Guizani, A. (2013). Dynamic modeling of a PEM fuel cell with temperature effects. *International Journal of Hydrogen Energy, 38*(20), 8532-8541. doi: 10.1016/j.ijhydene.2012.09.101

Vishnyakov, V. (2006). Proton exchange membrane fuel cells. *Vacuum, 80*(10), 1053-1065.

Vural, Y., Ingham, D. B., & Pourkashanian, M. (2009). Performance prediction of a proton exchange membrane fuel cell using the ANFIS model. *International Journal of Hydrogen Energy, 34*(22), 9181-9187.

Wee, J.-H. (2007). Applications of proton exchange membrane fuel cell systems. *Renewable and Sustainable Energy Reviews, 11*(8), 1720-1738. doi: 10.1016/j.rser.2006.01.005

Wu, S.-J., Shiah, S.-W., & Yu, W.-L. (2009). Parametric analysis of proton exchange membrane fuel cell performance by using the Taguchi method and a neural network. *Renewable Energy, 34*(1), 135-144.

Yanchun, Z., & Wei, Z. (2008). *An integrated framework for learning fuzzy cognitive map using RCGA and NHL algorithm.* Paper presented at the 2008 4th International Conference on Wireless Communications, Networking and Mobile Computing.

Yilanci, A., Dincer, I., & Ozturk, H. (2008). Performance analysis of a PEM fuel cell unit in a solar–hydrogen system. *International Journal of Hydrogen Energy, 33*(24), 7538-7552.

Youssef, M. E., Khalil, M. H., & AL-NAdi, K. E. (2010). Neural Network Modeling for Proton Exchange Membrane Fuel Cell(PEMFC). *Advances in Information Sciences and Service Sciences, 2*(2).

Zhang, L., Pan, M., & Quan, S. (2008). Model predictive control of water management in PEMFC. *Journal of Power Sources, 180*(1), 322-329.

Zhong, Z.-D., Zhu, X.-J., & Cao, G.-Y. (2006). Modeling a PEMFC by a support vector machine. *Journal of Power Sources, 160*(1), 293-298.

Zhong, Z.-D., Zhu, X.-J., Cao, G.-Y., & Shi, J.-H. (2007). A hybrid multi-variable experimental model for a PEMFC. *Journal of Power Sources, 164*(2), 746-751.

Zilouchian, A., & Jamshidi, M. (2000). *Intelligent control systems using soft computing methodologies*: CRC Press, Inc.

Appendix A

Electric Bicycle and Experimental Device

A.1 Electric Bicycle

An electric bicycle or e-bike becoming increasingly popular in many countries due to cheap and efficient mode of transportation. Figure below shows an electric bicycle uses a low-power source to turn a small motor located at the hub to the wheel. In electric bicycle, for maximize power to the wheel the rider can pedal in combination with the power.

A.2 System Description

The complete equipment consists of the Fuel Cell Stack with one cooling and one reaction air blower, the necessary auxiliaries to manage the hydrogen and the Electronic Control Unit (ECU).

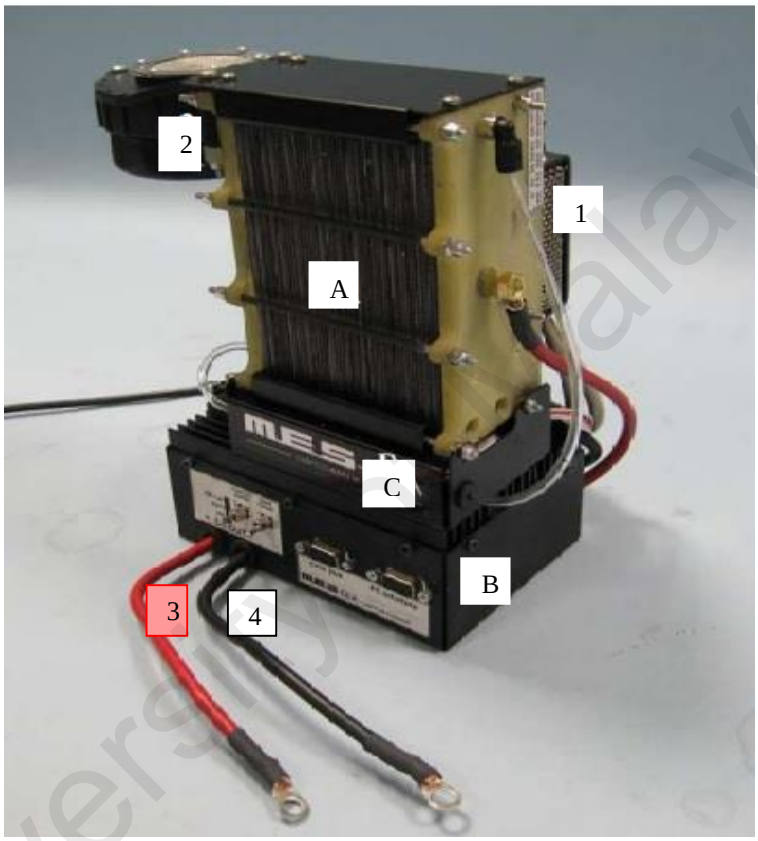

Item	Description
A	PEM- fuel cell stack
B	Electronic Control Unit
C	H_2 Auxiliary box
1	Cooling Air Blower
2	Reaction Air Blower
3	Power Output Terminal +
4	Power Output Terminal -

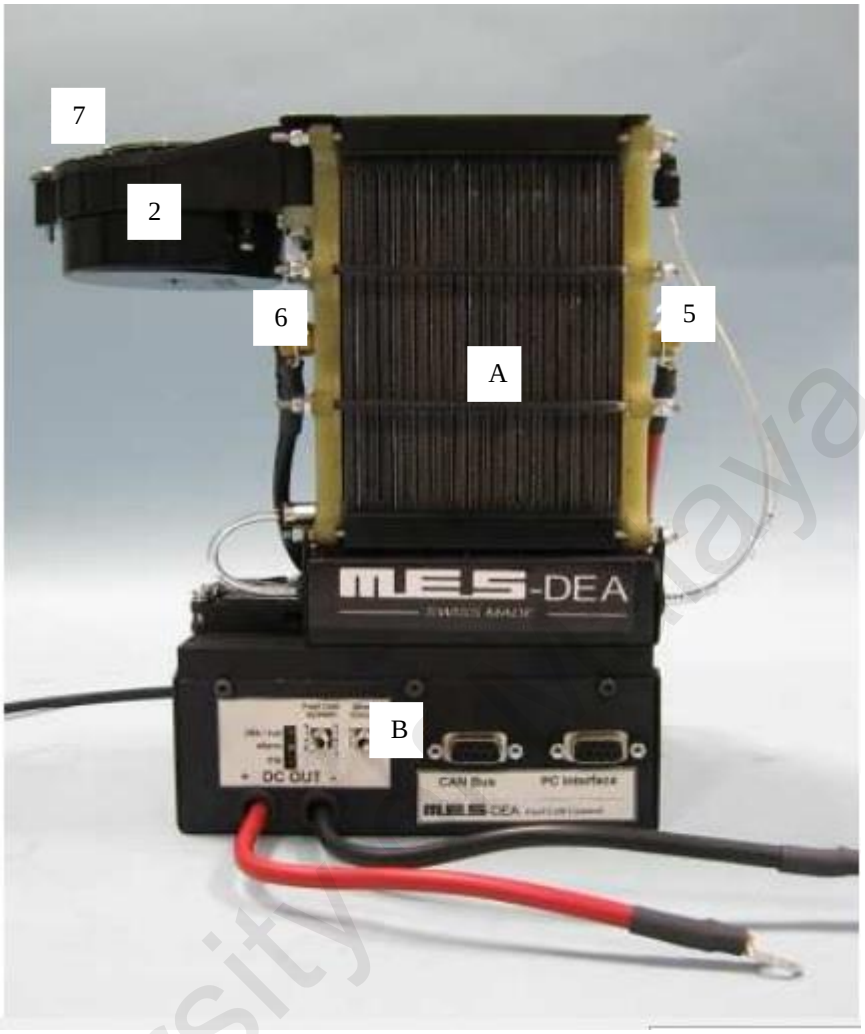

Item	Description
A	PEM- fuel cell stack
B	Electronic Control Unit
2	Reaction Air Blower
5	Hydrogen auxiliary pump (H_2 out)
6	H_2 inlet tube connector
7	H_2 purging tube connector

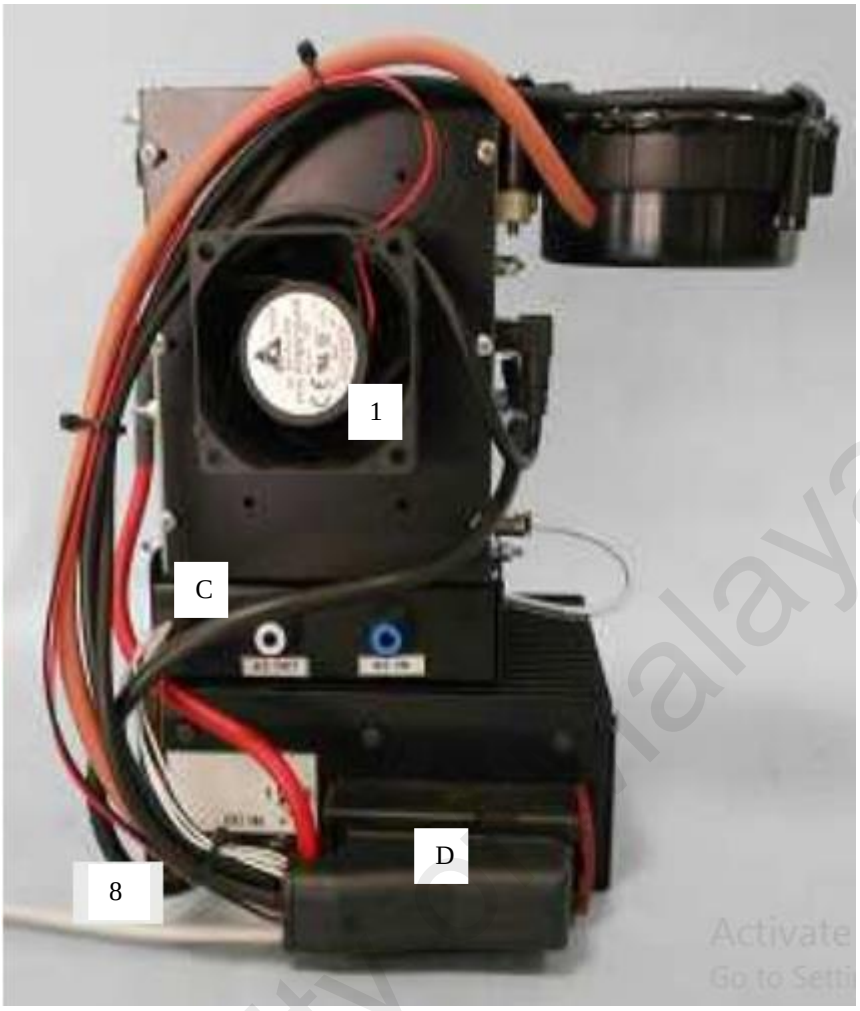

Item	Description
C	H_2 Auxiliary box
D	Signal Wiring
1	Cooling Air Blower
8	External connection cables

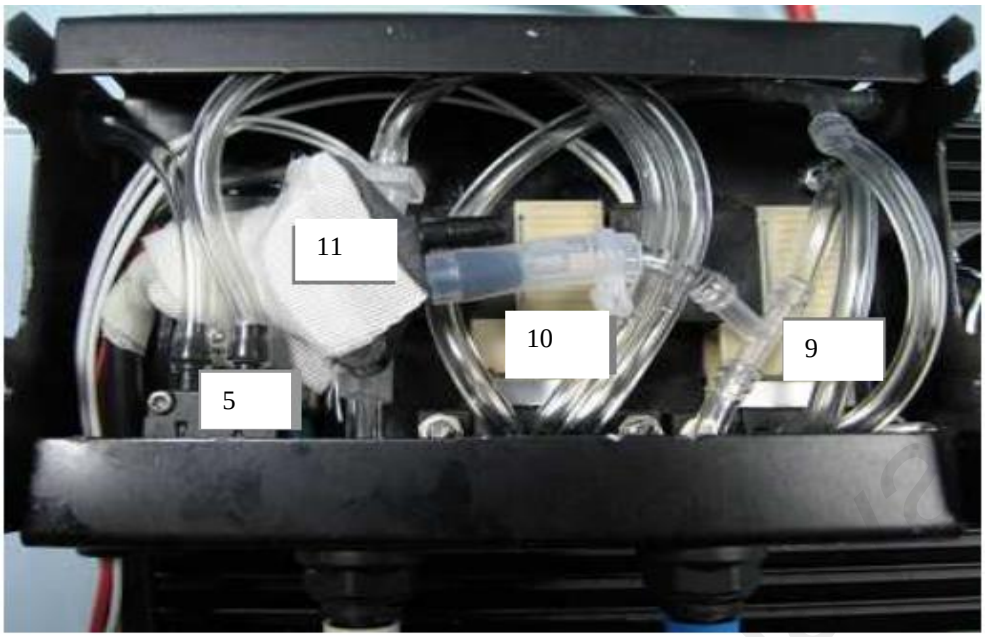

Item	Description
9	Hydrogen main valve (H_2 in)
10	Hydrogen purging valve (H_2 out)
11	Hydrogen pressure sensor
5	Hydrogen auxiliary pump (H_2 out)

Item	Description
13	H_2 inlet tube connector
14	H_2 purging tube connector
15	H_2 auxiliary cables

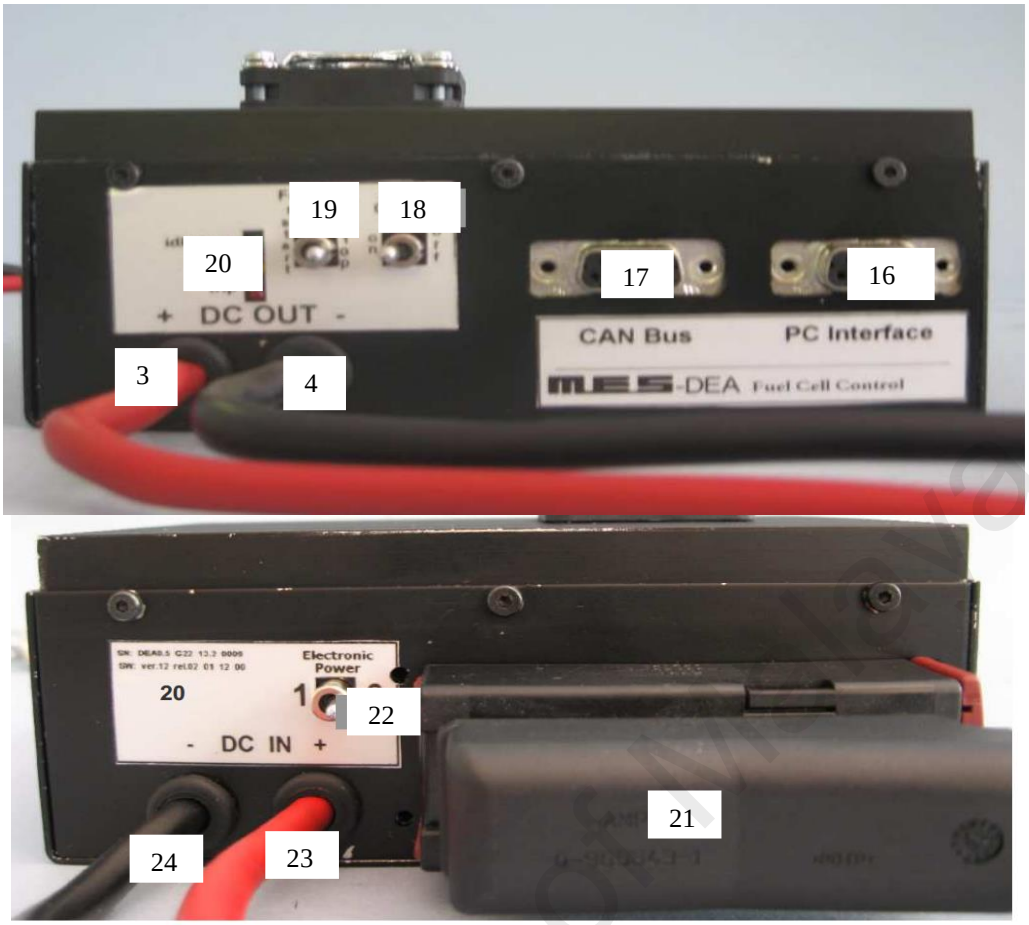

Item	Description
3	Power output terminal +
4	Power output terminal -
16	Serial communication port (RS232)
17	CAN Bus port
18	Short circuit on/off switch
19	Start/Stop switch
20	Status LED's (red, yellow & green)

Item	Description
21	Signal cable connector
22	Power On/Off switch
23	DC In cable +
24	DC In cable -

A.3 Electric Connection

If there is made any modification to the stack or ECU without the written consent of the manufacturer, MES does not warrant the correct function of the fuel cell system.

A.3.1 Connection of stack and ECU

First the connection between the ECU (B) and the auxiliary devices of the stacks (e.g. blowers, valves) has to be established. This is done by connecting the 42 pole AMP® connector (19) that unites all the signal cables (C) from the stack to its connector on the back side of the ECU.

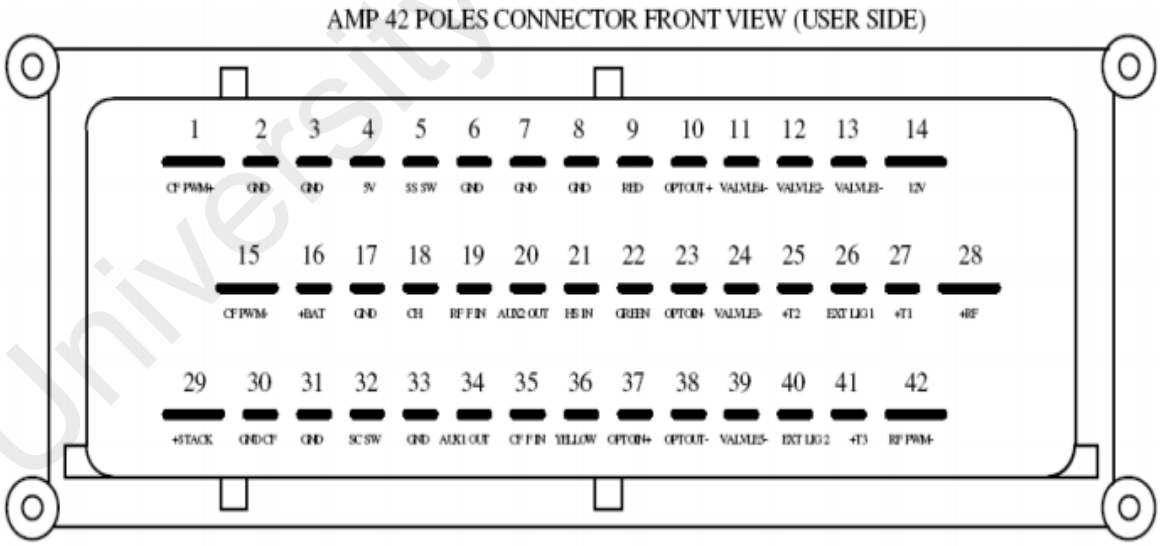

Contact	Description
27	Temperature sensor 1 +
25	Temperature sensor 2 +
41	Temperature sensor 3 + (no implemented on mDEA0.xx)
33	Temperature sensor Ground
4	Hydrogen Pressure Supply +
17	Hydrogen Pressure Supply -
34	Hydrogen Pressure Signal
4	Ambient sensor Supply +
17	Ambient sensor Supply -
21	Ambient RH
8	Ambient Temperature
1	Cooling blower power +
15	Cooling blower power pwm -
30	Cooling blower gnd
35	Cooling air blower fault signal
28	Reaction air blower + supply
31	Reaction air blower - supply
42	Reaction air blower PWM
19	Reaction air blower fault signal
14	Hydrogen main, auxiliary & purging valve + supply
13	Hydrogen main valve
12	Hydrogen purging valve
24	Hydrogen auxiliary pump
16	External battery +
3	External battery -

The connection of the power cables between the Fuel Cell Stack (A) and the ECU (B) is made according to the following scheme:

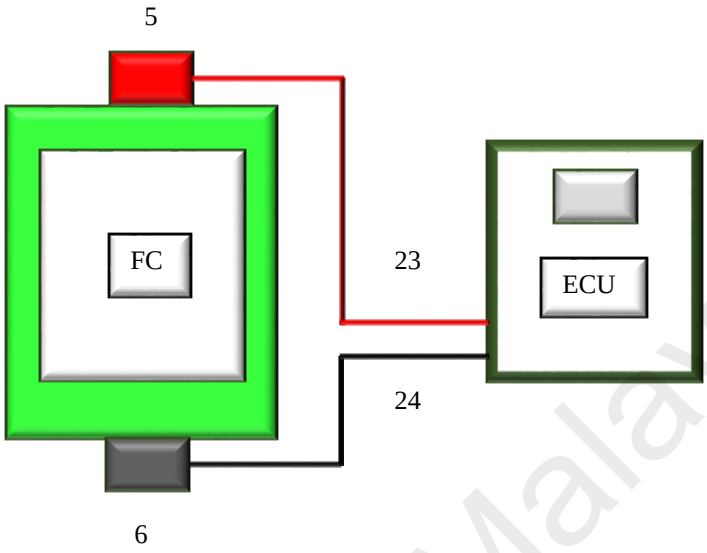

Connect the DC In cable + (23) to the positive (+) power output terminal (5) of the stack and the DC In cable – (24) to the negative (-) power output terminal (6). To do this you have to unscrew the M6 brass nut of the power output terminals of the stack, put the cable lug over the brass bolt and fix it with the M6 brass nut. In principle this connection is already done but be absolutely sure that the connections are made as described above.

Appendix B

Flow charts

B.1 State machine flow chart

The FC control is always in one of seven different states of operation. Sideways a representation of the possible changes of the state.

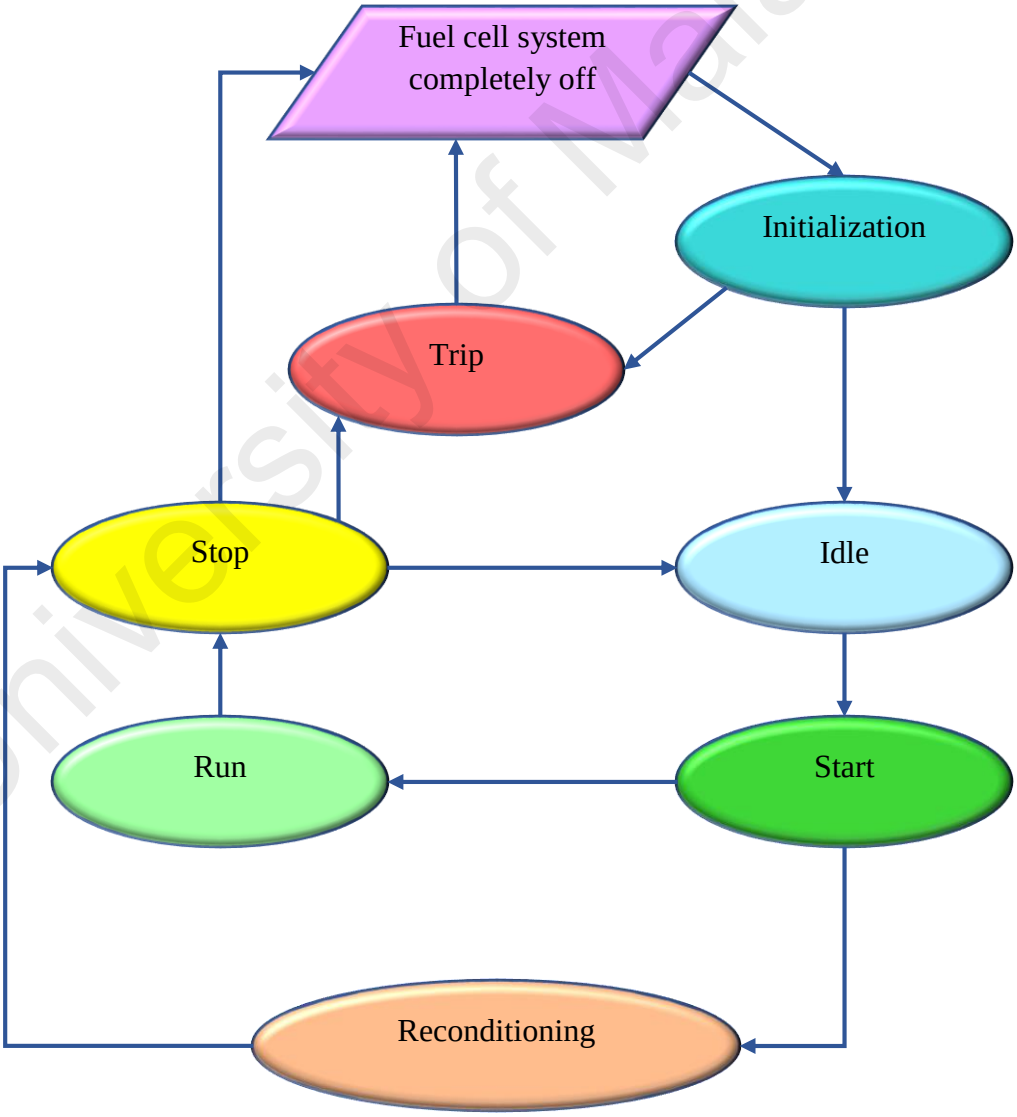

B.2 Start procedure flow chart

In the following flow chart is reported the possible logic sequences that bring to the start of the system:

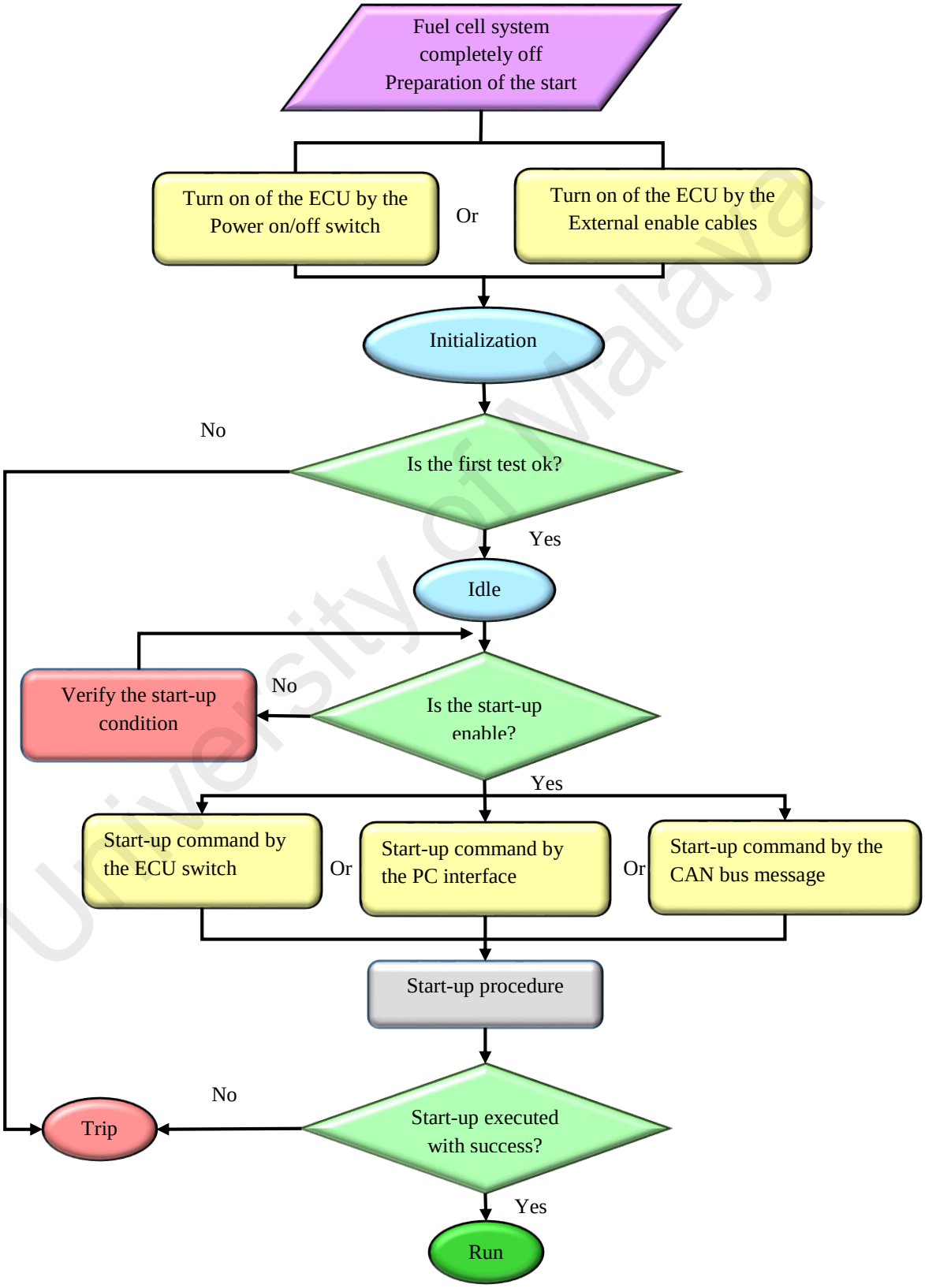

B.3 Stop procedure flow chart

In the following flow chart is reported the possible logic sequences that bring to the stop of the system:

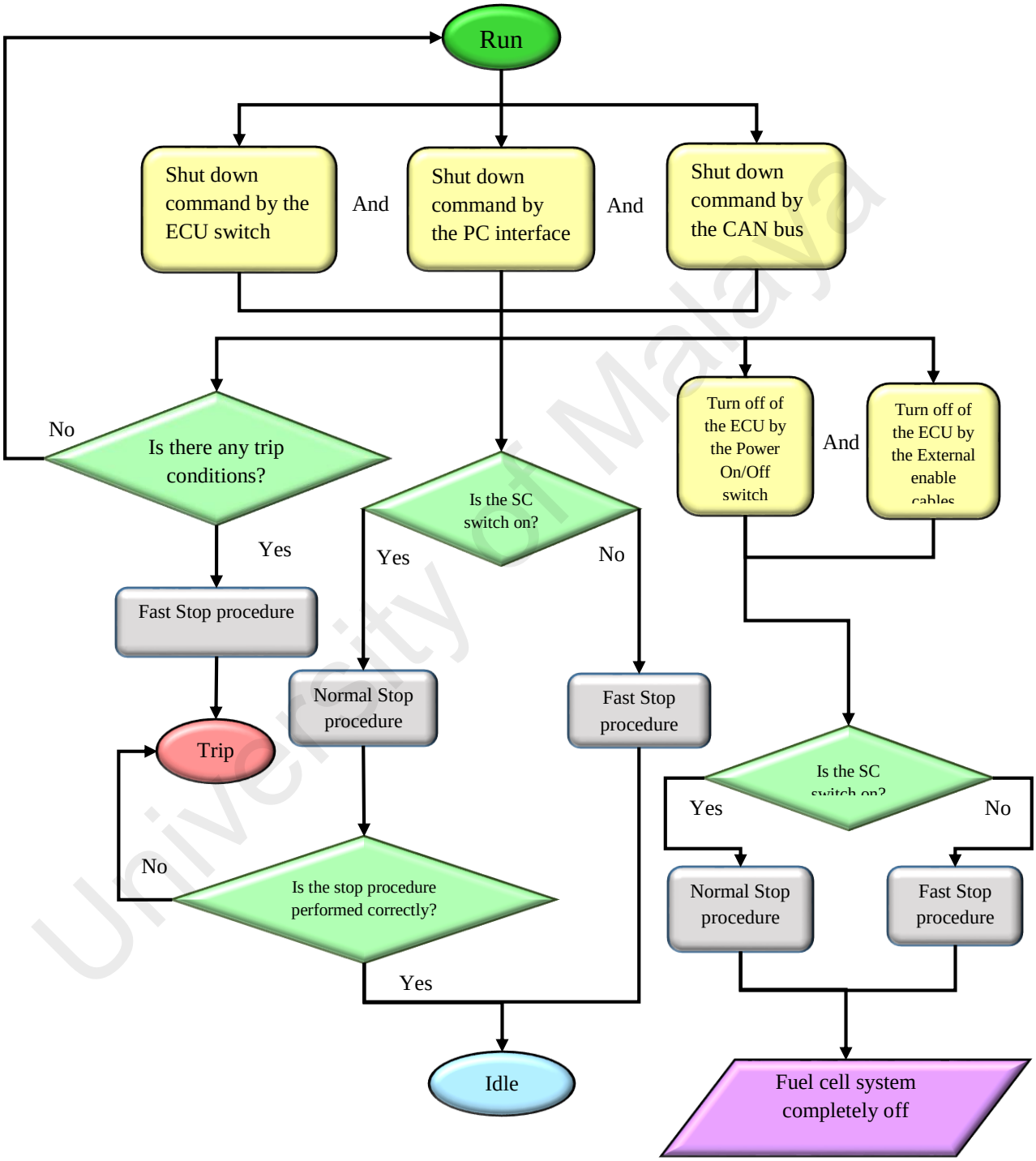

Appendix C

Fuel cell supervisor H2 software and data collection

Install the program Fuel Cell Supervisor H2 for collect the data. Figure below show the software of fuel cell supervisor H2.

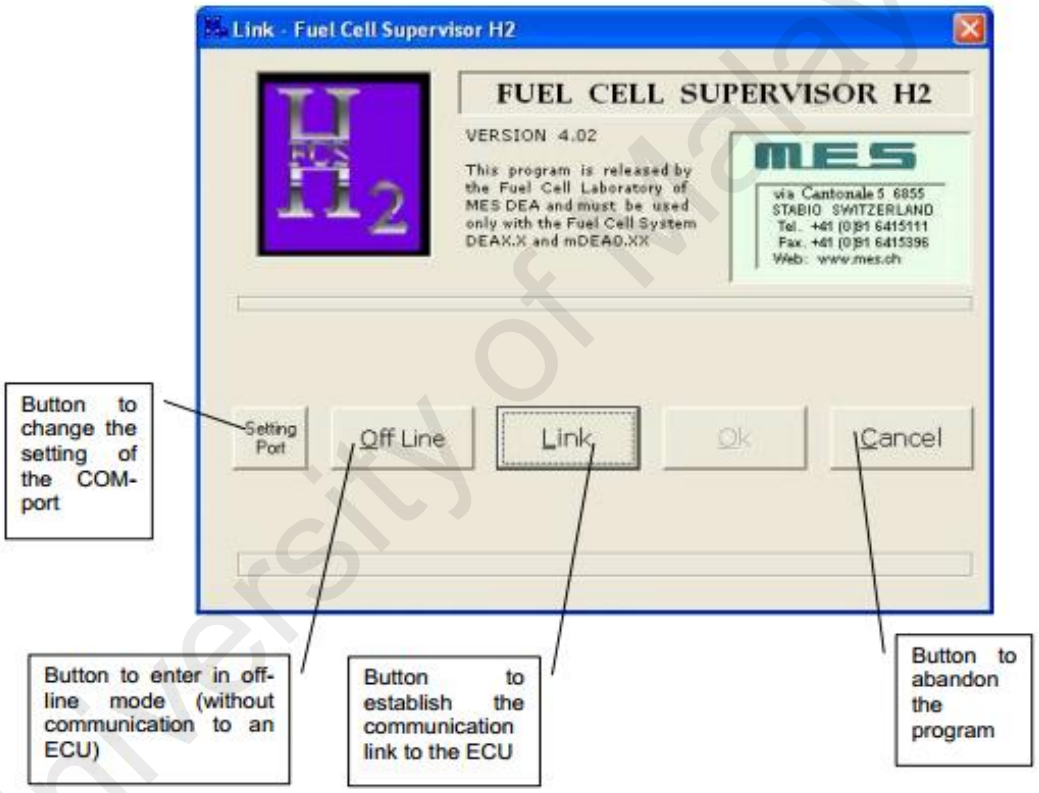

C.1 Fuel cell supervisor H2

In this program the operator can:

- View the general state of each part of the system
- Check the state of the system
- Check the elapsed total operation time of the fuel cell system
- Monitor the control flags of the ECU software
- Monitor the state of the alarm level of the ECU software

Figure below show the status bar:

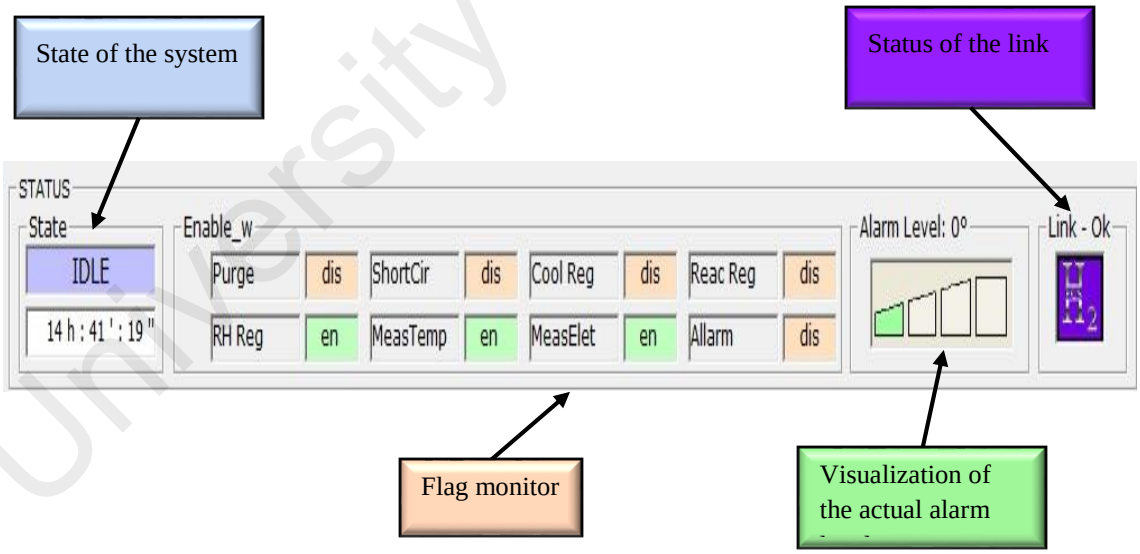

C.1.1 State of the system

In this box the operator can read the actual operational status of the Fuel Cell System control and the already elapsed total operation time of the fuel cell system:

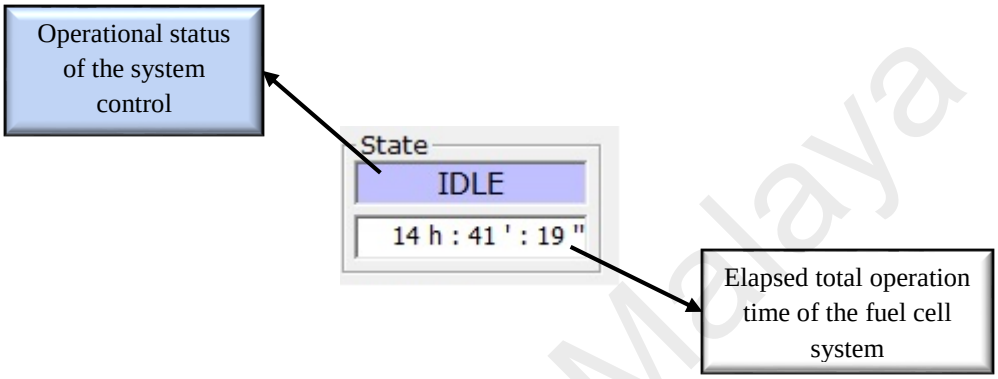

The picture above shows the system in HIDLE state (the control is active, but the fuel cell system is stopped). Other possible state are:

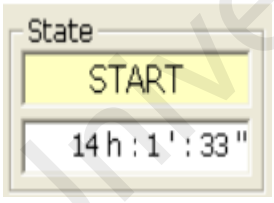

The control is active and the fuel cell system is executing the starting phase

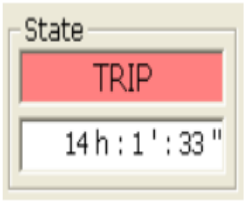

The control is active and the fuel cell system has been stopped, because a security shut off condition has occurred

The control is active and the fuel cell system is in RUN phase

The control is active and the fuel cell system has been realizing a power recovery procedure

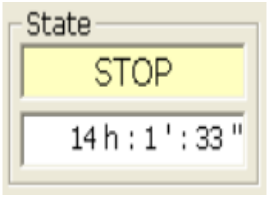

The control is active and the fuel cell is executing the stopping phase

C.1.2 System survey area

In this area the operator can check the general state of operation of the Fuel Cell System; it changes its configuration according to the size of the connected fuel cell system. The configuration for the single fuel cell stack systems is shown here:

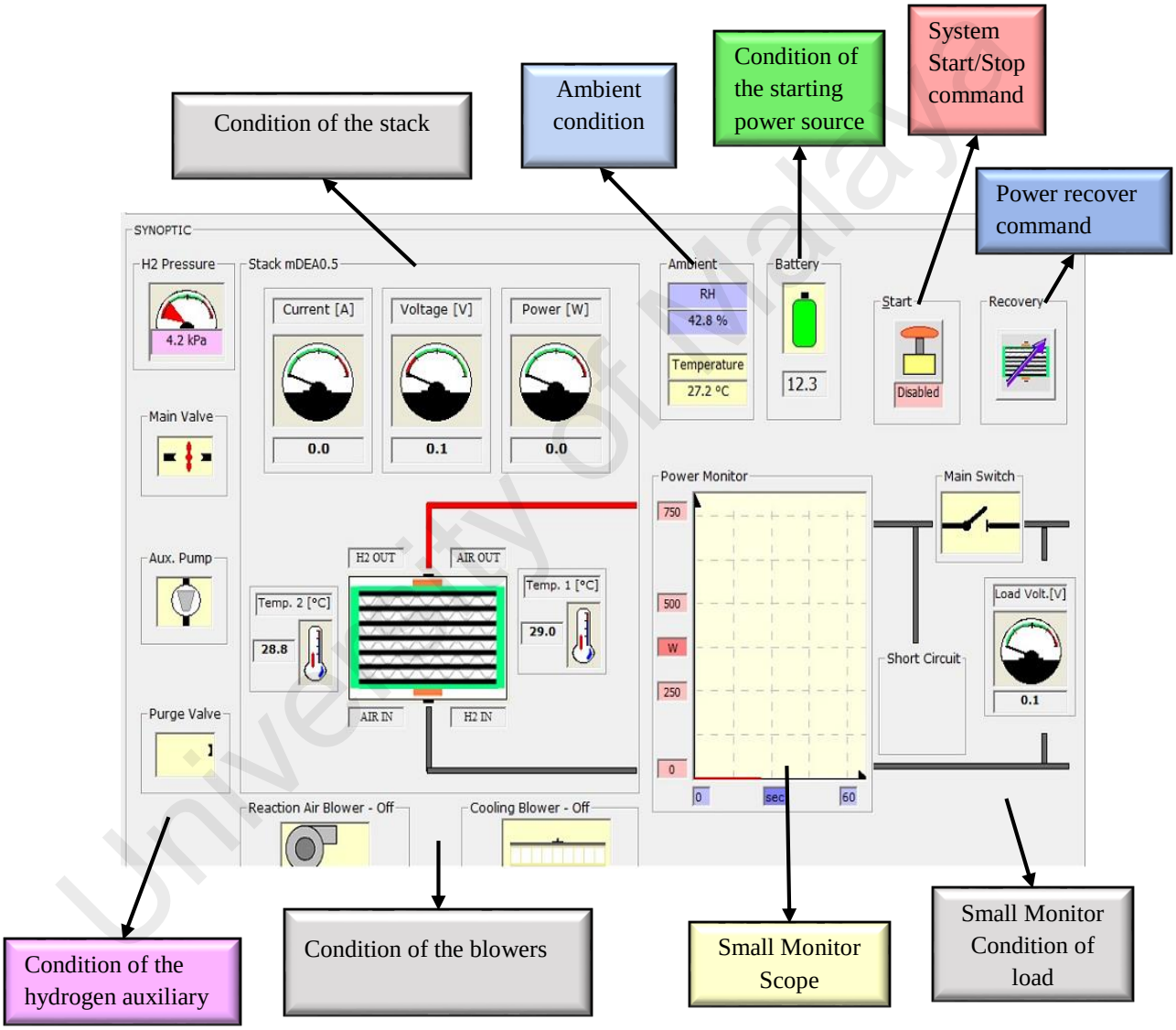

C.1.3 Data Collection

Data collected by Fuel cell supervisor H2 software in excel shown in figure below:

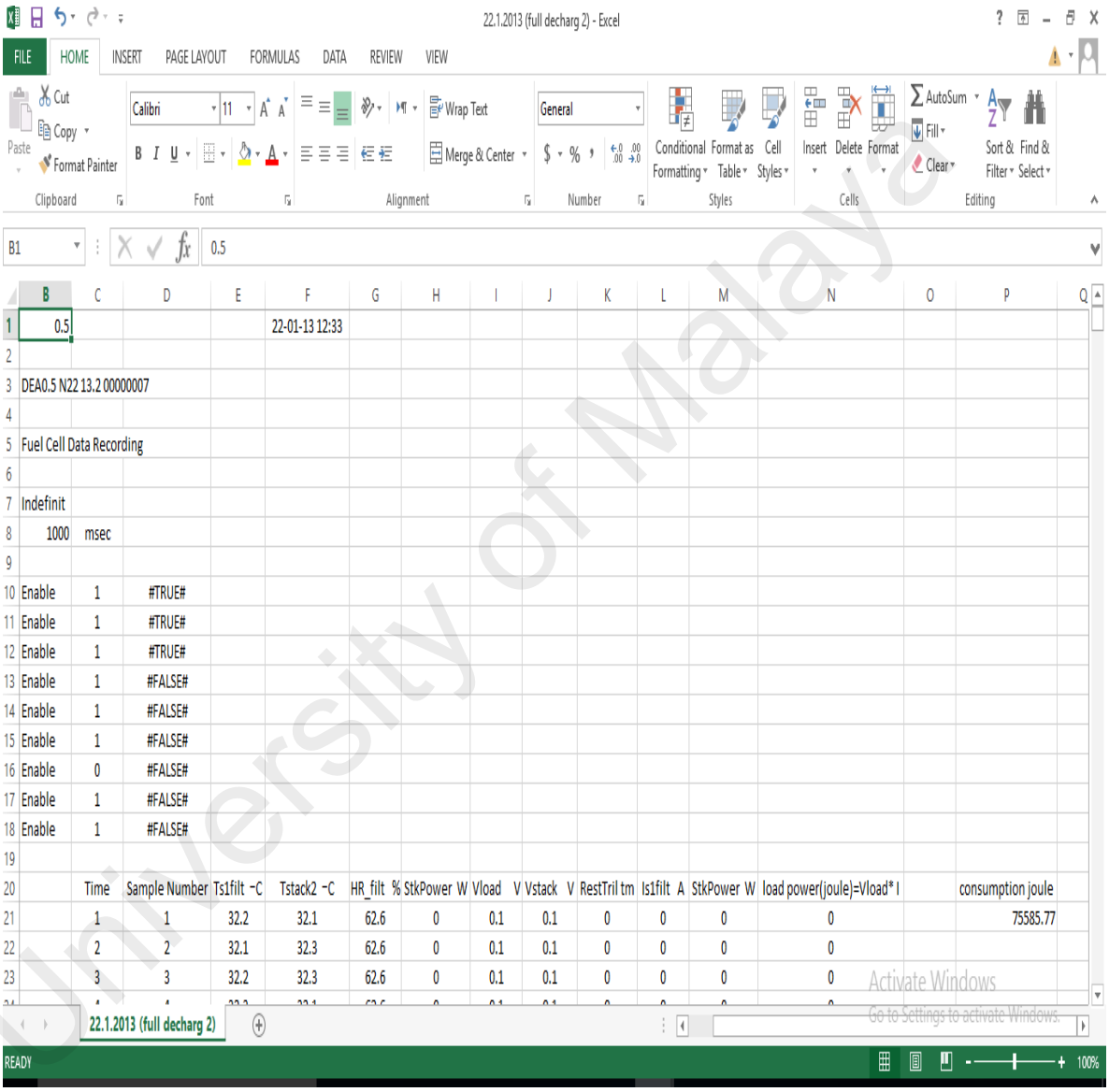

	B	C	D	E	F	G	H	I	J	K	L	M	N	O	P	Q
1	0.5				22-01-13 12:33											
2																
3	DEA0.5 N22 13.2 00000007															
4																
5	Fuel Cell Data Recording															
6																
7	Indefinit															
8	1000	msec														
9																
10	Enable	1	#TRUE#													
11	Enable	1	#TRUE#													
12	Enable	1	#TRUE#													
13	Enable	1	#FALSE#													
14	Enable	1	#FALSE#													
15	Enable	1	#FALSE#													
16	Enable	0	#FALSE#													
17	Enable	1	#FALSE#													
18	Enable	1	#FALSE#													
19																
20		Time	Sample Number	Ts1filt -C	Tstack2 -C	HR_filt %	StkPower W	Vload V	Vstack V	RestTril tm	Is1filt A	StkPower W	load power(joule)=Vload*I		consumption joule	
21		1	1	32.2	32.1	62.6	0	0.1	0.1	0	0	0	0		75585.77	
22		2	2	32.1	32.3	62.6	0	0.1	0.1	0	0	0	0			
23		3	3	32.2	32.3	62.6	0	0.1	0.1	0	0	0	0			

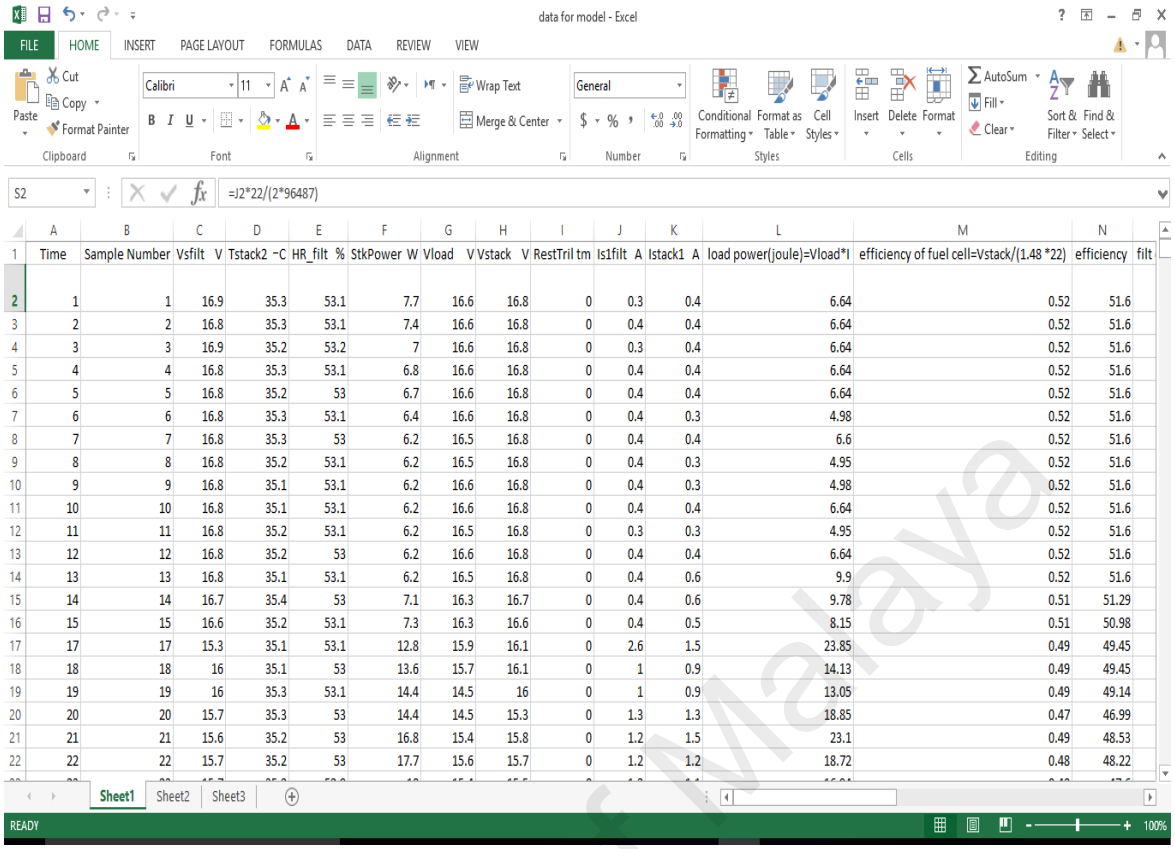

	A	B	C	D	E	F	G	H	I	J	K	L	M	N
1	Time	Sample Number	Vsfilt V	Tstack2 -C	HR_filt %	StkPower W	Vload V	Vstack V	RestTril tm	Is1filt A	Istack1 A	load power(joule)=Vload*I	efficiency of fuel cell=Vstack/(1.48 *22)	efficiency filt
2	1	1	16.9	35.3	53.1	7.7	16.6	16.8	0	0.3	0.4	6.64	0.52	51.6
3	2	2	16.8	35.3	53.1	7.4	16.6	16.8	0	0.4	0.4	6.64	0.52	51.6
4	3	3	16.9	35.2	53.2	7	16.6	16.8	0	0.3	0.4	6.64	0.52	51.6
5	4	4	16.8	35.3	53.1	6.8	16.6	16.8	0	0.4	0.4	6.64	0.52	51.6
6	5	5	16.8	35.2	53	6.7	16.6	16.8	0	0.4	0.4	6.64	0.52	51.6
7	6	6	16.8	35.3	53.1	6.4	16.6	16.8	0	0.4	0.3	4.98	0.52	51.6
8	7	7	16.8	35.3	53	6.2	16.5	16.8	0	0.4	0.4	6.6	0.52	51.6
9	8	8	16.8	35.2	53.1	6.2	16.5	16.8	0	0.4	0.3	4.95	0.52	51.6
10	9	9	16.8	35.1	53.1	6.2	16.6	16.8	0	0.4	0.3	4.98	0.52	51.6
11	10	10	16.8	35.1	53.1	6.2	16.6	16.8	0	0.4	0.4	6.64	0.52	51.6
12	11	11	16.8	35.2	53.1	6.2	16.5	16.8	0	0.3	0.3	4.95	0.52	51.6
13	12	12	16.8	35.2	53	6.2	16.6	16.8	0	0.4	0.4	6.64	0.52	51.6
14	13	13	16.8	35.1	53.1	6.2	16.5	16.8	0	0.4	0.6	9.9	0.52	51.6
15	14	14	16.7	35.4	53	7.1	16.3	16.7	0	0.4	0.6	9.78	0.51	51.29
16	15	15	16.6	35.2	53.1	7.3	16.3	16.6	0	0.4	0.5	8.15	0.51	50.98
17	17	17	15.3	35.1	53.1	12.8	15.9	16.1	0	2.6	1.5	23.85	0.49	49.45
18	18	18	16	35.1	53	13.6	15.7	16.1	0	1	0.9	14.13	0.49	49.45
19	19	19	16	35.3	53.1	14.4	14.5	16	0	1	0.9	13.05	0.49	49.14
20	20	20	15.7	35.3	53	14.4	14.5	15.3	0	1.3	1.3	18.85	0.47	46.99
21	21	21	15.6	35.2	53	16.8	15.4	15.8	0	1.2	1.5	23.1	0.49	48.53
22	22	22	15.7	35.2	53	17.7	15.6	15.7	0	1.2	1.2	18.72	0.48	48.22

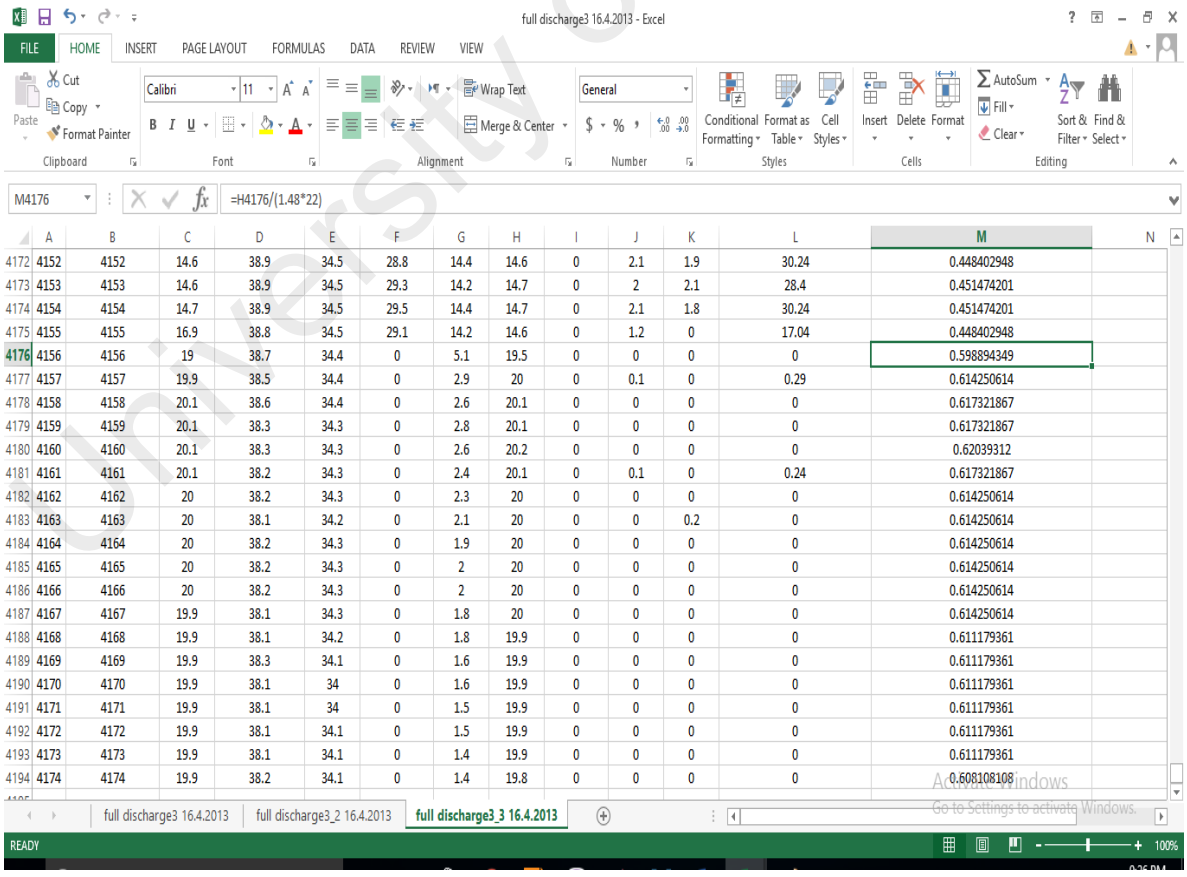

	A	B	C	D	E	F	G	H	I	J	K	L	M	N
4172	4152	4152	14.6	38.9	34.5	28.8	14.4	14.6	0	2.1	1.9	30.24	0.448402948	
4173	4153	4153	14.6	38.9	34.5	29.3	14.2	14.7	0	2	2.1	28.4	0.451474201	
4174	4154	4154	14.7	38.9	34.5	29.5	14.4	14.7	0	2.1	1.8	30.24	0.451474201	
4175	4155	4155	16.9	38.8	34.5	29.1	14.2	14.6	0	1.2	0	17.04	0.448402948	
4176	4156	4156	19	38.7	34.4	0	5.1	19.5	0	0	0	0	0.598894349	
4177	4157	4157	19.9	38.5	34.4	0	2.9	20	0	0.1	0	0.29	0.614250614	
4178	4158	4158	20.1	38.6	34.4	0	2.6	20.1	0	0	0	0	0.617321867	
4179	4159	4159	20.1	38.3	34.3	0	2.8	20.1	0	0	0	0	0.617321867	
4180	4160	4160	20.1	38.3	34.3	0	2.6	20.2	0	0	0	0	0.62039312	
4181	4161	4161	20.1	38.2	34.3	0	2.4	20.1	0	0.1	0	0.24	0.617321867	
4182	4162	4162	20	38.2	34.3	0	2.3	20	0	0	0	0	0.614250614	
4183	4163	4163	20	38.1	34.2	0	2.1	20	0	0	0.2	0	0.614250614	
4184	4164	4164	20	38.2	34.3	0	1.9	20	0	0	0	0	0.614250614	
4185	4165	4165	20	38.2	34.3	0	2	20	0	0	0	0	0.614250614	
4186	4166	4166	20	38.2	34.3	0	2	20	0	0	0	0	0.614250614	
4187	4167	4167	19.9	38.1	34.3	0	1.8	20	0	0	0	0	0.614250614	
4188	4168	4168	19.9	38.1	34.2	0	1.8	19.9	0	0	0	0	0.611179361	
4189	4169	4169	19.9	38.3	34.1	0	1.6	19.9	0	0	0	0	0.611179361	
4190	4170	4170	19.9	38.1	34	0	1.6	19.9	0	0	0	0	0.611179361	
4191	4171	4171	19.9	38.1	34	0	1.5	19.9	0	0	0	0	0.611179361	
4192	4172	4172	19.9	38.1	34.1	0	1.5	19.9	0	0	0	0	0.611179361	
4193	4173	4173	19.9	38.1	34.1	0	1.4	19.9	0	0	0	0	0.611179361	
4194	4174	4174	19.9	38.2	34.1	0	1.4	19.8	0	0	0	0	0.608108108	

Sample Number	T −C	HR_ %	Vload V	Iload A	P Load w	Effi	H_2 flow rate	O_2 flow rate
1	35.3	53.1	16.6	0.3	6.64	51.6	3.42015E-05	1.71007E-05
2	35.3	53.1	16.6	0.4	6.64	51.6	4.5602E-05	2.2801E-05
3	35.2	53.2	16.6	0.3	6.64	51.6	3.42015E-05	1.71007E-05
4	35.3	53.1	16.6	0.4	6.64	51.6	4.5602E-05	2.2801E-05
5	35.2	53	16.6	0.4	6.64	51.6	4.5602E-05	2.2801E-05
6	35.3	53.1	16.6	0.4	4.98	51.6	4.5602E-05	2.2801E-05
7	35.3	53	16.5	0.4	6.6	51.6	4.5602E-05	2.2801E-05
8	35.2	53.1	16.5	0.4	4.95	51.6	4.5602E-05	2.2801E-05
9	35.1	53.1	16.6	0.4	4.98	51.6	4.5602E-05	2.2801E-05
10	35.1	53.1	16.6	0.4	6.64	51.6	4.5602E-05	2.2801E-05
11	35.2	53.1	16.5	0.3	4.95	51.6	3.42015E-05	1.71007E-05
12	35.2	53	16.6	0.4	6.64	51.6	4.5602E-05	2.2801E-05
13	35.1	53.1	16.5	0.4	9.9	51.6	4.5602E-05	2.2801E-05
14	35.4	53	16.3	0.4	9.78	51.29	4.5602E-05	2.2801E-05
15	35.2	53.1	16.3	0.4	8.15	50.98	4.5602E-05	2.2801E-05
17	35.1	53.1	15.9	2.6	23.85	49.45	0.000296413	0.000148206
18	35.1	53	15.7	1	14.13	49.45	0.000114005	5.70025E-05
19	35.3	53.1	14.5	1	13.05	49.14	0.000114005	5.70025E-05
20	35.3	53	14.5	1.3	18.85	46.99	0.000148206	7.41032E-05
21	35.2	53	15.4	1.2	23.1	48.53	0.000136806	6.8403E-05
22	35.2	53	15.6	1.2	18.72	48.22	0.000136806	6.8403E-05
23	35.2	52.9	15.4	1.2	16.94	47.6	0.000136806	6.8403E-05
24	35.1	53	15.4	1.4	16.94	48.83	0.000159607	7.98035E-05
25	35.3	53	15	1.4	31.5	46.99	0.000159607	7.98035E-05
27	35.2	52.9	14.9	4.5	50.66	46.38	0.000513022	0.000256511
28	35.3	52.8	15.8	2.1	33.18	50.37	0.00023941	0.000119705
29	35.3	52.9	17	0.4	1.7	53.13	4.5602E-05	2.2801E-05
30	35.3	52.8	16.6	0.2	6.64	53.13	2.2801E-05	1.14005E-05
31	35.3	52.9	16.6	0.3	6.64	52.21	3.42015E-05	1.71007E-05
32	35.4	52.8	16.6	0.4	3.32	51.9	4.5602E-05	2.2801E-05
33	35.5	52.8	16.5	0.4	6.6	51.9	4.5602E-05	2.2801E-05
34	35.5	52.9	16.5	0.4	4.95	51.6	4.5602E-05	2.2801E-05
35	35.5	52.9	16.6	0.3	6.64	51.9	3.42015E-05	1.71007E-05
36	35.5	52.9	16.5	0.4	6.6	51.29	4.5602E-05	2.2801E-05
37	35.3	52.9	16.6	0.4	6.64	51.29	4.5602E-05	2.2801E-05
38	35.4	53	15.9	1.5	4.77	48.22	0.000171007	8.55037E-05
39	35.5	53.1	15.8	1.5	20.54	49.14	0.000171007	8.55037E-05
40	35.4	53.1	15.6	1	15.6	49.45	0.000114005	5.70025E-05
41	35.5	53.1	15.6	1	14.04	50.68	0.000114005	5.70025E-05
42	35.5	53.1	16.6	0.5	4.98	50.68	5.70025E-05	2.85012E-05
43	35.4	53.2	16.6	0.3	6.64	51.6	3.42015E-05	1.71007E-05
44	35.4	53.2	16.8	0.4	6.72	51.6	4.5602E-05	2.2801E-05
45	35.3	53.2	16.6	0.4	6.64	51.6	4.5602E-05	2.2801E-05

46	35.5	53.3	16.8	0.4	5.04	51.6	4.5602E-05	2.2801E-05
47	35.4	53.3	16.6	0.3	6.64	51.6	3.42015E-05	1.71007E-05
48	35.4	53.3	16.5	0.4	4.95	51.6	4.5602E-05	2.2801E-05
49	35.3	53.3	16.5	0.4	6.6	51.6	4.5602E-05	2.2801E-05
52	35.5	53.4	16.6	0.4	4.98	51.9	4.5602E-05	2.2801E-05
53	35.5	53.3	16	0.4	22.4	49.75	4.5602E-05	2.2801E-05
54	35.4	53.4	16	0.4	3.2	49.75	4.5602E-05	2.2801E-05
55	35.3	53.4	16.4	0.4	6.56	51.29	4.5602E-05	2.2801E-05
57	35.3	53.5	16.5	0.4	8.25	51.29	4.5602E-05	2.2801E-05
58	35.5	53.5	16.5	0.4	4.95	51.6	4.5602E-05	2.2801E-05
59	35.3	53.4	15.9	1.1	41.34	51.29	0.000125405	6.27027E-05
60	35.3	53.4	13.5	3.1	35.1	43.3	0.000353415	0.000176708
62	35.3	53.4	13.3	4.4	47.88	40.23	0.000501622	0.000250811
63	35.3	53.5	13.5	4.9	78.3	42.08	0.000558624	0.000279312
64	35.5	53.5	13.5	3.8	66.15	42.08	0.000433219	0.000216609
65	35.5	53.4	13.5	3.8	55.35	42.08	0.000433219	0.000216609
66	35.5	53.5	13.5	3.8	55.35	42.08	0.000433219	0.000216609
67	35.5	53.5	13.5	4	59.4	42.38	0.00045602	0.00022801
68	35.5	53.5	13.4	4.2	54.94	41.46	0.000478821	0.00023941
69	35.5	53.5	13.2	4	48.84	41.15	0.00045602	0.00022801
70	35.5	53.6	13.2	3.9	48.84	41.77	0.000444619	0.00022231
75	36	54.1	9.1	11	107.38	29.79	0.001254055	0.000627027
158	35.5	51.7	17.1	0.2	3.42	54.05	2.2801E-05	1.14005E-05
159	35.4	51.7	17.1	0.3	5.13	53.13	3.42015E-05	1.71007E-05
160	35.3	51.7	17	0.3	5.1	53.13	3.42015E-05	1.71007E-05
161	35.3	51.7	16.9	0.4	6.76	53.13	4.5602E-05	2.2801E-05
162	35.3	51.8	16.9	0.4	6.76	52.83	4.5602E-05	2.2801E-05
163	35.2	51.7	16.9	0.4	5.07	52.83	4.5602E-05	2.2801E-05
164	35.2	51.8	16.9	0.4	8.45	52.83	4.5602E-05	2.2801E-05
165	35.3	51.8	16.9	0.3	5.07	52.83	3.42015E-05	1.71007E-05
166	35.1	51.7	16.9	0.4	1.69	52.83	4.5602E-05	2.2801E-05
167	35	51.8	16.9	0.3	6.76	53.13	3.42015E-05	1.71007E-05
168	35.1	51.8	16.9	0.3	5.07	52.83	3.42015E-05	1.71007E-05
169	35.1	51.9	17	0.3	6.8	52.83	3.42015E-05	1.71007E-05
170	35	51.9	16.9	0.3	5.07	52.83	3.42015E-05	1.71007E-05
171	35	51.9	16.9	0.4	8.45	52.83	4.5602E-05	2.2801E-05
172	35	51.8	15.9	10.5	190.8	42.38	0.001197052	0.000598526
173	35	51.9	10.2	12.3	122.4	31.33	0.001402261	0.000701131
174	35	51.9	12.4	7.8	147.56	37.78	0.000889239	0.000444619
176	35.3	52	17.6	0.1	1.76	54.98	1.14005E-05	5.70025E-06
177	35.1	52.1	17.4	0.1	1.74	54.67	1.14005E-05	5.70025E-06
179	35.4	52.4	13	4.6	67.6	43	0.000524423	0.000262211
181	35.3	52.6	14.5	3.4	52.2	45.45	0.000387617	0.000193808
182	35.3	52.9	14.4	3.4	50.4	45.45	0.000387617	0.000193808
183	35.5	52.9	13.9	3.7	56.99	44.53	0.000421818	0.000210909
187	35.5	53.3	9	14.4	136.8	29.48	0.001641672	0.000820836
198	36.7	55.1	17	0.4	28.9	53.44	4.5602E-05	2.2801E-05

199	36.5	55.1	16.9	0.5	5.07	52.83	5.70025E-05	2.85012E-05
200	36.5	55.1	16.3	0.5	29.34	51.29	5.70025E-05	2.85012E-05
201	36.6	55.1	16.2	1	17.82	50.98	0.000114005	5.70025E-05
202	36.7	55	16	1	17.6	50.06	0.000114005	5.70025E-05
203	36.8	54.9	15.9	1.3	22.26	50.06	0.000148206	7.41032E-05
204	36.7	54.6	15.9	1.6	25.44	49.14	0.000182408	9.1204E-05
205	36.9	54.6	15.6	1.7	31.2	48.83	0.000193808	9.69042E-05
206	36.6	54.4	13.9	3.8	41.7	43	0.000433219	0.000216609
207	36.6	53.9	14.4	3.5	63.36	44.53	0.000399017	0.000199509
208	36.6	53.7	14.4	3.6	54.72	44.84	0.000410418	0.000205209
209	36.5	53.5	14.3	4.4	70.07	44.53	0.000501622	0.000250811
210	36.7	53.2	14.4	4.4	70.56	44.23	0.000501622	0.000250811
214	36.8	52.7	9.5	13.8	143.45	28.56	0.001573269	0.000786634
215	36.8	52.6	9.6	14.4	130.56	28.87	0.001641672	0.000820836
223	37.4	53.6	14.8	3.3	48.84	46.68	0.000376216	0.000188108
225	37.4	53.7	9.9	13.3	141.57	31.63	0.001516266	0.000758133
227	37.7	53.8	8.9	14.6	127.27	29.79	0.001664473	0.000832236
228	38.1	53.9	9.6	14.5	150.72	29.48	0.001653072	0.000826536
229	38	54	9.4	14.8	142.88	29.18	0.001687274	0.000843637
281	39.7	52.7	17.6	0.3	3.52	54.98	3.42015E-05	1.71007E-05
282	39.7	53.1	16.4	3.4	4.92	50.98	0.000387617	0.000193808
284	39.7	53.5	16.6	3	14.94	52.21	0.000342015	0.000171007
285	39.8	53.4	16.4	1.5	26.24	52.21	0.000171007	8.55037E-05
286	39.9	53.3	16.4	1.8	34.44	51.29	0.000205209	0.000102604
287	39.7	53.1	15.6	4.2	84.24	46.99	0.000478821	0.00023941
288	39.6	52.8	9.6	14.9	147.84	30.71	0.001698674	0.000849337
289	39.4	52.6	9.7	14.1	139.68	30.41	0.00160747	0.000803735
290	39.4	52.6	9.3	14.9	139.5	30.41	0.001698674	0.000849337
291	39.4	52.4	9.2	15.1	143.52	29.18	0.001721475	0.000860738
292	39.6	52.2	9.5	15.6	161.5	28.56	0.001778478	0.000889239
293	39.5	52	8.8	15.7	136.4	29.79	0.001789878	0.000894939
347	39.5	50.9	18	0.6	3.6	53.75	6.8403E-05	3.42015E-05
348	39.4	51	17.7	0.3	5.31	54.98	3.42015E-05	1.71007E-05
349	39.7	51	16.3	2.1	44.01	50.37	0.00023941	0.000119705
350	39.5	51	15.4	3.1	58.52	47.91	0.000353415	0.000176708
351	39.5	51	14.8	4.1	66.6	46.07	0.00046742	0.00023371
352	39.4	51	13.8	4.7	64.86	44.53	0.000535823	0.000267912
353	39.4	51.1	13.9	5.5	86.18	43.92	0.000627027	0.000313514
354	39.4	51.1	13.8	5.5	85.56	42.69	0.000627027	0.000313514
355	39.4	51.1	13.5	6.3	94.5	41.15	0.000718231	0.000359116
356	38.9	51	13.3	6.7	85.12	41.15	0.000763833	0.000381917
357	38.9	51	13.4	6.2	75.04	42.08	0.000706831	0.000353415
358	38.9	50.9	13.2	6	85.8	42.08	0.00068403	0.000342015
359	38.9	50.8	13.2	5.8	85.8	42.38	0.000661229	0.000330614
360	38.4	50.6	13	13.4	184.6	36.55	0.001527667	0.000763833
361	38.4	50.6	10.2	14.2	138.72	31.33	0.001618871	0.000809435
362	38.3	50.6	9.8	15.1	140.14	28.87	0.001721475	0.000860738

363	38.3	50.6	9.6	15.3	144.96	30.41	0.001744276	0.000872138
364	38.4	50.6	9.6	15.7	149.76	29.48	0.001789878	0.000894939
366	38.4	50.5	8.4	16	142.8	59.58	0.00182408	0.00091204
426	38.9	50.3	17.1	0.9	13.68	53.44	0.000102604	5.13022E-05
427	38.5	50.4	16.7	0.9	13.36	52.52	0.000102604	5.13022E-05
428	38.7	50.5	16.8	1.1	18.48	52.21	0.000125405	6.27027E-05
429	38.7	50.6	15.1	1.1	16.61	47.6	0.000125405	6.27027E-05
430	38.5	50.7	15.9	2.1	28.62	50.06	0.00023941	0.000119705
431	38.5	50.8	15.9	2.1	33.39	50.06	0.00023941	0.000119705
432	38.5	51	15.9	2.1	34.98	49.45	0.00023941	0.000119705
433	38.7	51	15.7	2.5	39.25	48.83	0.000285012	0.000142506
434	38.4	51	15.4	2.9	43.12	48.22	0.000330614	0.000165307
435	38.5	51	14.1	5.2	64.86	43.61	0.000592826	0.000296413
436	38.6	50.9	14.2	5.4	88.04	43.92	0.000615627	0.000307813
437	38.6	50.8	12.6	7.4	99.54	39.93	0.000843637	0.000421818
438	38.3	50.6	13.5	6.1	78.3	41.77	0.00069543	0.000347715
439	38.3	50.5	13.5	5.9	78.3	40.85	0.000672629	0.000336315
440	38.2	50.3	12.7	5.9	68.58	38.39	0.000672629	0.000336315
442	38.1	50	12.4	7.9	106.64	39.31	0.000900639	0.00045032
443	37.9	49.8	12.1	12	164.56	36.24	0.00136806	0.00068403
444	38.1	49.8	11.8	10.3	113.28	36.24	0.001174251	0.000587126
445	37.9	49.7	11.9	9.2	110.67	36.86	0.001048846	0.000524423
446	37.9	49.7	12	9.2	114	37.47	0.001048846	0.000524423
447	37.8	49.5	11.9	9	111.86	38.08	0.001026045	0.000513022
448	37.7	49.7	12.1	8.8	113.74	38.39	0.001003244	0.000501622
449	37.9	49.6	12.4	8.8	106.64	39	0.001003244	0.000501622
450	37.8	49.5	12.8	7.9	102.4	39	0.000900639	0.00045032
451	37.7	49.6	12.6	7.8	103.32	39.62	0.000889239	0.000444619
452	37.7	49.5	12.6	6.4	78.12	39.62	0.000729632	0.000364816
453	37.6	49.5	14.6	7.6	94.9	45.76	0.000866438	0.000433219
454	37.7	49.5	14.6	6	86.14	46.07	0.00068403	0.000342015
455	37.5	49.5	11.5	11.7	106.95	34.71	0.001333858	0.000666929
456	37.5	49.4	12.7	8.8	119.38	40.85	0.001003244	0.000501622
457	37.7	49.3	13.2	8.3	108.24	40.54	0.000946241	0.000473121
458	37.7	49.3	12.9	7.9	109.65	41.15	0.000900639	0.00045032
459	37.4	49.2	12.9	8.2	95.46	40.54	0.000934841	0.00046742
460	37.6	49.2	12.9	8.1	95.46	40.54	0.00092344	0.00046172
461	37.4	49.3	13	8.1	96.2	40.54	0.00092344	0.00046172
462	37.5	49.3	12.5	7.7	98.75	40.85	0.000877838	0.000438919
463	37.4	49.2	12.3	8.2	97.17	38.7	0.000934841	0.00046742
464	37.2	49.2	12.6	9.3	120.96	38.7	0.001060246	0.000530123
465	37.4	49.2	12.3	8.6	111.93	39	0.000980443	0.000490221
466	37.2	49.1	12.3	8.4	105.78	40.23	0.000957642	0.000478821
467	37.4	49.1	12.3	9	111.93	38.7	0.001026045	0.000513022
468	37.1	49.2	12.3	8.9	105.78	39.31	0.001014644	0.000507322
470	37.1	49.1	16	2.2	36.8	49.75	0.000250811	0.000125405
471	37.1	49.2	15.8	2.4	42.66	49.14	0.000273612	0.000136806

472	37.2	49.1	15.6	2.8	43.68	48.83	0.000319214	0.000159607
473	37	49.2	15.7	2.6	42.39	48.53	0.000296413	0.000148206
474	37.2	49.3	15.3	2.7	41.31	48.22	0.000307813	0.000153907
475	37	49.4	15.6	2.7	39	48.22	0.000307813	0.000153907
476	37.1	49.3	15.4	2.7	44.66	47.91	0.000307813	0.000153907
477	37.1	49.4	15.1	2.8	40.77	48.22	0.000319214	0.000159607
478	37	49.4	15.1	2.6	42.28	48.22	0.000296413	0.000148206
479	37.1	49.4	15	4.1	79.5	46.68	0.00046742	0.00023371
480	37.1	49.4	13.6	5.1	66.64	44.23	0.000581425	0.000290713
481	37.1	49.4	13.6	6.3	85.68	42.69	0.000718231	0.000359116
482	37.1	49.4	14.1	6	90.24	43	0.00068403	0.000342015
483	37.1	49.4	13.5	5.7	72.9	43	0.000649828	0.000324914
484	37.1	49.4	14	5.5	77	43.3	0.000627027	0.000313514
485	37.1	49.5	13.9	5.8	76.45	43	0.000661229	0.000330614
486	37.2	49.5	12.7	5.8	69.85	39.62	0.000661229	0.000330614
487	37.2	49.7	12.2	7	92.72	38.7	0.000798035	0.000399017
488	37.4	50	12.8	7.5	90.88	39.93	0.000855037	0.000427519
489	37.4	50.2	12.5	7.8	87.5	39.93	0.000889239	0.000444619
490	37.5	50.4	12.5	8	93.75	39.93	0.00091204	0.00045602
491	37.7	50.7	12.3	8.5	111.93	38.7	0.000969042	0.000484521
493	37.7	50.9	13	8.4	107.9	42.69	0.000957642	0.000478821
494	38	51.2	13.3	9.2	129.01	41.15	0.001048846	0.000524423
495	38	51.5	12.6	9.8	128.52	39.93	0.001117249	0.000558624
496	38.2	51.6	12.1	10.9	140.36	38.39	0.001242654	0.000621327
497	38.2	51.6	11.8	11.6	136.88	37.16	0.001322458	0.000661229
498	38.4	51.7	12	11.6	135.6	38.08	0.001322458	0.000661229
499	38.4	51.7	12.3	10.1	132.84	37.47	0.00115145	0.000575725
500	38.5	51.6	12.3	10.8	124.23	37.47	0.001231254	0.000615627
501	38.9	51.5	12	10.1	129.6	37.47	0.00115145	0.000575725
502	38.7	51.6	12	11.5	133.2	37.47	0.001311057	0.000655529
503	38.9	51.5	11.8	11.1	138.06	37.16	0.001265455	0.000632728
504	38.9	51.6	11.7	11.6	135.72	37.16	0.001322458	0.000661229
505	39.2	51.6	11.7	11.8	131.04	35.93	0.001345259	0.000672629
506	39.4	51.6	11.3	12	134.47	35.63	0.00136806	0.00068403
507	39.4	51.7	11.6	12	135.72	35.63	0.00136806	0.00068403
508	39.5	51.8	11.3	12	143.51	35.93	0.00136806	0.00068403
509	39.6	51.8	11.4	12.6	144.78	35.01	0.001436463	0.000718231
510	39.8	51.9	11.5	12.6	135.7	36.55	0.001436463	0.000718231
511	39.8	52.2	10.5	12.2	135.45	35.01	0.001390861	0.00069543
512	39.9	52.3	10.8	13.5	137.16	35.01	0.001539067	0.000769534
513	40.1	52.5	11	13.3	134.2	34.71	0.001516266	0.000758133
570	42.1	51.1	14.6	0.1	27.74	43.61	1.14005E-05	5.70025E-06
574	42.1	51.1	16.6	2.2	34.86	51.6	0.000250811	0.000125405
575	42.1	51.2	15.3	3.4	39.78	46.99	0.000387617	0.000193808
578	42.1	51.6	13.5	4.2	60.75	45.76	0.000478821	0.00023941
579	41.9	51.7	15.3	4.7	58.14	46.68	0.000535823	0.000267912
580	42.3	51.8	12	4.7	62.4	37.78	0.000535823	0.000267912

581	42.3	51.7	12.5	10.4	131.25	38.7	0.001185652	0.000592826
582	41.8	51.6	11.8	10	114.46	36.24	0.00114005	0.000570025
584	41.8	51.1	11.5	11.3	135.7	35.93	0.001288256	0.000644128
585	41.8	50.7	11.5	10.8	124.2	35.93	0.001231254	0.000615627
586	41.8	50.5	11.6	11.4	124.12	36.86	0.001299657	0.000649828
587	41.7	50.5	11.4	12	134.52	35.01	0.00136806	0.00068403
588	41.4	50.2	11	12.2	137.5	35.01	0.001390861	0.00069543
589	41.4	50	10.9	13.2	139.52	34.71	0.001504866	0.000752433
590	41.4	49.7	10.5	13.5	139.65	33.48	0.001539067	0.000769534
591	41.3	49.4	9.6	16.4	127.68	30.71	0.001869682	0.000934841
592	41.2	49.4	10	16.4	164	30.41	0.001869682	0.000934841
645	40.9	48.8	17.8	0.8	1.78	54.05	9.1204E-05	4.5602E-05
646	40.8	48.8	17.8	0.2	3.56	55.9	2.2801E-05	1.14005E-05
647	40.9	49	17.8	1.2	24.92	52.83	0.000136806	6.8403E-05
648	40.8	49	15.7	3.1	43.96	49.14	0.000353415	0.000176708
649	40.8	49	16.3	2	40.75	50.98	0.00022801	0.000114005
650	40.8	49	15.7	2.9	50.24	48.83	0.000330614	0.000165307
651	40.8	48.9	15.3	3.8	71.91	47.91	0.000433219	0.000216609
652	41	48.9	15	4.4	70.5	45.76	0.000501622	0.000250811
653	40.5	48.8	15	4.4	70.5	45.15	0.000501622	0.000250811
654	40.5	48.6	13.4	4.4	50.92	41.77	0.000501622	0.000250811
655	40.5	48.5	12.9	7.7	153.51	39	0.000877838	0.000438919
656	40.2	48.4	13.2	9.9	146.52	41.77	0.001128649	0.000564325
657	40.2	48.4	13.2	7.2	89.76	41.77	0.000820836	0.000410418
658	40.1	48.2	14.1	5.9	90.24	43.61	0.000672629	0.000336315
659	39.8	48.1	14.2	5.3	79.52	44.53	0.000604226	0.000302113
660	39.8	48	13.9	6.1	75.06	42.69	0.00069543	0.000347715
661	39.6	48	13.8	5.8	88.32	43	0.000661229	0.000330614
662	39.6	48	13.5	7.7	106.65	41.15	0.000877838	0.000438919
663	39.4	47.9	12.4	9.2	112.84	39	0.001048846	0.000524423
664	39.4	47.9	11.8	10.5	125.08	36.86	0.001197052	0.000598526
665	39.4	47.7	11.6	10.9	122.96	36.24	0.001242654	0.000621327
666	39.1	47.8	11.1	11.3	117.66	35.63	0.001288256	0.000644128
668	38.9	47.6	11.3	11.3	134.47	36.24	0.001288256	0.000644128
669	38.9	47.7	11.1	11.9	126.54	35.01	0.001356659	0.00067833
670	38.9	47.7	11.1	12.1	144.3	35.32	0.00137946	0.00068973
672	38.9	47.7	11.1	12.2	129.87	34.4	0.001390861	0.00069543
673	38.5	48	18	0.2	3.6	55.59	2.2801E-05	1.14005E-05
674	38.5	48.1	17.8	0.2	3.56	55.59	2.2801E-05	1.14005E-05
675	38.4	48.4	17.6	1.3	1.76	54.05	0.000148206	7.41032E-05
676	38.6	48.6	15.9	1.3	34.98	49.45	0.000148206	7.41032E-05
677	38.7	48.7	17.2	2.8	15.48	53.75	0.000319214	0.000159607
678	38.5	48.8	16.6	0.8	33.2	51.9	9.1204E-05	4.5602E-05
679	38.4	48.8	16.4	1.5	22.96	51.9	0.000171007	8.55037E-05
680	38.4	48.7	16.4	2.1	41	50.98	0.00023941	0.000119705
681	38.5	48.8	16.2	2.1	34.02	50.37	0.00023941	0.000119705
682	38.6	48.7	15.6	2.3	32.76	48.83	0.000262211	0.000131106

683	38.6	48.7	15.7	2.7	37.68	49.75	0.000307813	0.000153907
684	38.5	48.6	14	4.5	58.8	44.23	0.000513022	0.000256511
685	38.4	48.4	14.6	4.1	61.32	45.76	0.00046742	0.00023371
686	38.3	48.2	15.2	4.1	57.76	47.3	0.00046742	0.00023371
687	38.2	48.1	15	3.4	52.5	46.68	0.000387617	0.000193808
688	38.1	47.9	14.7	3.6	52.92	46.68	0.000410418	0.000205209
689	38.1	47.6	14.5	4.2	59.45	44.53	0.000478821	0.00023941
690	38	47.6	14.5	4.6	58	44.53	0.000524423	0.000262211
691	37.9	47.5	14.5	4.2	60.9	45.45	0.000478821	0.00023941
692	37.8	47.4	14.4	4.2	61.92	45.76	0.000478821	0.00023941
693	38	47.3	14.7	6.5	102.9	44.23	0.000741032	0.000370516
694	37.7	47.3	14.2	4.9	68.16	44.23	0.000558624	0.000279312
695	37.7	47.3	14.2	5	65.32	44.23	0.000570025	0.000285012
696	37.7	47.2	14.1	4.9	66.27	43.3	0.000558624	0.000279312
697	37.5	47.1	14.1	4.7	60.63	43.92	0.000535823	0.000267912
698	37.4	47.1	14.2	4.7	61.06	44.53	0.000535823	0.000267912
699	37.1	47.1	14.2	4.7	65.32	45.15	0.000535823	0.000267912
700	37	47	12.8	4.5	61.44	39.93	0.000513022	0.000256511

LIST OF PUBLICATIONS

1) Azadeh Kheirandish, Mohammad Saeed Kazemi, Mahidzal Dahari (2014) "Dynamic performance assessment of the efficiency of fuel cell-powered bicycle: An experimental approach" *International Journal of Hydrogen Energy (Q_1. Impact 3.5)*
2) Azadeh Kheirandish, Farid Motlagh, Niusha Shafiabady, Mahidzal Dahari (2016) "Dynamic Modelling of PEM Fuel Cell of Power Electric Bicycle System" *International Journal of Hydrogen Energy (Q_2. Impact 3.3)*
3) Azadeh Kheirandisha, Niusha Shafiabady, Mahidzal Dahari, Mohammad Saeed Kazemi, , Dino Isa "Modelling of Commercial Proton Exchange Membrane Fuel Cell Using Support Vector Machine" Journal: *International Journal of Hydrogen Energy (Q_2. Impact 3.3)*